

**Eap-functionalized liposomes as a
bioinspired delivery system for oral delivery
of colistin to treat intracellular *Salmonella*
*infection***

Dissertation
zur Erlangung des Grades
des Doktors der Naturwissenschaften
der Naturwissenschaftlich-Technischen Fakultät
der Universität des Saarlandes

von
Sara Menina

Saarbrücken

2020

Tag des Kolloquiums: 5. März 2021

Dekan: Prof. Dr. Jörn Erik Walter

Berichterstatter/in: Prof. Dr. Claus-Michael Lehr

Prof. Dr. Rolf W. Hartmann

Vorsitzende/r: Prof. Dr. Marc Schneider

Akad. Mitarbeiter/in: Dr. Jessica Hoppstädter

Die vorliegende Arbeit wurde vom June 2015 bis Oktober 2018 unter der
Leitung von Herrn Prof. Dr. Claus-Michael Lehr am Institut für Pharmazeutische
Technologie der Universität des Saarlandes und Helmholtz-Institut für
Pharmazeutische Forschung Saarland (HIPS) in der Abteilung für Wirkstoff-
Transport angefertigt

“Life is not easy for any of us. But what of that? We must have perseverance and, above all, confidence in ourselves. We must believe that we are gifted for something, and that this thing, at whatever cost, must be attained.”

-Marie Curie.

Table of Contents

Short Summary	I
Kurzzusammenfassung	II
List of Abbreviations	III
List of Figures	VII
List of Tables	X
List of Equations	XI
1 Introduction	1
1.1 Intracellular infections	1
1.2 Anti-infectives: past and present	5
1.3 Oral delivery	11
1.4 Liposomes as a delivery system	14
1.4.1 Liposome modulation to improve stability	16
1.4.2 Liposome modulation to improve permeability	19
1.5 Extracellular adherence protein (Eap)	24
2 Aim	26
3 Materials and Methods	28
3.1 Materials	28
3.2 Liposomes preparation	29
3.3 Characterization of liposomes	30
3.3.1 Colloidal characterization	30
3.3.2 Colistin quantification	31
3.3.3 Phospholipids quantification	32
3.3.4 Cholesterol quantification	32
3.3.5 Entrapment efficiency and loading capacity	33
3.3.6 Thermal characterization	33

3.4	Stability studies in biorelevant media	34
3.4.1	Fasted state simulated gastric fluid (FaSSGF)	35
3.4.2	Fasted state simulated intestinal fluid (FaSSIF)	36
3.4.3	Fed state simulated intestinal fluid (FeSSIF)	38
3.5	Liposomes functionalization	39
3.5.1	Determination of Eap concentration	40
3.5.2	Functionalization efficiency.....	42
3.5.3	Stability of Eap-functionalized liposomes	43
3.6	<i>In vitro</i> cell experiments.....	43
3.6.1	Cell culture	43
3.6.2	Cytotoxicity assessment.....	43
3.6.3	Uptake efficiency	45
3.6.4	TEER measurements	46
3.6.5	Cell Imaging	47
3.6.6	Immunostaining of Caco-2 monolayer	48
3.6.7	Uptake mechanism.....	48
3.7	<i>In vitro</i> infection studies	50
3.7.1	Bacterial growth curve.....	51
3.7.2	Minimum inhibitory concentration (MIC)	51
3.7.3	Anti-bacterial efficacy	51
3.7.4	Colistin dose-response and Eap titration studies.....	54
3.8	<i>In vivo</i> assessment of anti-infective efficacy	55
3.9	Statistical analysis	56
4	Results.....	57
4.1	Unloaded liposomes	57
4.1.1	Colloidal characterization	57

4.1.2	Unloaded liposomes stability	57
4.2	Colistin-loaded liposomes	60
4.2.1	Colloidal characterization	60
4.2.2	Liposomes morphology	61
4.2.3	Colistin loading	62
4.3	Stability studies for the oral route	64
4.4	Eap-functionalized liposomes containing colistin	69
4.5	<i>In vitro</i> cellular studies	73
4.5.1	Intestinal barrier model	73
4.5.2	Cytotoxicity assessment	74
4.5.3	Eap mediates the binding/internalization of liposomes into epithelial cells.....	76
4.6	<i>Salmonella enterica</i> growth curve and MIC determination	82
4.7	Impact of Eap-functionalized liposomes on infected cells	85
4.7.1	Infection parameters determination	85
4.7.2	Antibacterial efficacy of EapCol-Lip-3.....	86
4.7.3	Cell viability during infection studies	87
4.7.4	Eap dose titration.....	89
4.7.5	Colistin-dose response	90
4.8	<i>In vivo</i> pilot study	91
5	Discussion	93
5.1	Colistin-loaded liposomes for oral delivery	93
5.2	Eap mediates the internalization of liposomes	96
5.3	Impact of Eap-functionalized liposomes containing colistin on intracellular infection	102
6	Conclusion.....	105
7	References	106

8	Supplementary Figures	137
	Acknowledgements	146
	Contributions	149
	Curriculum Vitae.....	Fehler! Textmarke nicht definiert.
	Award.....	150

Short Summary

Bacterial infections continue to prove difficult to treat due to the increase of drug resistance, but also in the case of intracellular pathogens, poorly permeable anti-infectives are usually not effective. Encapsulation of anti-infectives into nanoparticulate delivery systems, such as liposomes, has been shown to result in an enhancement of intracellular delivery. The aim of this study was to formulate liposomes for oral delivery of a poorly permeable anti-infective, colistin, and functionalize them with a bacterial invasion moiety to enhance their intracellular delivery. Different combinations of phospholipids and cholesterol were employed to produce colistin-loaded liposomes. Long alkyl chain-containing liposomes showed improved stability in terms of colloidal parameters as well as colistin retention when compared to the other formulations tested in gastrointestinal biorelevant media. The stable formulation was then functionalized with extracellular adherence protein (Eap), a *Staphylococcus aureus*-derived invasion protein. Eap-functionalized liposomes loaded with colistin were able to invade HEp-2 and Caco-2 monolayers with high efficiency. Treatment of HEp-2 and Caco-2 monolayers infected with the enteroinvasive bacteria *Salmonella enterica*, with colistin containing Eap-functionalized liposomes showed a significant reduction in the infection load when compared to control i.e. non-functionalized liposomes. This indicates that such bio-invasive nanocarriers were able to promote successful cellular uptake of colistin and mediate anti-infective effect intracellularly. Eap-functionalized liposomal nanocarriers offer a promising strategy for intracellular infections treatment.

Kurzzusammenfassung

Bakterielle Infektionen erweisen sich aufgrund der zunehmenden Arzneimittelresistenzen weiterhin als schwierig zu behandeln. Zudem sind bei intrazellulären Bakterien schlecht permeable Antiinfektiva normalerweise nicht wirksam. Es wurde gezeigt, dass die Einkapselung von Antiinfektiva in nanopartikuläre Trägersysteme, wie beispielsweise Liposomen, zu einer Verbesserung des Transports in Zellen führt. Diese Studie zielte darauf ab, Liposomen für die orale Applikation des schlecht permeablen Antibiotikums Colistins zu formulieren und diese mit einem bakteriellen Invasionsmolekül zu funktionalisieren, um ihre intrazelluläre Verfügbarkeit zu verbessern. Unterschiedliche Kombinationen von Phospholipiden und Cholesterin wurden verwendet, um mit Colistin beladene Liposomen herzustellen. Lange Alkylketten enthaltende Liposomen zeigten im Vergleich zu den anderen in simulierten Magen-Darm-Medien getesteten Formulierungen eine verbesserte Stabilität sowohl hinsichtlich ihrer kolloidalen Stabilität als auch der Colistinretention. Diese stabile Formulierung wurde dann mit extrazellulärem Adhäsionsprotein („extracellular adherence protein“ Eap), einem von *Staphylococcus aureus* gewonnenen Invasionsprotein, funktionalisiert. Mit Colistin beladene Eap-funktionalisierte Liposomen konnten mit hoher Effizienz in dichte Zellschichten von HEp-2- und Caco-2-Zellen eindringen. Die Behandlung von HEp-2- und Caco-2-Monoschichten, die mit dem enteroinvasiven Bakterium *Salmonella enterica* infiziert wurden, mit Colistin-beladenen; Eap-funktionalisierten Liposomen führten zu einer signifikanten Verringerung der Infektionslast im Vergleich zur Behandlung mit nicht funktionalisierten Liposomen. Dies ist ein Beleg dafür, dass solche bio-invasiven Nanocarrier die erfolgreiche zelluläre Aufnahme von Colistin fördern und somit die intrazelluläre antiinfektiöse Wirkung ermöglichen können. Somit bieten die entwickelten Eap-funktionalisierten Liposomen eine vielversprechende Strategie zur Verbesserung der Therapie intrazellulärer Infektionen des Magen-Darm-Trakts.

List of Abbreviations

Acr/Bis	N, N'-Methylenebisacrylamide
AMR	Anti-microbial resistance
APS	Ammonium persulfate
BCA	Bicinchoninic acid assay
BCV	Bacteria-containing vacuole
BSA	Bovine serum albumin
Caco-2	Human epithelial colorectal adenocarcinoma
CBA	Colistin base activity
CEACAMs	Carcinoembryonic antigen-related cell adhesion molecules
CFU	Colony forming unit
C ₄ H ₁₁ NO ₃	Tris base
C ₆ H ₁₃ NO ₄ S	2-(N-morpholino) ethanesulfonic acid
C ₁₉ H ₁₀ Br ₄ O ₅ S	Bromophenol blue
CHOL	Cholesterol
CMS	Colistin methanesulfonate
CLSM	Confocal Laser Scanning Microscopy
CO ₂	Carbon dioxide
Col-Lip	Colistin-loaded liposomes
CPP	Cell-penetrating peptide
DLS	Dynamic light scattering
DMPC	1, 2-dimyristoyl- <i>sn</i> -glycero-3-phosphocholine
DMTMM chloride	4-(4,6-dimethoxy-1,3,5-triazin-2-yl)-4-methyl-morpholinium chloride
DNA	Deoxyribonucleic acid

List of Abbreviations

DOPC	1,2-dioleoyl- <i>sn</i> -glycero-3-phosphocholine
DOPE	1, 2-dioleoyl- <i>sn</i> -glycero-3-phosphoethanolamine
DPPC	1, 2-dipalmitoyl phosphatidylcholine
DPPE	1, 2-dipalmitoyl- <i>sn</i> -glycero-3-phospho-ethanolamine-N-(Glutaryl) sodium salt
DSC	Differential scanning calorimetry
DSPC	1, 2-distearoyl- <i>sn</i> -glycero-3-phosphocholine
DSPE	1, 2-distearoyl- <i>sn</i> -glycero-3-phosphoethanolamine
Eap	Extracellular adhesion protein
EapCol-Lip	Eap-functionalized liposomes containing colistin
ECM	Extracellular matrix
FDA	Food and Drug Administration
EDC	Ethylcarbodiimide hydrochloride
EE	Encapsulation efficiency
EMA	European Medicines Agency
FACS	Fluorescence-activated cell sorting
FaSSGF	Fasted state simulated gastric fluid
FaSSIF	Fasted state simulated intestinal fluid
FaSSIF-enz	Fasted state simulated intestinal fluid containing enzymes
FE	Functionalization efficiency
FeCl ₃ .6H ₂ O	Ferric 3-chloride-hexahydrate
FeSSIF	Fed state simulated intestinal fluid
gC1q-R	Complement receptor
GI	Gastrointestinal
HCl	Hydrochloric acid
HEp-2	Human Epithelial type 2

List of Abbreviations

HEPES	Hydroxyethyl-piperazineethane-sulfonic acid buffer
HGF	Hepatocyte growth factor
HPLC	High performance liquid chromatography
ICAM-1	Intercellular adhesion molecule 1
InIA	Internalin A
InIB	Internalin B
InvA	Invasin A protein
IU	International Unit
LC	Loading capacity
Lip	Unloaded liposomes
LAS AF	Leica Application Suite Advanced Fluorescence software
M cells	Microfold cells
MDR	Multidrug resistant
MOI	Multiplicity of infection
mRNA	Messenger ribonucleic acid
MTT	3-(4,5-Dimethylthiazol-2-yl)-2,5-diphenyltetrazolium bromide
MWCO	Molecular weight cut off
NHS	N-hydroxysuccinimide
NH ₄ SCN	Ammonium thiocyanate
PBS	Phosphate buffered saline
PC	Phosphatidylcholine
PDI	Polydispersity index
PDR	Pandrug-resistant
PEG	Polyethylene glycol
PLGA	Poly (lactic-co-glycolic acid)
Rhod	Rhodamine

List of Abbreviations

Rpm	Revolutions per minute
RPMI	Roswell Park Memorial Institute cell culture medium
rRNA	Ribosomal ribonucleic acid
SDS-PAGE	Sodium dodecyl sulfate polyacrylamide gel electrophoresis
SE	Standard error of the mean
SEM	Scanning electron microscopy
SIPs	Salmonella invasion proteins
SUV	Small unilamellar vesicle
TEER	Transepithelial electrical resistance
TEMED	N, N, N', N'-tetramethylethylenediamine
T _m	Transition temperature (melting temperature)
WHO	World Health Organization
XDR	Extensively drug-resistant tuberculosis
ZO	Zonula Occludens

List of Figures

<i>Figure 1.1. Mechanisms of bacterial entry into host cells</i>	2
<i>Figure 1.2. Anti-infective mechanisms of action</i>	5
<i>Figure 1.3. A history of anti-infective discovery and corresponding evolution of bacterial-resistance</i>	7
<i>Figure 1.4. Colistin structure and mechanism of action</i>	10
<i>Figure 1.5. Gastrointestinal tract challenges for oral delivery</i>	13
<i>Figure 1.6. Liposomal structure</i>	14
<i>Figure 1.7. Strategies for the oral delivery of liposomes</i>	21
<i>Figure 3.1. Liposomes preparation</i>	30
<i>Figure 3.2. Stability study workflow</i>	35
<i>Figure 3.3. Scheme illustrating FaSSIF-enz preparation protocol</i>	37
<i>Figure 3.4. Scheme illustrating FeSSIF preparation protocol</i>	38
<i>Figure 3.5. Functionalization methods</i>	40
<i>Figure 3.6. Scheme illustrating SDS-PAGE principle</i>	42
<i>Figure 3.7. MTT assay principle</i>	44
<i>Figure 3.8. TEER measurement setup</i>	47
<i>Figure 3.9. Uptake mechanism pathways</i>	50
<i>Figure 3.10. Optimization of infection assay</i>	53
<i>Figure 3.11. Antibacterial efficacy protocol</i>	54
<i>Figure 3.12. Experimental plan of the in vivo study</i>	56
<i>Figure 4.1. Colloidal characteristics of unloaded liposomes</i>	58
<i>Figure 4.2. Unloaded liposomes stability</i>	59
<i>Figure 4.3. Colloidal parameters of colistin-loaded liposomes</i>	61
<i>Figure 4.4. Liposomes morphology</i>	62

Figure 4.5. Colistin-loaded liposomes properties	63
Figure 4.6. Stability characteristics of colistin-loaded liposomes	65
Figure 4.7. Colloidal characteristics in simulated media	67
Figure 4.8. Colistin release kinetics in simulated media	68
Figure 4.9. Functionalization efficiency	70
Figure 4.10. Colloidal characteristics of Eap-functionalized liposomes	71
Figure 4.11. Stability of Eap-functionalized liposomes	72
Figure 4.12. Caco-2 monolayer properties	73
Figure 4.13. Cytotoxicity results	75
Figure 4.14. Uptake efficiency	77
Figure 4.15. Uptake imaging	79
Figure 4.16. Uptake mechanism kinetics	81
Figure 4.17. Salmonella characteristics	83
Figure 4.18. Salmonella minimum inhibitory concentrations	84
Figure 4.19. Intracellular infection optimization	85
Figure 4.20. Antibacterial efficacy	87
Figure 4.21. Cell viability after infection studies	88
Figure 4.22. Eap-dose titration	89
Figure 4.23. Colistin-dose response	90
Figure 4.24. Liposomal treatment of Salmonella-mouse modal	92
Figure 8.1. Colistin analytic analysis	137
Figure 8.2. Thermal Characterization	138
Figure 8.3. 3D fluorescence imaging	139
Figure 8.4. Ortho-CLSM images of Eap-Col-Lip-3 uptake	141
Figure 8.5. Liposomal morphology after stability studies in FaSSIF-Enz	142
Figure 8.6. EapCol-Lip-3 uptake comparison	143

Figure 8.7. Eap- and InvA197-functionalized col-Lip-3 comparison144
Figure 8.8. Cell imaging during infection145

List of Tables

Table 1. Material used in this study	28
Table 2. Liposomes composition	29
Table 3. Simulated media composition	36
Table 4. Characteristics of colistin-loaded liposomes (4 mg/mL) after optimization	64

List of Equations

<i>Equation 1: Entrapment efficiency</i>	33
<i>Equation 2. Loading capacity</i>	33
<i>Equation 3: Functionalization efficiency</i>	42
<i>Equation 4. Infection percentage</i>	52

1 Introduction

1.1 Intracellular infections

Bacterial infections are among the most frequent life-threatening diseases worldwide, with over 10 million deaths registered every year (Kraker et al. 2016; PLOS Medicine Editors. 2016). These pathogens can be found either extracellularly living as free microorganisms in their habitats, or creating complex forms by invading their surrounding niches and causing intracellular infections (McClure et al. 2017). Nowadays, intracellular infections still represent a major threat to human and animal populations, as they have proven themselves to be targets which are hard to reach. These species of pathogens can be internalized by host cells following passive or active pathways. In the passive mode of invasion, pathogens are internalized by phagocytosis which is a common route used by professional phagocytic host cells such as macrophages, dendritic cells and neutrophils. During this process, the bacteria do not require an energy-dependent activity such as mycobacteria (Pieters 2008) and legionellae (Weissgerber et al. 2003). However, other bacterial species are able to invade non-phagocytic cells, upon attachment to certain receptors or via virulence factor-mediated mechanisms. The zipper strategy used by *Yersinia* and *Listeria* spp. involves the ligation of pathogenic agents to specific receptors on the host cell membrane such as integrins or cadherins. These interactions stimulate cytoskeletal pseudopod-like structures, leading to the engulfment of pathogens (Ham et al. 2011; Ribet and Cossart 2015) (**Figure 1.1 a, b**). On the other hand, salmonellae and shigella possess a type III secretion system, which can penetrate the host cell membrane and secrete virulence factors called the trigger mechanism to induce cytoskeletal rearrangements. This results in engulfment of the bacteria via membrane protrusions named ruffles (Cossart and Roy 2010; Pizarro-Cerdá and Cossart 2006) (**Figure 1.1 c, d**). After their internalization, these pathogenic agents are capable of replicating inside intracellular compartments called vacuoles (a strategy used by bacteria such as *Salmonella* and *Mycobacterium*), or escaping into the cytosol where further replication occurs (as occurs for example with *Listeria* and *Shigella*) (Ham et al. 2011).

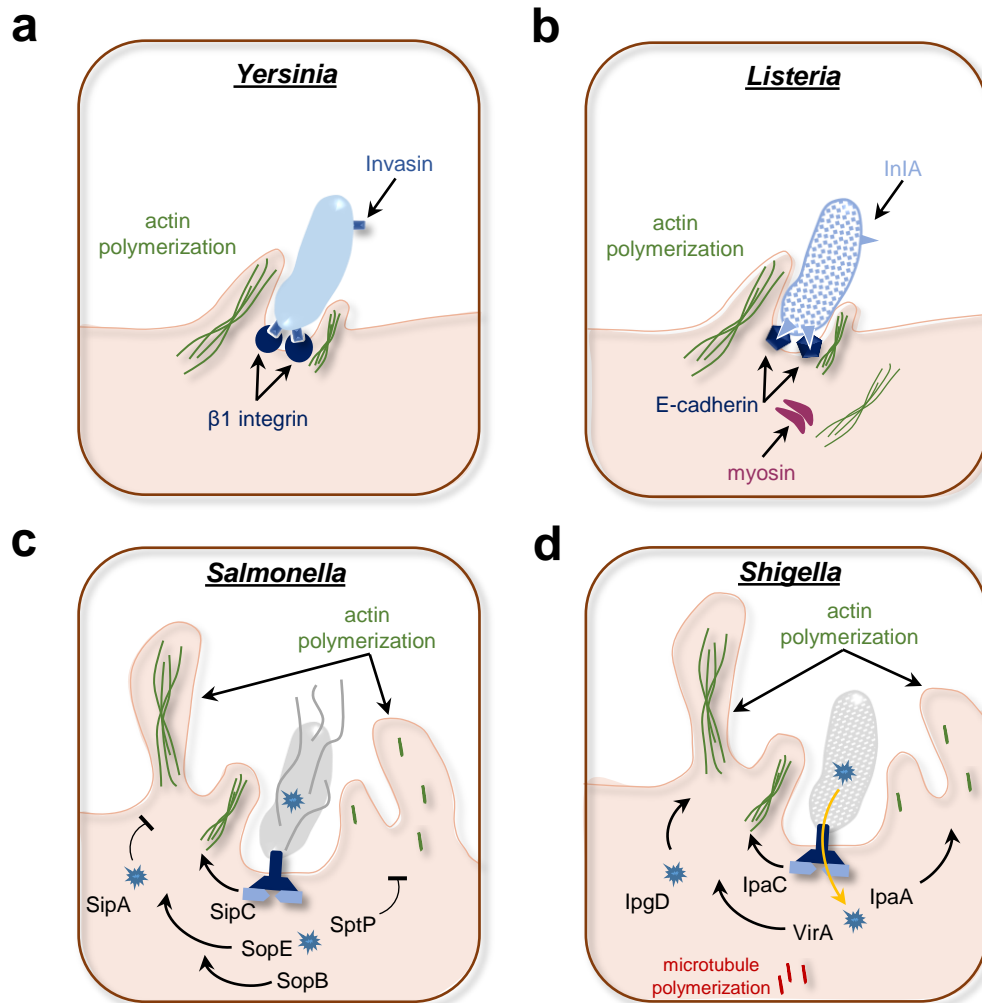


Figure 1.1. Mechanisms of bacterial entry into host cells

Invasion routes of Yersinia (a), Listeria (b) using the zipper strategy characterized by receptor-mediated internalization through the binding of invasins (Yersinia) to Integrin receptors and Internalin A (InlA, Listeria) to E-cadherin receptors. Salmonella (c) and Shigella (d) applying the trigger strategy via their type III secretion system mediating the secretion of different proteins (SipA, SipC, SopE, SptP and SopB in Salmonella infection) and (IpgD, IpaC, VirA and IpaA in shigella infection) which regulate actin cytoskeleton dynamics. Figure adapted from (Cossart and Sansonetti 2004).

Such invasive strategies, among others, allow these bacteria to escape immune detection and elimination in response to the body signals. Once taken up by

macrophages, organisms which cannot survive intracellularly are mainly digested within a maximum of 30 min during fusion of the phagosome with lysosome. Digestion is ensured by the content of phagosomes, including nitric oxide and oxygen species, as well as antimicrobial peptides present for example in some epithelial cells and neutrophils (Hasset and Cohen 1989; Nicolas and Mor 1995). However, intracellular bacteria possess, and are capable of developing if needed, a variety of strategies to overcome phagosome-lysosome digestion. *Yersinia* spp. have the ability to prevent phagocytosis by interacting with phagocyte receptors and blocking the process (Fällman et al. 2001). *Shigella* and *Listeria* spp. secrete toxins, which are able to lyse phagosomes and therefore facilitate bacterial escape into the cytosol (Paz et al. 2010; Pizarro-Cerdá et al. 2016). In contrast, *Legionella* spp. interfere with phagosome and lysosome fusion, while *Mycobacterium* spp. impede acidification of the phagolysosome which generally occurs as a result of phagosome and lysosome fusion (Pizarro-Cerdá et al. 2016; Levitte et al. 2016). *Salmonella* spp. employ yet another different mechanism, which involves alteration of phagocytosis mechanism and resistance to the antimicrobial activity into the phagolysosome (Pizarro-Cerdá et al. 1997). Besides evading the action of the immune system, these pathogenic agents may also be capable of resisting the action of anti-infectives such as beta-lactams, or presenting a hard target to access for other antibiotics to access – this may be a result of poor intracellular retention, as is the case for macrolides and fluoroquinolones, or due to low antibiotic permeability, as is exhibited by aminoglycosides (Salouti and Ahangari 2014).

Regardless of the type of entry mechanism these pathogens employ, once able to reside and replicate within host cells, they can induce complicated and life-threatening diseases such as pneumonia as well as foodborne illnesses. *Salmonella* is one of the global causes of foodborne illnesses. 550 million people are affected each year by this diarrheal disease, including over 220 million children, as stated by the World Health Organization in February 2018. *Salmonella*, the rod-shaped motile Gram-negative bacteria from the Enterobacteriaceae family, is divided in two species: *S. bongori*, and *S. enterica* (Su and Chiu 2007). *S. enterica* has six subspecies, which include more than 2600 serotypes (Gal-Mor et al. 2014). From a clinical perspective, *Salmonella* is

divided into two categories: typhoidal (invasive) or non-typhoidal (non-invasive) *Salmonella* (Okoro et al. 2012). Non-typhoidal serotypes can infect either animals or humans, and the disease can be transferred from animal to human. As intracellular pathogens, they can invade the cellular barrier of the gastrointestinal (GI) tract causing salmonellosis, where the symptoms are usually self-limiting such as fever, abdominal pain, diarrheas, and sometimes vomiting. However, these invasive serotypes can cause more serious complications such as paratyphoid fever, which requires anti-infective therapy in most cases. On the other hand, typhoidal serotypes are restricted to human hosts, and are characterized by their ability to invade the GI tract barrier and make their way through the lymphatic system to the bloodstream (causing typhoid fever). Moreover, they can disseminate further into different organs and release toxins causing septic shock, which usually requires anti-infective treatment and intensive care (Ryan et al. 2004). Regarding the treatment, this is generally not required in healthy individuals with mild or moderate symptoms. However, some exceptions occur in the case of children and the elderly; treatment may also prove necessary in immunocompromised individuals. Ampicillin, chloramphenicol and sulfamethoxazole-trimethoprim, which were previously the first line of treatment in this case, are no longer an appropriate choice due to the increase in bacterial resistance to these anti-infectives; fluoroquinolones and third generation cephalosporins are therefore now taking the lead in the treatment scheme. The lower susceptibility of *Salmonella* towards these anti-infective classes has however led to considerable concern regarding treatment of such pathogens. In addition, the Food and Drug Administration (FDA) reported in July 2018 warnings concerning fluoroquinolone prescriptions, stating that the use of these anti-infectives might lead to hypoglycemia and neural system dysfunction. Therefore, there is a major need for new drugs or new therapeutic strategies for the treatment of such intracellular pathogenic agents.

1.2 Anti-infectives: past and present

In 1947, Selman Waksman first introduced the world to the word “Antibiotic”, a term defined as a small molecule derived from pathogenic agents, capable of either inhibiting the growth of a micro-organism or eliminating it altogether (Clardy et al. 2009). An antibiotic interferes with bacterial survival via a specific mechanism of action, which also requires a specific therapeutic concentration. This specific therapeutic concentration should be sufficient to achieve high efficacy regarding inhibition or elimination of the pathogenic agent while causing minimal toxicity (Ren et al. 2015).

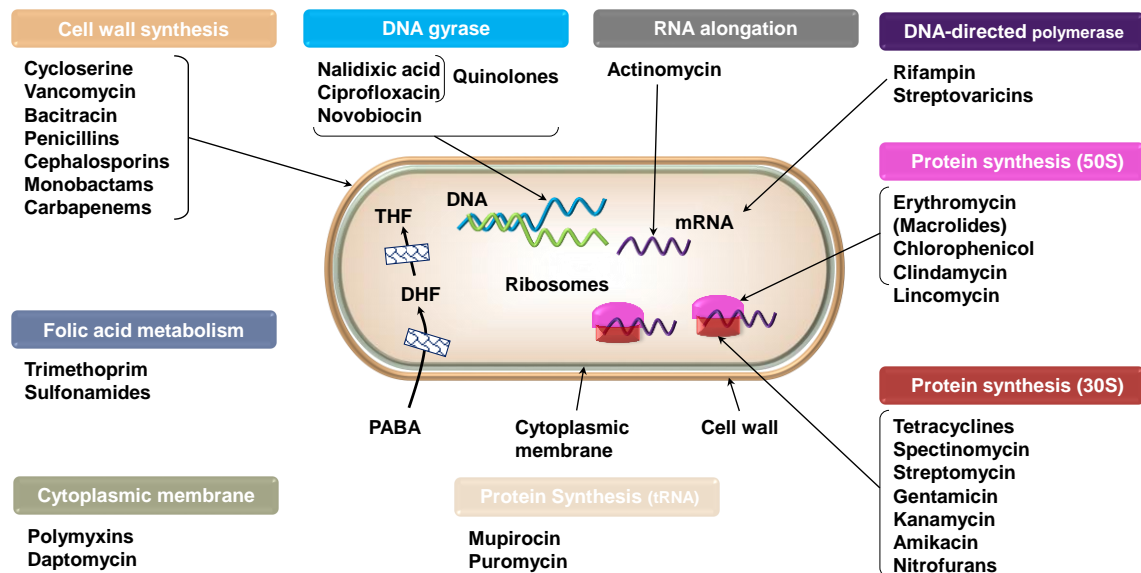


Figure 1.2. Anti-infective mechanisms of action

Illustration showing classification of antibiotics and their mechanisms of action. Different bacterial sites including the cell wall and membrane, DNA, RNA and protein synthesis are targeted by different antibiotic molecules. Figure adapted from (Bbosa et al. 2014).

Beta lactams including penicillins, cephalosporins, carbapenems and monobactams act on the bacterial cell wall, leading to the inhibition of synthesis of peptidoglycan and causing lysis of bacterial cells (Peterson and Kaur 2018). Following their penetration into the bacterial cell, other antibiotics are able to inhibit protein synthesis by targeting the ribosomal subunits. Tetracyclines and

aminoglycosides interfere with mRNA translation by interacting with rRNA of the 30S subunit, while chloramphenicol, oxazolidinones and macrolides interact with the 50S ribosomal subunit (Vannuffel and Cocito 1996; Wise 1999). Quinolones on the other hand are able to inhibit DNA replication by interacting with the bacterial enzyme DNA gyrase (Higgins et al. 2003), while rifampicin acts on the RNA polymerase; sulfonamides as well as trimethoprim interfere with folic acid metabolism by inhibiting distinct steps involved in its synthesis (Yoneyama and Katsumata 2006) (**Figure 1.2**). However, due to the ability of several bacterial pathogens to acquire sophisticated survival strategies to overcome antibiotic activity, the spread of anti-microbial resistance (AMR) is accelerating leaving humanity with major challenges (Coates et al. 2011; Aslam et al. 2018).

Since discovery of the first antibiotic Penicillin by Alexander Fleming in 1928, and the beginning of its use for treatment of infections in 1942, more than 20 classes of antibiotics have been discovered and marketed – this occurred in the period between 1940 and 1960, which is considered as the Antibiotic Golden Age (Powers 2004; Coates et al. 2002). In fact in 1970, Surgeon General William Stewart stated that it was time “to close the book on infectious diseases,, and focus more on hard-to-treat diseases such as cancer” (WHO 2018). Since that period only two antibiotic classes have been discovered and some analogues of existing classes have reached the market (Infectious Diseases Society of America 2010; Venter et al. 2017; Dahal and Chaudhary 2018) (**Figure 1.3**).

Currently, approximately 20% of worldwide deaths are related to infectious diseases, despite a 36% increase in antibiotic usage (Martens and Demain 2017; Laxminarayan et al. 2016). Therefore, in 2017 the World Health Organization (WHO) released a global priority list of anti-microbial resistant bacteria in order to help scientists prioritize their research to develop alternative treatments. This list includes multiple drug resistance (MDR) *Pseudomonas aeruginosa*, *Enterobacteriaceae*, *Salmonella* and *Shigella* (WHO Report 2017).

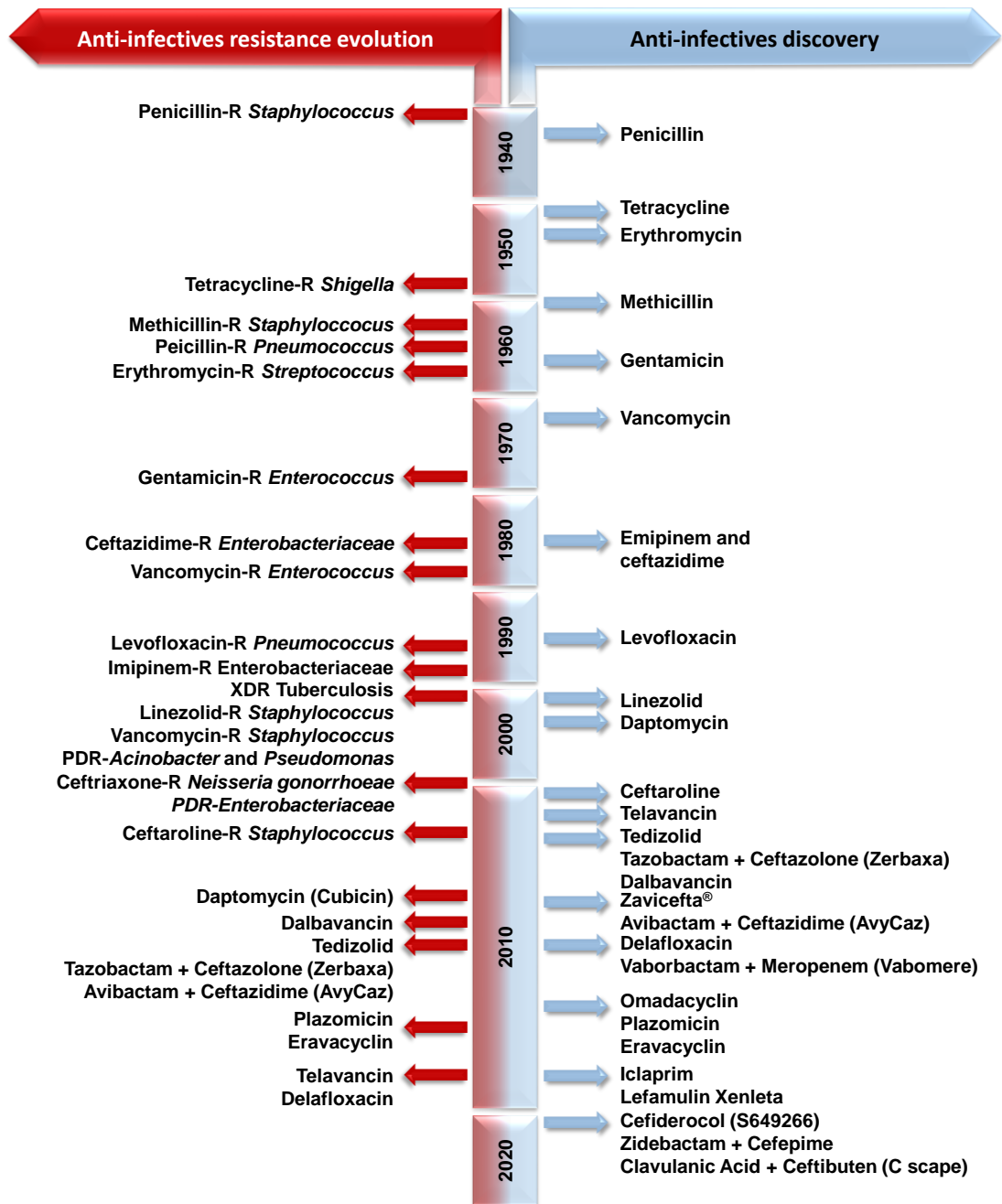


Figure 1.3. A history of anti-infective discovery and corresponding evolution of bacterial-resistance

Timeline illustrating the history of antibiotics discovery since 1940 in comparison to the appearance of different bacterial resistance over time. Figure adapted from (amr-bioMérieux 2019).

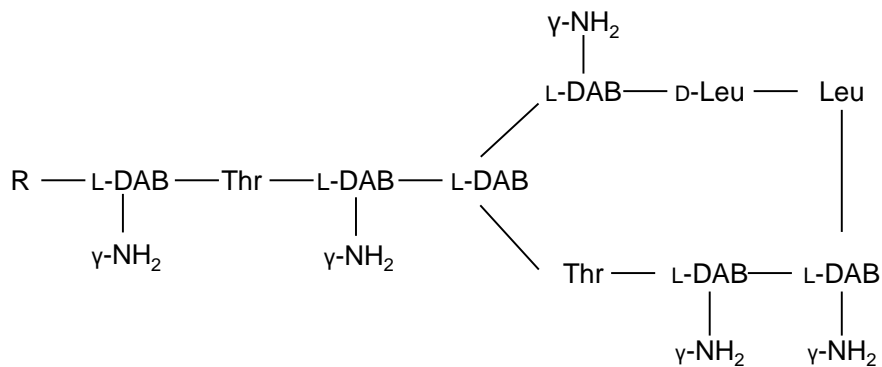
The Polymyxin class of anti-infectives, and in particular colistin, a polypeptide anti-infective discovered in the late 1950s, initially fell out of favor but are now being increasingly used as a last resort treatment Gram negative for MDR

infections. After the discovery of colistin and its immediate use in the clinic, several toxicity cases were reported (Koch-Weser 1970). However, due to the lack of alternative treatments for such infections at that time, colistin was considered as the only choice despite the lack of a proper understanding of its pharmacokinetics and pharmacodynamics properties. Shortly after the emergence of aminoglycosides (which exhibited a lower toxicity compared to colistin) in the early 1980s, the use of polymyxins was gradually phased out (Li et al. 2006).

Colistin, with a molecular weight of 1750 Da, consists of a cationic heptapeptide ring linked to a tripeptide side chain, conferring hydrophilic properties on the molecule. In addition, the side chain is coupled through an α -amide linkage to a fatty acid chain, functioning as a hydrophobic tail (Falagas and Kasiakou 2005). Colistin is furthermore a multicomponent anti-infective, composed mainly of Colistin A and B which differ in the length of their fatty acid tails (6-methyloctanoic acid in colistin A and 6-methylheptanoic acid in colistin B) (Li et al. 2005). As a bactericidal agent, it interacts with lipopolysaccharide (LPS) molecules mainly Lipid A of the Gram-negative bacterial membrane through electrostatic interactions (**Figure 1.4**). This interaction leads to a displacement of the cations Mg^{+2} and Ca^{+2} which disturbs the outer membrane, leading to a leakage of the cell contents and subsequently cell death (Biswas et al. 2012). Commercially, colistin is available as colistin sulfate and colistin methanesulfonate (CMS). The latter is a prodrug of colistin and the more commonly used form, due to its lower toxicity compared to colistin sulfate. It is used for parenteral administration or as a nebulized formulation for pulmonary infections (Gurjar 2015; Landersdorfer et al. 2017; Yapa et al. 2013). Colistin sulfate is only administered topically for skin infections, or in very limited way orally for bowel decontamination, due to its low bioavailability (Yahav et al. 2012; Falagas and Kasiakou 2005). Several studies have been performed in recent years to understand and optimize the dosage of colistin and investigate in a detailed manner its pharmacokinetics and pharmacodynamics properties in healthy as well as in ill patients (Karaiskos et al. 2015; Rao et al. 2014). The dosage of CMS intravenously recommended by the FDA is 2.5 to 5 mg CBA/kg (colistin base activity), corresponding to 31250 to 62500 International Unit (IU)/kg per day divided into 2 to 4 equal doses, for an

individual with normal creatinine clearance (≥ 80 mL/min). In contrast, the European Medicines Agency (EMA) approved dose per day is 9 million IU (approximately 300 mg CBA) (Nation et al. 2016). However, approximately 30% of CMS is converted to colistin while most of it is eliminated in urine – this makes treatment using CMS less efficient in terms of colistin dose after conversion, but less harmful compared to colistin in terms of toxicity (Jacobs et al. 2016).

To improve the use of colistin for infection therapy via a range of administration routes, several strategies have been explored, such as using nanoparticulate delivery systems. These systems have shown to play a major role in improving the efficacy of different drugs by increasing their concentration at the site of action and extending their half-life to achieve an optimal effect at the site of action. The improvement of drug efficacy is also due to the enhanced permeation using nanocarriers especially for hydrophilic drugs such as colistin (Mohammed et al. 2016; Salama and Aburahma 2016).

a

Colistin A → R = (+) 6-methyloctanoic acid
Colistin B → R = 6-methylheptanoic acid

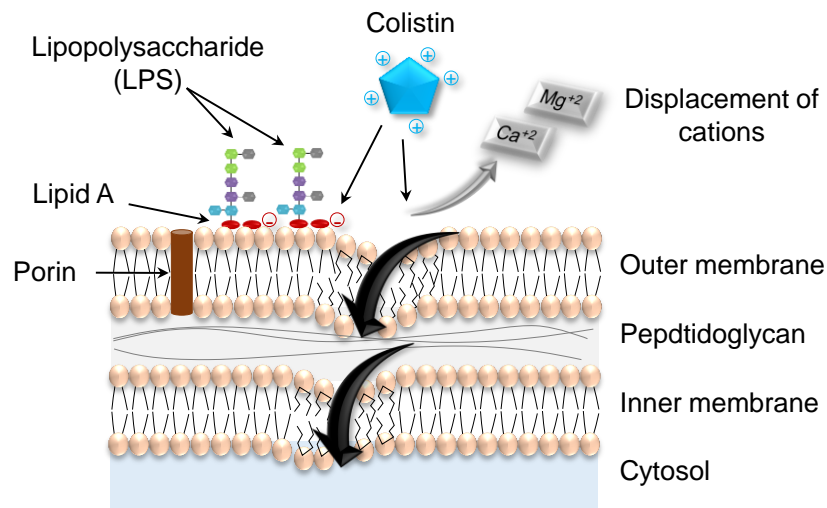
b

Figure 1.4. Colistin structure and mechanism of action

(a) Chemical structure of colistin, which consists of D-Leucine, L-threonine and L- α - γ -diaminobutyric acid. (b) Colistin mechanism of action indicating the interaction of positively charged colistin amino acids with Lipid A of LPS which displaces cations leading to disruption of the membrane and cell death. Figure adapted from (Bialvaei and Samadi K. H. 2015).

1.3 Oral delivery

Oral administration of drugs remains the most preferred route due to its simplicity and high patient compliance, as it offers a high degree of convenience in terms of self-medication, flexibility especially for chronic conditions. This route is also of interest for economic reasons as it does not require sterile conditions and complex production procedures, both of which can inflate manufacturing costs. Oral administration is also of interest due to physiological reasons. The gastrointestinal (GI) tract has an extensive surface area of 180-300 m², allowing for a large drug absorption capability through diverse cell types (Ensign et al. 2012; Hunter et al. 2012). The GI tract contains epithelial cells, namely enterocytes, which are largely responsible for the absorption of nutrients and/or drugs. Other cells may be involved in the absorption process as well such as goblet cells, Paneth cells and Microfold (M) cells associated with Peyer's patches, which transport antigens through dendritic cells (DCs) (Pawar et al. 2014; Pridgen et al. 2015). However, various hydrophilic and hydrophobic drugs such as aminoglycosides and polyene anti-infectives exhibit a poor bioavailability following oral administration as a result of physicochemical and/or biopharmaceutical limitations including solubility, stability and/or permeability problems (Leo et al. 2010; Thornton and Wasan 2009; Hamman et al. 2005).

Several studies have proven that the use of nanocarriers can alter the stability, permeability and solubility of many drugs and therefore improve their bioavailability following oral delivery (Ross et al. 2004; Smart et al. 2014). However, the preclinical development of such nanoparticulate systems requires specific design considerations for each region of the GI tract to ensure better drug absorption and less side effects (Pandey and Khuller 2007; Liu et al. 2018; Gao et al. 2013).

- **Gastrointestinal tract environment**

The complexity of the GI tract is characterized by the presence of enzymes and varying environmental pH, as well as numerous chemical and physical barriers. This represents a significant challenge for the successful delivery not only of drugs and biologics, but also for sophisticated nanomedicines – in particular lipid-

based nanoparticulate systems, such as liposomes (liposomes will be described further in Section 1.4) (Garg et al. 2014; Lipp 2013). Following oral administration, nanocarriers encounter various conditions in the GI tract. As a first obstacle, the pH within the stomach ranges from 1 to 3 and can increase to 5 in the presence of food. From the pyloric region of the stomach to the ileum in the small intestine, the pH shifts to a basic environment ranging from 5.7 to 7.7. However, pH values decrease in the cecum again to a value of approximately 6, before increasing gradually to a value of 7 within the colon. This acidic environment and variations of pH throughout the GI tract disrupt the majority of nanoparticulate structures and lead to their instability and leakage of their payload. In addition to pH considerations, a variety of enzymes and molecules are present at each level (He et al. 2019). Gastric fluids contains lipases and proteases, while at the small intestine level, the duodenum contains bile salts and various enzymes including trypsin, amylase and lipase. Furthermore, the small intestine is rich in a variety of pancreatic enzymes, namely pancreatin, peptidases, lipases and maltase. This extremely acidic and enzymatically harsh habitat can affect the stability of lipid-based nanocarriers such as liposomes as well as their payload before they even reach the cellular level of the GI tract. Majority of liposomal formulations following their incubation for 2 h with biorelevant media, show colloidal deformation such as irregular shapes and damaged lipid bilayers. Moreover, presence of bile salts and lipases induce hydrolysis of liposomal phospholipids in particular lipids with lower transition temperature that lead to disruption of liposomes structure (Liu et al. 2015; Tian et al. 2016; He et al. 2019). At the cellular level, the mucus layer lining the surface of the GI tract plays a major role in determination of the absorption of orally administrated drugs. The epithelial cells underlying this mucus layer are additionally connected by tight junctions which acts as an effective barrier against absorption of macromolecules and fluids, allowing these cells to act as the gatekeepers of the GI tract (**Figure 1.5**) (Choonara et al. 2014; Nguyen et al. 2016; Raza et al. 2019).

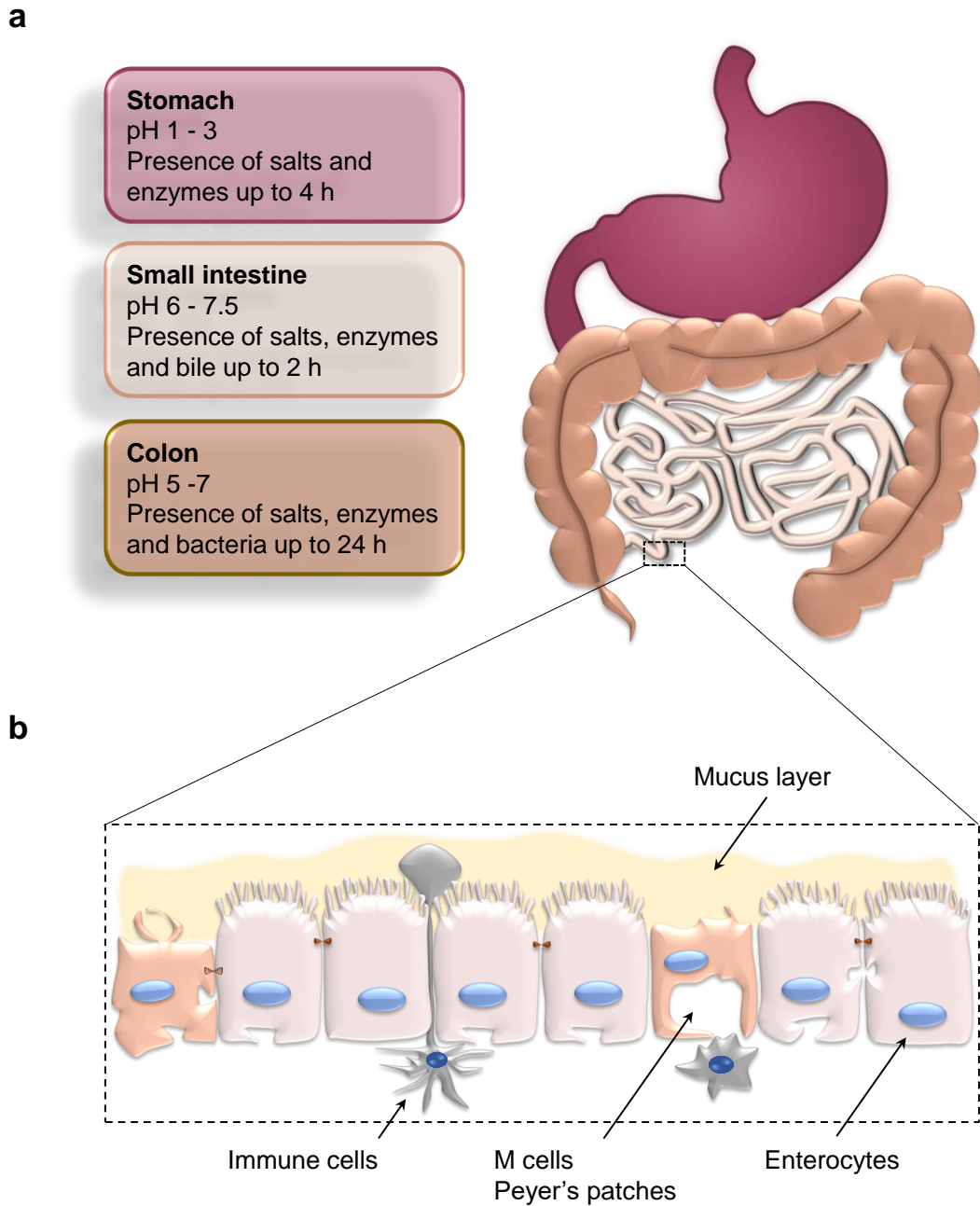


Figure 1.5. Gastrointestinal tract challenges for oral delivery

(a) Schematic representation illustrating gastrointestinal environment including pH and different compositions of fluid in the stomach, small and large intestine. (b) Zoom in view of the small intestine illustrating chemical and physical barriers including mucus layer and different cell types such as enterocytes, M cells bound to Peyer's patches and the underlying immune cells. Figure adapted from (Truong-Le et al. 2015).

Despite these challenges, considerable efforts have been and are still currently focused on improving the ability of various nanocarriers (including liposomes) to withstand these harsh environmental conditions and counter the highly protective cellular barriers. The stability of these carriers in order to provide continuous cargo protection is of particular concern, as an ultimate means to overcome the intestinal biological barrier and deliver the incorporated drug to its site of action.

1.4 Liposomes as a delivery system

Over 50 years ago, the British biophysicist Alec Bangham described liposomes for the first time (Bangham et al. 1965). The discovery was a result of his observation that phospholipids dispersed in water form vesicles which are structurally and functionally similar to cell membranes, enclosing two compartments; lipid bilayer and an aqueous cavity (**Figure 1.6**) (Düzgüneş and Gregoriadis 2005). Since then, liposomes have progressed from being a biophysical phenomenon to a successful delivery system, and widely used for several applications (Jesorka and Orwar 2008; Bulbake et al. 2017).

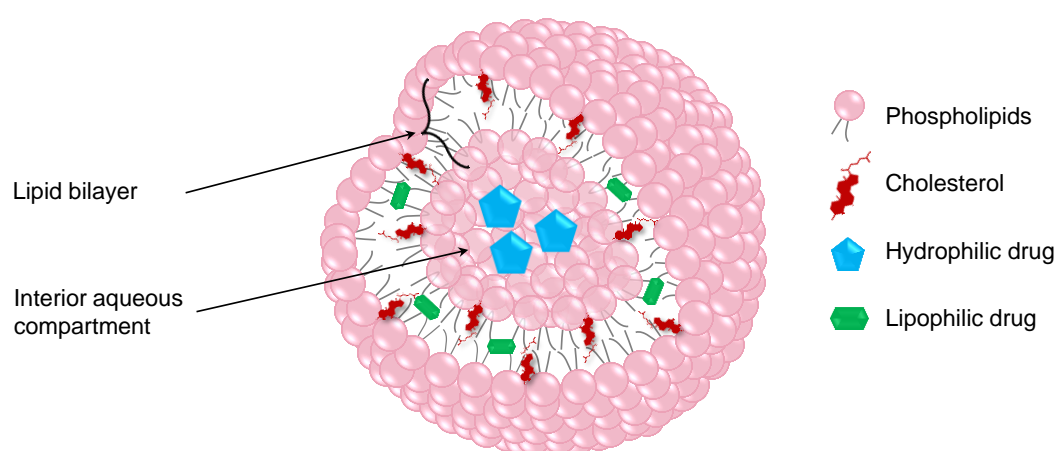


Figure 1.6. Liposomal structure

Illustration of unilamellar liposome, characterized by a spherical-shaped lipid bilayer made from phospholipids and cholesterol, in which hydrophobic drugs are incorporated. Lipid bilayer enclose an aqueous compartment in which hydrophilic drugs can be encapsulated. Figure adapted from (Talegaonkar et al. 2006).

Since 1995 in particular, tremendous progress in liposomal technology has resulted in the market approval of numerous liposomal formulations such as

Doxil[®] (100 nm stealth liposomes encapsulating doxorubicin hydrochloride) (Barenholz 2012), and AmBisome[®] (Amphotericin B encapsulated in liposomes of 70 nm size) (Adler-Moore and Proffitt 2002). Despite the appearance of several pharmaceutical carriers over the years, the interest in liposomes remains high – approximately 5000 articles concerned with various applications of liposomes have been published in the last 5 years, equating to approximately 3 articles per day (statistics from Springer Link). While various applications have been investigated, liposomes have mostly been employed to date as a delivery system for pharmaceuticals (Karmali and Chaudhuri 2007; Sercombe et al. 2015), as components of a membrane model (Mouritsen 2011), or as chemical micro-reactors (Lemièrre et al. 2015). Such studies have led to major breakthroughs, which have driven the rapid development of liposomes as pharmaceutical therapeutics over the last 15 years. New preparation methods and formulation approaches have further been developed in order to enhance their usage (Samad et al. 2007), including introduction of various amphiphilic components into the liposomal bilayer to increase their blood circulation half-life (e.g. using stealth moieties). Interaction of conventional liposomes following their administration into the circulation with proteins has traditionally resulted in poor liposomal stability and high clearance rate. By modulating the physical characteristics of liposomes such as their size and charge, coating of liposomes with a neutral water soluble polymer e.g. polyethylene glycol (PEG) confers the ability to extend their circulation time and evade opsonization (Pasut et al. 2015; van Slooten et al. 2001; Nag and Awasthi 2013). Another strategy employed to develop liposomes with better penetrating capabilities for topical applications, is the addition of single-chain surfactants. These molecules act as membrane modifiers causing destabilization of liposomal lipid bilayer, resulting in an increased liposome deformability and an increased capacity to squeeze between skin compartments (Elsayed et al. 2006; Hussain et al. 2016; Karande and Mitragotri 2009). Interestingly, although extensive studies of liposome applications have been carried out, few studies have shown that liposomes can be employed for the oral delivery of anti-infectives (and especially hydrophilic anti-infective molecules). The instability of these lipid-based nanoparticulate systems once exposed to different aspects of the gastrointestinal (GI) environment presents a major

challenge that often ultimately to low absorption of the encapsulated drug. (Wu et al. 2015).

1.4.1 Liposome modulation to improve stability

Modification of liposomal compositions and/or surface properties has emerged as a trend to change the fate of liposomes following their oral administration and overcome the aforementioned GI-related challenges (**Figure 1.7**).

- **Lipid composition**

Conventional liposomes consist of phospholipids and most commonly cholesterol, with similarities to cellular membranes. The phase transition temperature of lipids – defined as the temperature required to induce a physical state change from fully extended and well packed hydrocarbons chains, known as the crystalline gel state, to a disordered fluidic state known as the liquid crystalline state (Jacobson and Papahadjopoulos 1975) – plays a major role in liposome stability. This parameter is influenced by various factors including fatty acid chain length and degree of saturation, as well as head group type and/or charge. Incorporation of long alkyl chain phospholipids into liposomal compositions reinforces van der Waals interactions, leading to a greater energy requirement for disruption of the liposomal closely packed bilayer and therefore, increases the phase transition temperature (T_m) above 37 °C. On the other hand, presence of unsaturated bond in the alkyl chain induces a steric hindrance that increases distances between the molecules and prohibits the closed packaging of the lipid bilayer. This lead to reduced chain-to-chain interactions and therefore rendering the liposomal membrane less stable (Ali et al. 2013; Briuglia et al. 2015). Additionally, incorporation of cholesterol at a specific molar ratio percentage (~ 30%) into the bilayer leads to a condensing action. This has been shown to improve liposomal integrity by mediating phospholipid hydrophobic chain alignment, enabling an orderly behavior of lipid alkyl chains (Parmentier et al. 2012; Briuglia et al. 2015; Róg and Pasenkiewicz-Gierula 2001).

Liposomes containing specific lipids or cholesterol analogues are also capable of serving as an adaptable system for the delivery of poorly permeable or unstable drugs (Muramatsu et al. 1996). Parmentier and his colleagues showed that

liposomes containing dipalmitoyl phosphatidylcholine (DPPC) and tetraether lipids derived from *Sulfolobus acidocaldarius* improved the bioavailability of the encapsulated octapeptide octreotide after oral administration in rats by approximately 4 fold using different types of tetraether lipid derivatives (Parmentier et al. 2011). Another study revealed that substitution of cholesterol with plant-derived sterols such as ergosterol resulted in the formation of liposomes capable of protecting insulin against GI tract degradation, and induced a significant hypoglycemic effect in rats (Cui et al. 2015). Several bile salts such as sodium taurocholate and sodium deoxycholate have also been incorporated into liposomes for the delivery of antigens (Shukla et al. 2008; Aburahma 2016), poorly soluble small drug molecules (Aburahma 2016; Guan et al. 2011) and macromolecules (Niu et al. 2012; Niu et al. 2011) . Although the underlying mechanism by which bile salt incorporation into liposomes improves oral drug bioavailability has not been completely clarified, offsetting the degrading potential of endogenous bile salts present in GI tract could be the main drive for this enhancement (He et al. 2019).

- **Surface coating**

As another approach to overcome the harsh conditions of the GI tract, coating of liposomal surfaces with various polymers has emerged. In early development stages, enteric polymers such as the Eudragits were utilized to protect liposomes in the acidic environment of stomach (Hosny et al. 2013). However, these Eudragit-coated liposomes could not sustain the destructive effect of bile salts (Barea et al. 2010; Barea et al. 2012). Various polysaccharides have also been employed as coating materials for liposomes, including O-palmitoylpullulan (Carafa et al. 2006; Lee et al. 2005), pectin (Smistad et al. 2012; Willats et al. 2006) and chitosan (Alshraim et al. 2019; Nguyen et al. 2014; Venkatesan and Vyas 2000). Among these various coating materials, charged polymers have shown greater achievements in terms of liposomes protection as well as interaction with cell membranes. Chitosan as a cationic polymer ensures an optimal coating of negatively charged liposomes and therefore, is able to provide an optimal shield against GI tract acidity and enzymes. Additional to the aforementioned coating materials, polyelectrolytes have emerged as innovative

nanocarriers in drug delivery – in particular, oral delivery of proteins (Dwivedi et al. 2010; Mohanraj et al. 2010) and some drugs (Jain and Kumar et al. 2012; Jain and Patil et al. 2012; Li et al. 2012). As an example of this strategy, a layer by layer approach was used in order to coat doxorubicin-loaded liposomes, consisting of a deposition of the anionic poly(acrylic acid) followed by the cationic polyallyl amine hydrochloride. This led to the formation of stable coated vesicles termed 'layersomes' (Jain and Kumar et al. 2012; Jain and Patil et al. 2012).

- **Interior thickening**

The colloidal stability of liposomes may also be modulated by increasing the size of the interior aqueous compartment. This alteration can be achieved by modification of the interior compartment viscosity, or by incorporation of hydrogel beads (Kazakov 2016; Miguel et al. 1995). Liposomes containing charged and cross-linked polysaccharides within their central cores have also been found to be stable carriers for proteins (Hoegen 2001; Miguel et al. 1995). Another study showed that incorporation of polymerized PEG–dimethacrylate to the aqueous core of liposomes consisting of soybean PC and cholesterol led to an improvement of their structural properties (Petalito et al. 2014).

- **Other approaches**

Filtration of prepared liposomes through glass filters coated with lipid bilayers, as performed by Ebato and his colleagues, was shown to result in a considerable increase in the ability of encapsulated salmon calcitonin to decrease calcium levels in blood, as compared to calcitonin incorporated within conventional liposomes (Ebato et al. 2003). An improvement of the hypoglycemic effect was also achieved using similar strategy by Katayama and his colleagues (Katayama et al. 2003). In another study, egg phosphatidylcholine/cholesterol (PC/CHOL) liposomes were stabilized by adding gelatin as a thickening platform in which liposomes were embedded (Pantze et al. 2014). This system was employed as an optimal dosage form for the controlled release of highly water soluble macromolecules.

1.4.2 Liposome modulation to improve permeability

- **Mucoadhesives**

Coating of liposomes with mucoadhesive-acting materials such as cationic polymers has shown to result in an increase in the absorption of either liposome-associated payloads, or the payload alone. The positive polymeric charge increases the possibility of liposome interaction with the negatively charged mucus layer of the small intestine, therefore slowing liposome clearance. Liposomes coated with various chitosan derivatives have been reported to show a more prolonged efficacy compared to un-coated vesicles (Manconi et al. 2010; Sugihara et al. 2012). However, the molecular weight of chitosan has a great impact on the degree of mucoadhesion and thereby influences the *in vivo* efficacy of the delivery system (Thongborisute et al. 2006). Coating of liposomes with PEG showed also an extended penetrating effect in the GI tract due to the ability of PEG to penetrate deeply into mucosal barrier, leading to an enhanced uptake of liposomes (Minato et al. 2003).

- **Bio-enhancers**

Incorporation of oral bio-enhancers such as cetylpyridinium chloride, stearylamine and cholylsarcosine into liposomes has also been found as an effective strategy to orally deliver hydrophilic molecules. Beside their role in increasing the oral absorption, without exhibiting any typical drug activity, these bio-enhancers are able to inhibit degradation in the GI tract by affecting e. g. the efflux pumps and some metabolic enzymes (Kesarwani and Gupta 2013). Parmentier and his colleagues investigated the impact of various bio-enhancers with different properties on the oral absorption of fluorescein isothiocyanate-dextran, by assessing their permeation capacity and cytotoxicity (Parmentier et al. 2010). The study was conducted *in vitro* using Caco-2 monolayers as a GI tract model, with results showing that each of the investigated bio-enhancers (when used at a specific percentage) enhanced permeation of the payload. A potential shortcoming of this study however is that non-cellular aspects of the GI tract, namely the intestinal fluids and the mucus layer, were not represented. Liposomes containing surfactants such as sodium glycocholate have been found

to have a greater GI stability, as mentioned above; inclusion of sodium glycocholate within liposomes has also proven to significantly enhance their permeation through the intestinal barrier (Guan et al. 2011). Non-ionic surfactants such as Tween 80 have further been incorporated into liposomes containing PC and cholesterol to form elastic vesicles encapsulating catechin. The produced liposomes showed an optimal stability in simulated intestinal fluids and greater accumulation of the drug at the target site compared to the control (Huang et al. 2011).

- **Muco-penetrators**

As an example of muco-penetrating systems, thiomers-coated liposomes were formulated by Gradauer and her group, using the modified chitosan derivative chitosan–thioglycolic acid further conjugated with 6, 6'-dithionicotinamide, resulting in a chitosan–thioglycolic acid 6-mercaptonicotinamide-conjugate. Owing to the ability to resist degradation, these liposomes exhibited a potential to form disulfide bonds with the mucus layer and thereby enhanced the permeation of salmon calcitonin across the mucosal barrier in rats (Gradauer et al. 2013). Pluronic F127, a synthetic tri-block copolymer of poly(ethylene oxide)-poly(propylene oxide)-poly (ethylene oxide), was found to improve intestinal mucus penetration of various payloads encapsulated within liposomes and mediate their cellular uptake after oral administration (Li, X. et al. 2011; Zhu et al. 2013).

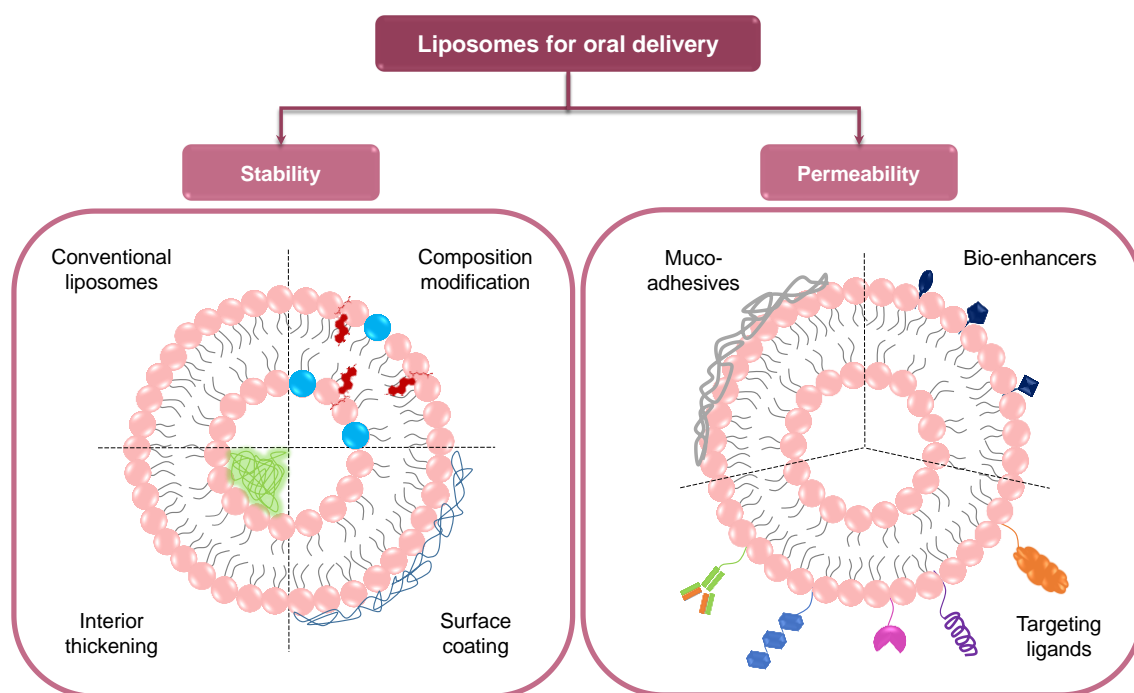


Figure 1.7. Strategies for the oral delivery of liposomes

Scheme illustrating different strategies to enhance liposomal stability in order to withstand challenges associated with the GI tract environment. These strategies include modifying the lipid composition, coating of the liposomal surface or increasing the innermost bilayer leaflet of the liposomes (left panel). The right panel demonstrates possibilities to enable and/or improve the trafficking of liposomes through the mucosal barrier including the use of mucoadhesive agents, incorporation of bio-enhancers or insertion of specific targeting moieties such as antibodies, sugars or proteins. Figure adapted from (He et al. 2019).

- **Invasive moieties for active targeting**

The progress in nanotechnology research in recent years has resulted in different strategies to further optimize nanoparticulate delivery systems such as liposomes to overcome their lack of specificity and insufficient delivery of the payload. Several parameters may play a role and have an effect on their behavior once applied either in *in vitro* simple cellular setups, or within complicated *ex/in vivo* systems. Size, shape and surface charge, as well as nanocarrier composition can determine their delivery pathway and affect their function, with the impact of modulating composition on stability and permeability having been discussed above. Functionalization of nanocarrier surfaces has further emerged as an

additional design step, aimed at the fabrication of more sophisticated nanocarriers able to be directed to particular target sites and manipulated with respect to their cell interactions and uptake. Diverse ligands and moieties including vitamins, synthetic and natural compounds as well as peptides have been used to achieve active targeting of delivery systems towards cancer cells, increase their circulation life, or improve their internalization into various eukaryotic cells. Since most lipids and proteins within the mucosal lining of the intestine are glycosylated, lectins, a family of proteins able to bind mono- and oligo-saccharides with high affinity, emerged as possible targeting moieties in 1988. Although lectins were identified much earlier, in 1860, when Stillmark described in his thesis the agglutination phenomenon of ricin (Bies et al. 2004), it was not until more than 100 years later that Woodley described lectins as promising moieties for GI tract targeting (Naisbett and Woodley 1994). Lehr and colleagues later demonstrated that tomato lectin-functionalized polystyrene microspheres were able to bind to enterocytes, however the presence of mucin was seen to reduce this interaction (Lehr et al. 1992). Since that time, discovery of various lectins from plant or animal origins as well as their usage has increased dramatically. Wheat germ agglutinin (WGA) was coupled to poly(lactide-co-glycolide) nanoparticles for delivery of anti-tuberculosis drugs in guinea pigs. Results showed a significant improve of rifampicin, isoniazid and pyrazinamide absorption, in which three doses were sufficient to eradicate mycobacterial colonies versus 45 doses of oral free drug (Sharma et al. 2004). Sashini and his co-authors described in their study on oral ulcerative lesions that liposomes with conjugated WGA and loaded with a β -lactam antibiotic were able to immediately bind to epithelial cells and ensure sustained and localized drug release (Wijetunge et al. 2018).

Since the penetration ability of the transactivator of transcription (Tat) peptide was demonstrated, cell-penetrating peptides (CPPs) – short peptides that facilitate cellular intake/uptake of various - have been widely used either conjugated to drug molecules as delivery systems (Kristensen et al. 2015; Morishita et al. 2007) or functionalized to nanocarrier surfaces as penetrating moieties (Torchilin et al. 2003). Penetration of insulin-labeled with fluorescein and conjugated to Tat was shown to be significantly enhanced compared to free

insulin, however the study was only conducted *in vitro* (Liang and Yang 2005). In another study, interferon- β was coupled to either oligoarginine or penetratin as cell-penetrating peptides, with an increase in the intestinal absorption noted only with penetratin (Kamei et al. 2008). Various studies have suggested an instability of these CPPs, due to relative susceptibility to peptidases and proteases in the GI tract. This lack of stability plays a major role in their limited usage to date for oral delivery (Khafagy and Morishita 2012).

An interesting, related approach has been employed recently, which is based on imitating natural strategies employed by some pathogenic agents to cross biological barriers in our bodies and establish a niche in order to replicate, disseminate and cause serious complications. Such pathogens use an arsenal of virulence factors which are expressed on their cell surface for a direct interaction with host cells, or are secreted either into the host cellular compartments. As a prominent example, internalins of *Listeria* (InIA, InIB) are located on the bacterial surface and mediate bacterial adhesion and internalization into various cell types. It has been shown that InIA interacts with E-cadherin receptors on epithelial cells and promotes the invasion of *Listeria* through the intestinal cell barrier of the GI tract. On the other hand, the combinations “InIB - HGF” (hepatocyte growth factor) and “InIB – gC1q-R” (complement receptor) lead to the internalization of *Listeria* into endothelial cells as well as hepatocytes. *Neisseria* spp. exhibit extracellular virulence proteins Opa and Opc that promote their binding to several receptors including CEACAMs (carcinoembryonic antigen-related cell adhesion molecules), as well as the integrins $\alpha_7\beta_3$ and $\alpha_5\beta_1$ via interaction with extracellular matrix membrane (ECM) proteins, which moderate its uptake by a variety of host cells. Moreover, *Yersinia* spp. exhibit several invasion proteins, with invasin (InvA) being one of the most well characterized. InvA promotes the internalization of *Yersinia* spp. into M cells of the intestinal barrier via interaction with β_1 integrin receptors. It has been shown that the last 197 amino acids C-terminal fragment of InvA is able to function as an efficient ligand during the invasion of *Yersinia* into epithelial cells (Dersch and Isberg 1999). Keeping in mind - the efficiency of the above mentioned pathogens to invade easily our cellular barriers- it could be beneficial to functionalize nanocarrier surfaces with these proteins, thereby simulating the mechanism of bacterial entry via their own invasive tools to achieve

maybe the same efficiency with our nanoparticulate delivery systems. Previous studies adopting this strategy have shown the promising aspect of using these bacterial invasive proteins to enhance the uptake of non-invasive pathogens (Haggar et al. 2003) as well as nanocarriers (Labouta et al. 2015; Menina et al. 2016). Liposomes functionalized with InvA497, a transmembrane protein of *Yersinia* species that plays a major role in the binding and entry of the pathogen into mammalian cells through interaction with β_1 integrin receptors, were used to facilitate the intracellular delivery of the poorly permeable anti-infective gentamicin. Treatment of HEP-2 cells infected with either *Yersinia pseudotuberculosis* or *S. enterica* showed that this formulation was able to reduce the infection load of both pathogens, indicating that such a strategy holds a great promise for the delivery of anti-infectives intracellularly (Lehr et al. 2016).

1.5 Extracellular adherence protein (Eap)

In the early 90s, different groups of scientists were able to independently identify and isolate from the wide *Staphylococcus aureus* repertoire of secreted molecules a protein named Eap. This protein has been found to play a major role in the pathogenicity of *S. aureus* not only by promoting adhesion to targeted surfaces but also by interfering with the host defense system (McGavin et al. 1993; Vogt et al. 1983; Harraghy et al. 2003). The structure was found to exhibit a modular architecture consisting of 4 to 6 tandem repeats of ~ 97 residue EAP domain. Depending on the bacterial strain, the molecular mass of Eap is around 50 – 70 kDa, and comprises four to six repeats linked with 9 – 12 residue regions of unknown structure. The biochemical characteristics of these domains have further not been well studied, which presents a major hurdle in understanding the full functionality of Eap (Hammel et al. 2007). Early investigations of Eap showed that this protein is able to bind to a wide array of plasma and ECM proteins, including fibrinogen, fibronectin and vitronectin as well as to pro-inflammatory cell surface receptors such as intracellular Adhesion Molecules 1 (ICAM-1) (Chavakis et al. 2002). Eap has also shown the capability to re-bind to *S. aureus* surfaces following secretion; this effect was investigated and proved by Hussain and colleagues by adding free Eap to *Staphylococcus* cultures or adding various types of pathogens to immobilized Eap (Hussain et al. 2002). The mechanism of

Eap binding to host/mammalian cell surfaces is still unclear, however Palma et al., suggested that Eap binding is due to non-specific interactions Eap-surface interactions, and a receptor-mediated process is unlikely (Palma et al. 1999). Adherence of Eap to eukaryotic cells has also been investigated using an *eap* mutant strain of *S. aureus* Newman. The study demonstrated a significant decrease of the internalized number of bacteria into fibroblasts and epithelial cells in comparison to the wild type. However, the internalization capacity was restored to some extent after addition of external Eap. Moreover, the addition of anti-Eap antibodies led to inhibition of the internalization process. This indicates the ability of Eap to bind not only to bacterial surfaces and proteins but also to eukaryotic cells, promoting the internalization of pathogens (Haggar et al. 2003). Eap adhesive properties demonstrate that this protein could be a promising candidate to promote the internalization of nanoparticulate delivery systems into eukaryotic cells. Microspheres and beads have previously been coated with Eap for functional determination, without therapeutic purpose (Joost et al. 2011); to the best of our our knowledge, the current study is the first to investigate the ability of Eap to mediate the internalization of nanocarriers for drug delivery.

2 Aim

The aim of the current study is to develop a stable nanocarrier capable of improving the cellular internalization of the poorly permeable colistin, as a strategy for combating hard-to-treat intracellular infections. Colistin, despite being an old anti-infective, it has gained attention due to its high efficacy against MDR bacteria. Moreover, the low intrinsic permeability and the possible gain in the safety profile which, could be achieved by employing liposomes as a delivery system were behind the motivation of using colistin as payload. The oral route is interesting not only due to patient compliance but also as a step-down therapy following intravenous administration in serious infections. However, from a delivery point of view, the oral route is highly challenging for liposomes, in which the release of colistin in the intestinal lumen should be minimized and high intracellular delivery should be achieved. In order to address the latter point, the uptake into non-phagocytic cells of the GI tract, a bio-invasive strategy, mimicking one of the bacterial pathways of internalization was utilized.

The main objectives of this thesis were as following:

- I. Formulation of liposomes loaded with colistin aimed to be achieved by formulating first unloaded liposomes with different compositions and subject them to colloidal stability studies. Selected formulations will be loaded further with different colistin concentrations in order to identify the optimal concentration which shows the highest entrapment efficiency.
- II. Challenge of colistin-loaded liposomes stability against various simulated media of the GI tract in order to evaluate its capacities to withstand its different conditions.
- III. Functionalization of liposomes with an invasive moiety as a strategy to improve the intracellular delivery of the nanoparticulate system. Different methods of coupling will be investigated. The invasive moiety was kindly provided by our collaboration partner Prof. Markus Bischoff from the Institute of Medical Microbiology and Hygiene (Institute of Infectious Medicine, Saarland University Hospital).

- IV. Assessment of the capacity of the system to facilitate the internalization of colistin to the interior of epithelial cells and achieve an intracellular eradication of the pathogen. A comparison between Eap and our previously investigated invasive moiety InvA497 will be performed to evaluate the efficiency of each system to internalize colistin-loaded liposomes. InvA497 was kindly provided by Prof. Rolf Müller's group (Microbial Natural Products group at the Helmholtz Institute for Pharmaceutical Research Saarland).

3 Materials and Methods

3.1 Materials

Table 1. Material used in this study

Material	Abbr.	Properties	Provider
1,2-Dipalmitoyl phosphatidylcholine (Lipoid E PC)	DPPC	-	Gift from Avanti Lipids (Alabama, USA)
1,2-distearoyl-sn-glycero-3-phosphocholine	DSPC	-	
1,2-Dipalmitoyl-sn-glycero-3-phosphoethanolamine-N-(lissamine rhodamine B sulfonyl) (ammonium salt)	Rh-DPPE	-	Avanti Polar Lipids (Ludwigshafen, Germany)
1,2-Dipalmitoyl-sn-glycero-3-phosphoethanolamine-N-(Glutaryl)(Sodium salt)	DPPE-GA	-	
Cholesterol	CHOL	≥ 99%	
N-Ethyl-N-(3-dimethylaminopropyl) carbodiimide hydro-chloride	EDC	≥ 99%	
Ammonium thiocyanate	NH ₄ SCN	≥ 97.5%	Sigma Aldrich (Steinheim, Germany)
Newborn calf serum (heat inactivated, sterile-filtered)	NCS		
Trypsin		0.5 g/L	
Chloroform	CHCl ₃	≥ 99.9%	
Colistin sulfate	Col	USP Grade	Adipogen AG (Liestal, Switzerland)
Potassium dihydrogen phosphate	KH ₂ PO ₄	-	
Ferric 3-chloride-hexahydrate	FeCl ₃ .6H ₂ O	-	Merck KGaA (Darmstadt, Germany)
Sodium hydroxide	NaOH	-	
Methanol	CH ₃ OH	≥ 99.9%	VWR Chemicals (Fontenay-sous-Bois, France)
Hydroxysuccinimide	NHS	≥ 99.0%	Carbolution Chemicals (St. Ingbert, Germany)
All other chemicals and solvents used were of an analytical grade.			

3.2 Liposomes preparation

Lipid film hydration method described previously by Bangham and his colleagues was used to prepare liposomes (Bangham et al. 1965). Briefly, DPPC and DSPC as main phospholipids were mixed either separately with cholesterol or as a combination of the two phospholipids together with cholesterol to form liposomes (**Table 2**). DPPE-GA was added to all formulations in a molar ratio of 0.2 (w/w) to facilitate the functionalization of these nanocarriers through their carboxylic groups. The mixtures were dissolved in chloroform: methanol (2:1 v/v) in round-bottomed flask. A 10 µg/ml of Rh-DPPE was added to label the liposomes for the imaging experiment (red fluorescence).

Table 2. Liposomes composition

Name	Composition	Molar Ratio
Lip-1	DPPC:DPPE-GA:CHOL	1:0.2:1
Lip-2	DSPC:DPPE-GA:CHOL	1:0.2:1
Lip-3	DPPC:DSPC:DPPE-GA:CHOL	1:1:0.2:1

Rotary evaporator (BUCHI Laboratory AG, Switzerland) set at 200 mbar, 120 rpm and equipped with a heating bath set at either 70° C for DPPC-containing liposomes or 75° C for DSPC-containing liposomes, was used to evaporate the solvent mixture for 1 h. A following evaporation step (40 mbar for 30 min) was used to ensure the complete evaporation of the organic solvent. The dry lipid film was hydrated with either phosphate buffer saline (PBS, pH 7.4) solution to prepare unloaded liposomes (Lip-1, Lip-2 and Lip-3) or with different concentrations of colistin from 1 mg/mL to 10 mg/mL in PBS to obtain colistin-loaded liposomes (Col-Lip-1, Col-Lip-2 and Col-Lip-3). The hydration step was performed by setting the rotation at 75 rpm and the heating bath at 50° C for DPPC-containing liposomes or 55° C for DSPC-containing liposomes for 1 h. The formed vesicles were then extruded 10 times through 200 nm polycarbonate membrane using LiposoFast LF-50 extruder (Avestin, Germany) (**Figure 3.1**) to obtain small unilamellar liposomes (SUV).

Centrifugal ultrafiltration was used to purify the liposomal suspensions and remove the non-encapsulated colistin. Briefly, liposomes were placed into Centrisart® tubes (Sartorius AG, Germany) equipped with a membrane of 300.000 MWCO and centrifuged two cycles at 3270 g and 4° C for 30 min each. After each cycle, the filtrate was collected to quantify the non-encapsulated colistin and fresh PBS was added to the liposomal suspension instead of the filtrate. Liposomes were stored afterwards at 4° C in glass scintillation vials.

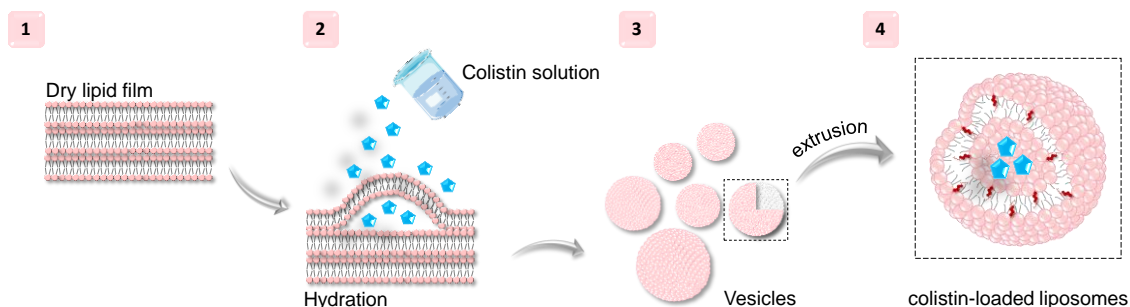


Figure 3.1. Liposomes preparation

Scheme illustrating liposomes preparation steps, (1) starting with a formation of dry lipid film by evaporating solvent mixture, which was used to dissolve different phospholipids and cholesterol (2) Evaporation step was followed by hydration of the dry lipid film with colistin solution for liposomes loaded with colistin or only PBS to prepare unloaded liposomes. The formation of multi-lamellar vesicles (3) was followed by an extrusion process (4) through 0.2 μm membrane to obtain small unilamellar colistin-loaded liposomes.

3.3 Characterization of liposomes

3.3.1 Colloidal characterization

Colloidal parameters of nanocarriers is an important factor which influences their stability, uptake and release of the payload at the target site. Therefore, liposomes were subjected to size, polydispersity index (PDI) and ζ -Potential measurements.

Hydrodynamic diameter and size distribution of liposomes were measured using dynamic light scattering technique (DLS) (Nano Zetasizer, Malvern Instruments,

Germany). DLS measurement is based on the Brownian motion of the vesicles in a fluid, a transfer of energy is induced due to the collision of particles with the fluid molecules leading to particles movement. Direction of the laser towards the sample, scatters the light due to particles movement and invoke fluctuations in intensity signal over time which is used then to determine the size using the Stokes-Einstein equation (Stetefeld et al. 2016). Briefly, purified liposomal samples were diluted 1:1000 in PBS and then measured at 25° C using a refractive index of 1.33 (Dorrington et al. 2018).

Laser Doppler Micro-electrophoresis technique on the other hand was applied to determine the surface charge of liposomes. The principle of this technique is based on the induction of an electric field to the liposomal suspension, in which the direction and particles velocity is proportional to their electrical voltage and therefore their charge. Measurements were conducted after a dilution of 1:1000 of the liposomal samples with PBS in folded capillary cell using Nano Zetasizer.

3.3.2 Colistin quantification

An ultimate 3000 high performance liquid chromatography (HPLC) system from Dionex equipped with diode array detector, a column oven, an autosampler and a pump (Thermo Scientific, Germany) was used to quantify colistin. Briefly, the detection of colistin two main peaks (Colistin A and B) was achieved using a method previously described by Bai and his colleagues with some modifications (Bai et al. 2011). A mobile phase composed of acetonitrile: 0.1% trifluoroacetic acid (TFA) was used to elute colistin through LiChrospher® 100, RP-18 (5 µm), 125 x4 column (Merck KGaA, Germany) in a gradient mode from 20:80 (v/v) to 50:50 (v/v) during 10 min. The elution in a flow rate of 1 mL/min was followed by 5 min washing step with 50:50 (v/v) acetonitrile: 0.1% TFA for 2 min and then increased gradually back to 20:80 (v/v). A 100 µL volume was used to analyze samples and the column oven was set at 30° C during all the analysis. A stock solution of 500 µg/mL of colistin was prepared by dissolving colistin in 0.1% TFA solution, then diluted 1:5 with acetonitrile. Standards from 10 µg/mL to 100 µg/mL were prepared accordingly, and then analyzed in HPLC vials.

Colistin standards were prepared each time freshly to validate the method in which precision, specificity, linearity, accuracy, detection limit and quantification limit were determined. Standards aliquots were also stored at 4°C for intra- and inter-day validation analysis.

Samples were prepared by diluting purified liposomes 3:7 (v/v) in same eluent used to prepare standards (0.1% TFA: Acetonitrile 20:80 v/v) and analyzed in triplicates. The amount of colistin was determined by plotting the sum of the area under the curve (AUC) of both colistin peaks A and B detected at a wavelength of 210 nm into the equation.

3.3.3 Phospholipids quantification

Phospholipids content was quantified utilizing a colorimetric assay previously described by Stewart (Stewart 1980). The assay is based on the measurement of the optical density of phospholipids - ammonium ferrothiocyanate complex at 485 nm. The assay reagent was prepared by dissolving $\text{FeCl}_3 \cdot 6\text{H}_2\text{O}$ and NH_4SCN in water. Standards (5, 10, 20, 30, 40 and 50 $\mu\text{g/mL}$) were prepared from 0.1 mg/mL DPPC or DSPC stock solutions in chloroform, each at a final volume of 2 mL in screw cap round-bottomed glass tubes. A 100 μL of liposomes (1:10 in PBS) was mixed with 1.9 mL chloroform and then 2 mL of ferrothiocyanate reagent was added to the samples and to the standards. Samples as well as standards were vortexed for 20 seconds and then centrifuged at 300 g for 10 minutes to obtain two phases in which the lower phase containing liposomal lipids dissolved in chloroform (total amount). Lipids-chloroform mixture transferred to a glass cuvette was subjected to an optical density measurement at 485 nm. The amount of phospholipids in liposomes was determined by plotting samples values in the corresponding calibration curve equation.

3.3.4 Cholesterol quantification

Cholesterol was quantified using the above described HPLC system (**Section 3.3.2**), using a method described previously by Simonzadeh (Simonzadeh 2009). A mobile phase composed of acetonitrile: methanol (70:30 v/v) with a flow rate of 2 mL/min was used to elute the samples with an injection

volume of 100 μL in an isocratic mode. Cholesterol's peak was detected at a wavelength of 210 nm after 15 min analysis time. Standards were prepared from a stock solution of 200 $\mu\text{g}/\text{mL}$ of cholesterol in 50:50 (v/v) acetonitrile: methanol/ethyl acetate (1/1 v/v). Whereas, samples were prepared by mixing 400 μL of liposomes (1:10 in PBS) with 1 mL of acetonitrile: methanol/ethyl acetate mixture. The amount of cholesterol in each sample was determined by comparing their absorbance values to that of standards.

3.3.5 Entrapment efficiency and loading capacity

The encapsulation efficiency of colistin-loaded liposomes was calculated using the **Equation 1** (Papadimitriou and Bikiaris 2009) after direct determination of the amount of encapsulated colistin using HPLC as described previously in **Section 3.3.2**.

Equation 1: Entrapment efficiency

$$EE \% = \frac{\text{Amount of encapsulated drug}}{\text{Amount of initial used drug}} \times 100$$

After the determination of the amount of all liposomal components including phospholipids, cholesterol and colistin, loading capacity was determined using **Equation 2** (Papadimitriou and Bikiaris 2009) as following:

Equation 2. Loading capacity

$$LC \% = \frac{\text{Amount of encapsulated drug}}{\text{Amount of all liposomal components}} \times 100$$

3.3.6 Thermal characterization

In order to determine the thermo-physical properties of liposomes mainly the transition temperature which could be an indicator of liposomal stability, differential scanning calorimetric technique (DSC) was performed (Bunjes and

Unruh, 2007). DSC is a direct thermo-analytical technique for determination of the enthalpy of biomolecules and nano-sized materials. This technique is based on the measurement of the thermo-dynamic properties of materials by determining the temperature and the heat flow associated with material transitions as a function of time and temperature (Demetzos, 2008), (Mabrey and Sturtevant, 1976). The basic principle underlying this technique is to compare the rate of heat flow to the sample and to an inert material which are heated or cooled at the same rate. Changes in samples' heat absorption induce change in the differential heat flow resulting in a peak. The area under the peak is proportional to the enthalpy change and its direction indicates the type of the thermal event either endothermic or exothermic.

Briefly, liposomes and gentamicin loaded liposomes were firstly frozen for 4 hours at -80°C and then placed on the freeze dryer (CHRIST Lyocube 4-8 LSC Freeze Dryer, Germany) to obtain a powdered form. Around 3 to 5 mg of Col-Lip-1, Col-Lip-2 and Col-Lip-3 were weighted in separated hermetic aluminum sample pans (PerkinElmer, USA) and covered with hermetic aluminum Lids (PerkinElmer, USA) and closed. Liposomes were subjected to a heating rate of 10°C/min in the 20 - 80°C using DSC 8000 (PerkinElmer, USA). The data were analyzed using Pyris - Instrument Managing Software (Version 11 PerkinElmer, USA)

3.4 Stability studies in biorelevant media

Liposomal suspensions were incubated with simulated media (1:10 v/v) in 24-well plate, three wells for each time point. The plates were incubated at 37° C for 5 hours at 180 rpm. At each time point, samples were collected and 100 µL was used for immediate colloidal properties measurements and the left was placed in Centrisart tubes for a purification step to remove the released colistin (as described previously in **Section 3.2**). Afterwards, samples were analyzed with HPLC to determine colistin content.

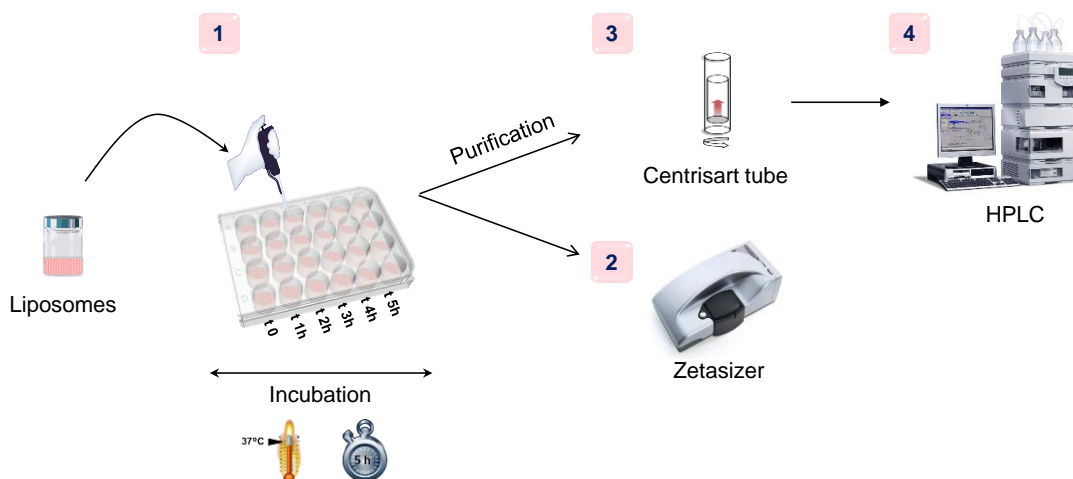


Figure 3.2. Stability study workflow

Liposomes were incubated in 24-well plate containing different media separately (1) for 5 h at 37° C at least 3 wells for each time point, afterwards Size, PDI and ζ -potential of collected samples were measured directly (2). Then samples were purified (3) to remove the amount of released colistin and then analyzed using HPLC to quantify colistin concentration (4).

3.4.1 Fasted state simulated gastric fluid (FaSSGF)

The gastric medium was prepared as described previously (Jantratid et al. 2008). Briefly, a lipid film was prepared by evaporating the organic solvent of 160 μ L phosphatidylcholine (0.125 μ M in chloroform) using a gentle nitrogen stream. Afterwards, a 43.01 mg of sodium taurocholate dissolved in 100 mL of HCL (0.02 M) pre-warmed to 37° C was added to hydrate the lipid film and form micelles. After mixing, the suspension was kept for stirring at 37° C overnight and protected from light. In the meanwhile, in another bottle 100 mg of pepsin and 1.999 g of sodium chloride were dissolved in 100 mL of pre-warmed HCL (0.02 M) and stirred overnight at 37° C as well. Afterwards, the contents of the two bottles were mixed and then 700 mL of pre-warmed HCL (0.02 M) was added. After mixing, the pH of the prepared medium was adjusted to 1.6 with HCL (1 M), and the volume to 1 L with Milli-Q water. The final concentrations of each component of the medium are shown on **Table 3**.

Table 3. Simulated media composition

Composition	FaSSGF ^{a)}	FaSSIF ^{b)} FaSSIF-Enz ^{c)}	FeSSIF ^{d)}
Sodium taurocholate (mM)	0.08	3	15
Phosphatidylcholine (mM)	0.02	0.75	3.75
Pepsin (mg/mL)	0.1	-	-
Sodium chloride (mM)	34.2	105.9	65.1
Oleic acid (mM)	-	-	5
Monoolein (mM)	-	-	2.5
Maleic acid (mM)	-	-	100
Sodium azide (mM)	-	-	3
Lipase (Pancreatin) (USP/mL)	-	600 ^{e)}	-
Ad. deionized water (mL)	1000	500	50
pH	1.6	6.5	6.5

^{a)}FaSSGF: fasted state simulated gastric fluid. ^{b)}FaSSIF: fasted state simulated intestinal fluid. ^{c)}FaSSIF-Enz: fasted state simulated intestinal fluid containing enzymes (pancreatin). ^{d)}FeSSIF: fed state simulated intestinal fluid. ^{e)}Pancreatin was added only in FeSSIF.

3.4.2 Fasted state simulated intestinal fluid (FaSSIF)

The simulated intestinal fluid in fasted state was prepared either without enzymes (FaSSIF) (Jantratid et al. 2008) or with enzymes (FaSSIF-Enz) (Sassene et al. 2014). A blank FaSSIF was prepared first by dissolving 0.348 g of NaOH, 3.438 g of NaH₂PO₄, and 6.186 g of NaCl in 1 L of Milli-Q water. Afterwards, the pH of

the buffer was adjusted to 6.5 and the volume to 1 L. Then, 1.65 g of sodium taurocholate was dissolved in 250 mL of blank FaSSIF and 5.9 mL of phosphatidylcholine (100 mg/mL in dichloromethane) was added. After mixing, the organic solvent was evaporated by placing the mixture on the rotary evaporator using a vacuum set at 250 mbar for 15 min followed by another 15 min at 100 mbar (water bath set at 40° C). After cooling, the volume of the mixture was adjusted to 1 L with blank FaSSIF. Simulated intestinal fluid-containing enzymes was prepared in a similar manner to FaSSIF, with the addition of an enzyme mixture to bile salts and phospholipids after the evaporation step. The suspension of enzymes was prepared by dissolving 7.48 g of porcine pancreatin in 37.4 mL of blank FaSSIF, and then centrifuged at 4° C, 4500 rpm for 7 min. The supernatant of the solution containing the enzymes was added then to the bile salts and phospholipids mixture to a final concentration of 600 U/mL of lipase in the simulated medium (**Figure 3.3**).

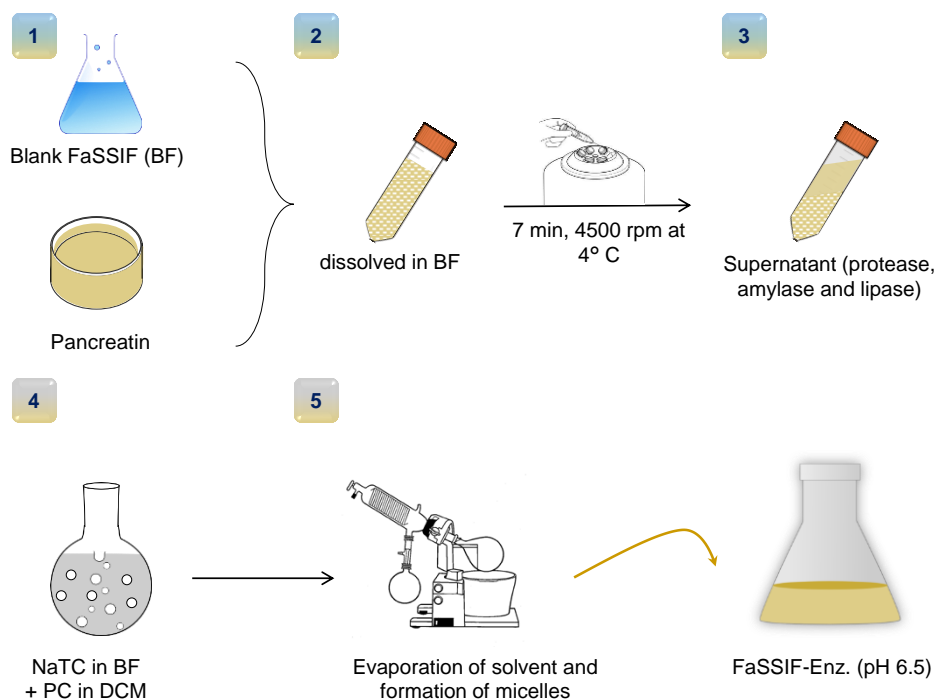


Figure 3.3. Scheme illustrating FaSSIF-enz preparation protocol

(1) Blank FaSSIF pre-prepared with different salts at pH 6.5 was used to dissolve pancreatin. (2) A centrifugation of pancreatin suspension at 4500 rpm and 4° c for 7 min was performed in order to extract the enzymes in supernatant and sediment all undesired components. (3) The supernatant containing enzymes

mixture was collected. (4) Sodium taurocholate (NaTC) dissolved in blank FaSSIF was mixed with phosphatidylcholine (PC) dissolved in dichloromethane (DCM). (5) Evaporation of the solvent lead to a formation clear suspension containing micelles, and then (6) enzymes mixture was added to NaTC/PC suspension to obtain FaSSIF-Enz.

3.4.3 Fed state simulated intestinal fluid (FeSSIF)

As described previously by Nielsen and his colleagues (Nielsen et al. 2013), FeSSIF was prepared by mixing 3 mL of phosphatidylcholine (125 mM) and 0.625 mL of oleic acid (800 mM) / mono-olein (400 mM) in blue-capped bottle. The organic solvent was evaporated with gentle nitrogen stream in order to form a dry lipid film. Afterwards, 20 mL of maleic acid (500 mM)/sodium azide (15 mM) and 26.04 mL of NaCl containing 0.8066 g of sodium taurocholate was added to hydrate the lipid film and form micelles in the suspension. A volume of 20 mL Milli-Q water was added and the bottle kept for stirring overnight at 37° C. The following day, the pH of the mixture was adjusted to 6.5 and the volume to 100 mL with Milli-Q water (**Figure 3.4**).

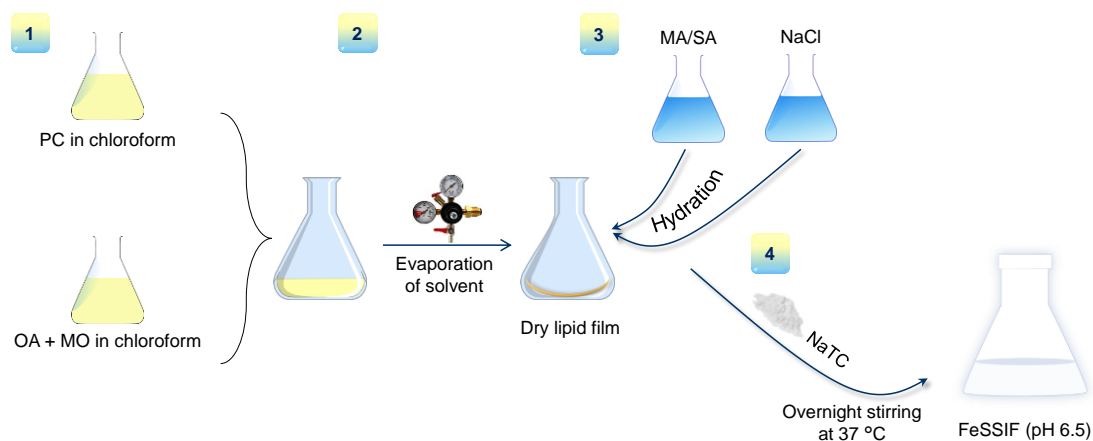


Figure 3.4. Scheme illustrating FeSSIF preparation protocol

(1) Phosphatidylcholine (PC) and mixture of oleic acid/monoolein (OA/MO) were dissolved in chloroform in separate Erlenmeyer flasks. (2) The dissolved lipid and fatty acids were mixed together and a nitrogen stream was used to evaporate the organic solvent resulting on lipid film. (3) Sodium chloride (NA) and oleic acid/sodium azide (OA/SA) solutions prepared in separate Erlenmeyer flasks

were added the lipid film for hydration. (4) Sodium taurocholate (NaTC) was added to the suspension and stirred overnight at 37° C to obtain FeSSIF with a pH of 6.5.

3.5 Liposomes functionalization

To enhance the internalization of liposomes into epithelial cells, liposomes were functionalized with the invasive moiety Extracellular Adherence Protein (Eap) using two different methods. The adhesive nature of Eap allowed for physical adsorption (ads) on the liposomal surface and the presence of carboxylic groups on liposomes enable the possibility for a covalent coupling (cov). Surface adsorption was achieved by incubating 2 mL of liposomes (1:10 in PBS) with 40 µg/mL of Eap. The suspension was kept for stirring (180 rpm) at room temperature for 1 h. Whereas, covalent coupling was performed in two steps procedure; activation of liposomal carboxylic groups using either 4-(4, 6-dimethoxy-1,3,5-triazin-2-yl)-4-methyl-morpholinium chloride (DMTMM) reagent or 1-ethyl -3- (3-dimethylaminopropyl) carbodiimide hydrochloride (EDC) / N-hydroxysuccinimide (NHS) reagents in order to determine the efficient method to achieve high functionalization efficiency (**Figure 3.5**). Briefly, 2 mL of liposomes were mixed with 300 µL of DMTMM (1 mg/mL) and stirred for 2 h at room temperature, or 300 µL of EDC/NHS (48 mM and 19 mM respectively) (Menina et al. 2016) for 3 h at 4°C. Afterwards, 40 µg/mL of Eap solution was added to liposomes and kept for stirring for another hour at room temperature. Liposomal suspensions were all purified using Centriscart tubes (as described previously in **Section 3.23.2**) to remove the unbound Eap and excess of reagents. After centrifugation, liposomes were subjected to two cycles of sonication of 50% amplitude for 30 seconds each with an interval of 2 min using ultrasonic probe Sonicator S-250D model (Branson Ultrasonics, USA) to disperse the liposomal suspension.

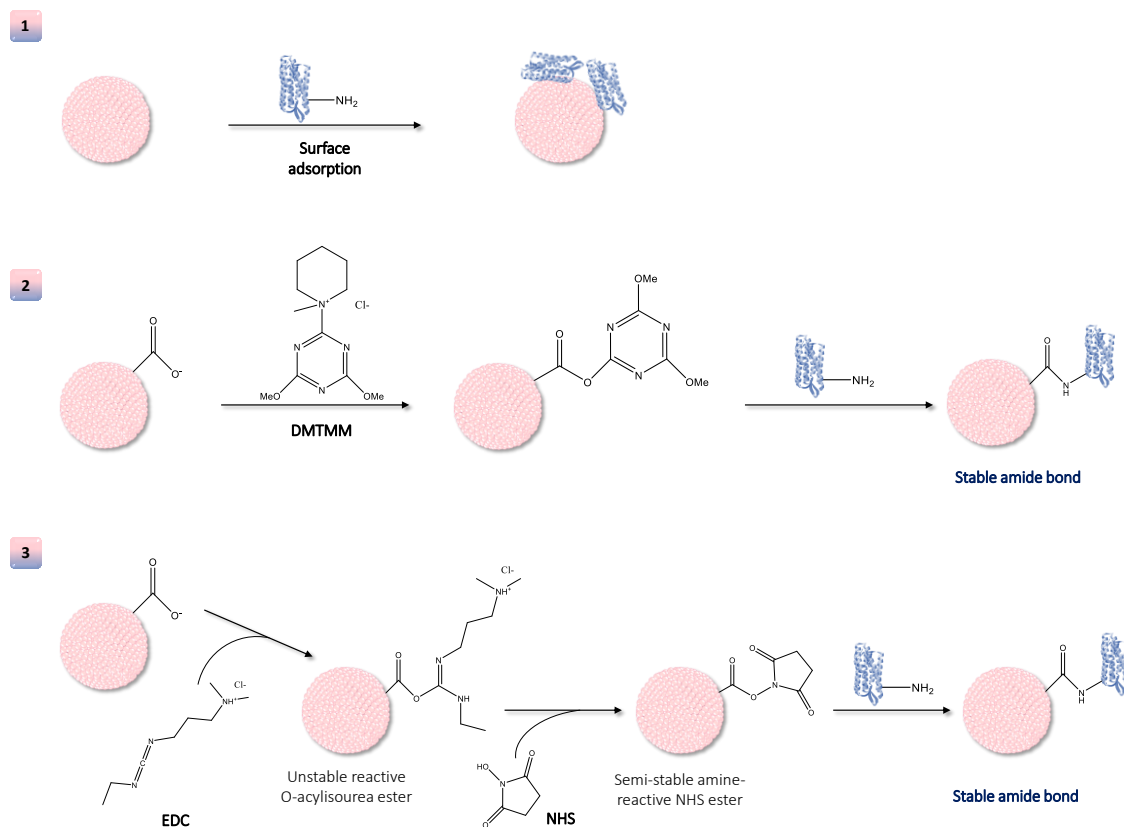


Figure 3.5. Functionalization methods

(1) Surface adsorption achieved by adding Eap to liposomal suspension which lead to adsorption of Eap onto liposomes (2) A covalent coupling of Eap to liposomal surface using DMTMM reagent, which activates the carboxylic groups on surface to form an amide bound between Eap amino groups. (3) A covalent coupling achieved using EDC reagent, which activates the carboxylic groups on liposomal surface, forming an unstable ester intermediate, stabilized by the addition of NHS reagent, and lead to a link with Eap amino groups via amide bound.

3.5.1 Determination of Eap concentration

Due to the interference of colistin; as a polypeptide, with the common protein quantification assays such as Bicinchoninic Acid Protein Assay (BCA) and Bradford assay, SDS-PAGE as a semi-quantitative method was used on one hand to confirm the presence of Eap on liposomal surface, and on the other hand to estimate Eap amount present on liposomal surface. The method is based on

migration of charged protein molecules in an electric field towards the positive side. Samples are treated with SDS detergent to denature proteins secondary, tertiary and quaternary structures by disturbing non-covalent forces including hydrogen-bonding, hydrophobic and ionic interactions. SDS also as anionic detergent gives a negative charge to protein molecules (Bhuyan 2010). Moreover, a treatment with 2-Mercapthoethanol as a reducing reagent is applied to cleave their disulfide bounds. This allows the proteins to be unfolded to linear chains and migrated through the gel matrix in a proportional manner to the polypeptide chain length (**Figure 3.6**).

The gel was based on 12% (w/v) acrylamide with a thickness of 0.75 mm, prepared by mixing 3.4 mL of Milli-Q water, 2.5 mL of resolving buffer (1.5 M Tris-HCL, pH 8.8), 100 μ L of 10 % SDS solution and 4 mL of N, N'-Methylenebisacrylamide solution (Serva, Germany). Afterwards, 50 μ L of 10% ammonium persulfate (APS) and 5 μ L of N, N, N', N'-tetramethylethylenediamine (TEMED) (Carl Roth GmbH, Germany) were added to the mixture and stirred gently with pipette tip in order to initiate the polymerization. Standards and samples were mixed (1:1 v/v) with a reducing agent that cleaves disulfide bonds. Afterwards, samples were loaded as well as protein ladder then placed into electrophoresis chamber containing electrophoresis buffer composed of 3.03 g Tris base, 14.4 g glycine and 1 g SDS (pH 8.3). Electrophoresis was conducted at 120 mV for 40 min. Page Blue Protein staining was used to stain the gel after a washing step with water for 1 h under a gentle shaking. The gel was then rinsed again with water and destained overnight in a water bath at room temperature and gentle shaking. Gel DocTM EZ imager (Bio-Rad, Germany) was used to image the gel and ImageJ software to process the images.

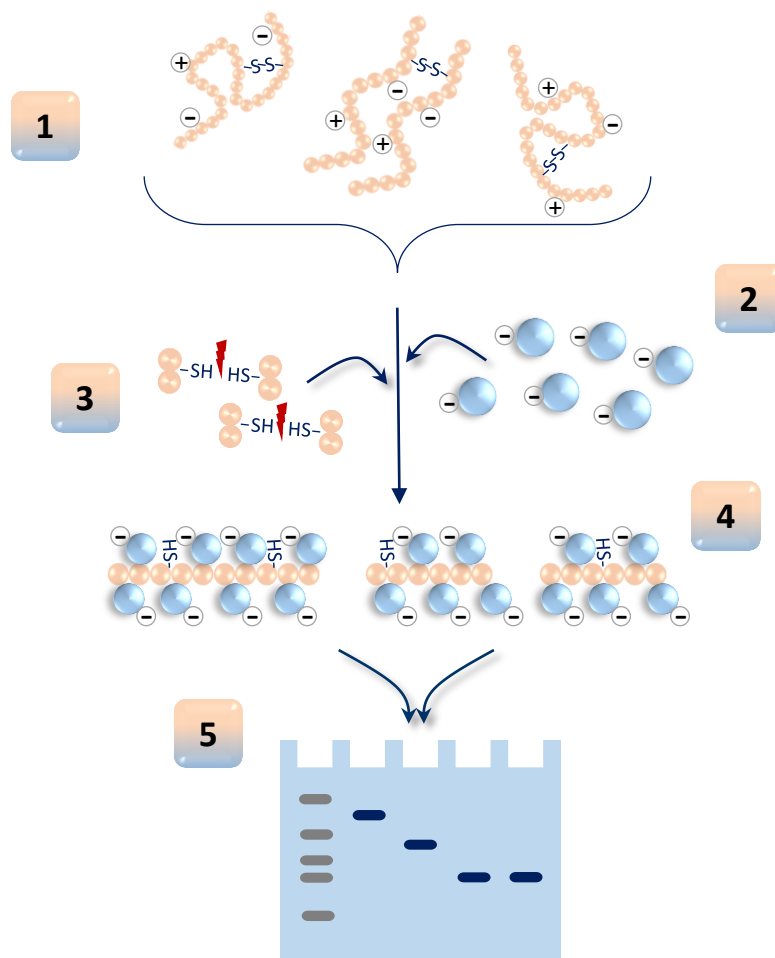


Figure 3.6. Scheme illustrating SDS-PAGE principle

(1) *Folded proteins with negative and positive charges. (2) In presence of SDS, proteins were charged negatively and denatured by cleavage of non-covalent interactions and (3) disulfide bonds in presence of reducing agent to form linear negatively-charged structures (4). Separation of proteins based on their polypeptide molecular weight on polyacrylamide gel (5).*

3.5.2 Functionalization efficiency

The amount of Eap was determined using SDS-PAGE and expressed as functionalization efficiency calculated using the following equation:

Equation 3: Functionalization efficiency

$$FE (\%) = \frac{\text{Amount of quantified Eap}}{\text{Initial amount of Eap}} \times 100$$

3.5.3 Stability of Eap-functionalized liposomes

Due to the adhesive nature of Eap, functionalization of liposomes with Eap resulted on formation of clumps after the purification step which was needed to eliminate the unbounded protein and the excess of coupling reagents. Therefore, a sonication step was applied to restore liposomes physical characteristics. Eap-functionalized liposomes containing colistin were subjected to a short stability study after sonication to ensure that liposomal suspension remain homogeneous in terms of size distribution and no clumps were formed again after storage . Colloidal parameters were monitored over a week at 4° C.

3.6 *In vitro* cell experiments

3.6.1 Cell culture

Human Larynx Carcinoma cell line (HEp-2 cells) received from the group of Prof. Petra Dersch, collaboration partner at HZI Braunschweig, and Human Colonic Adenocarcinoma cell line (Caco-2 cells) HTB-37 Clone purchased from (ATCC, Germany) were cultured in 75 cm² flasks. Roswell Park Memorial Institute medium (RPMI 1640) obtained from (Gibco Life technology, Germany), supplemented with 10% Fetal Calf Serum (Sigma Aldrich, Germany) was used for HEp-2 cells. While, Caco-2 cells were cultured in Dulbecco's Modified Eagle Medium (Gibco Life technology, Germany) supplemented with 10% FCS and 1% Non-Essential Amino Acids Solution (NEAA) purchased from (Gibco Life technology, Germany). Cells were incubated at 37° C, 5% CO₂, and 95% humidification. Cells were splitted once a week when reaching confluence and the medium was changed every second day.

3.6.2 Cytotoxicity assessment

A colorimetric assay was used to evaluate the cell metabolic activity after liposomes application on both cell lines in order to assess the cytotoxicity of the

formulations. MTT assay based on the ability of cells to reduce the reagent 3-(4, 5-dimethylthiazol-2-yl)-2, 5-diphenyltetrazolium bromide to its purple insoluble form formazan was used (**Figure 3.7**). Viable cells number is therefore proportional to the amount of formazan detected at 550 nm wavelength (Riss et al. 2004).

HEp-2 cells and Caco-2 cells were seeded on 96-well plates at a density of 10.000 cell/well and 20.000 cell/well respectively prior the assay for two days. Cells were washed with Hank's Balanced Salt Solution (HBSS) (Gibco Life technology, Germany) two times and then incubated with different concentrations of colistin, empty liposomes, colistin-loaded liposomes and Eap-functionalized liposomes containing colistin at 37° C, 5% CO₂ for 4 h. Cells were washed afterwards with HBSS again two times and then MTT reagent was added to a final concentration of 1 mg/mL. After 4 h incubation, the reagent was removed and cells were incubated 15 min with dimethyl sulfoxide (DMSO) at 37° C in order to dissolve formazan crystals. The absorbance was measured at 550 nm using a plate reader (Tecan Trading AG, Switzerland). Determination of cell viability was calculated by setting Triton X-100 treated cells as 0% viability and cells without particle treatment were set as 100% viability.

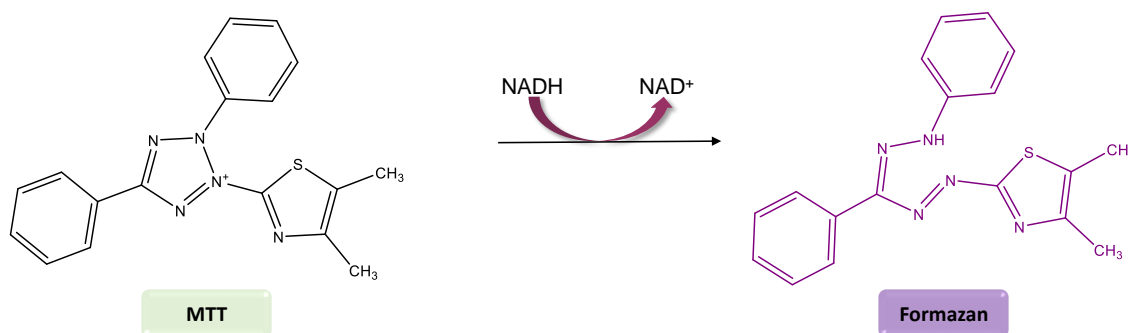


Figure 3.7. MTT assay principle

The MTT reagent is reduced in living cells to an insoluble purple compound, which will be solubilized and analyzed with spectrophotometer at 550 nm.

3.6.3 Uptake efficiency

Evaluation of the efficiency of Eap to facilitate the internalization of liposomes was investigated on epithelial cells of HEp-2 and Caco-2 cell lines. HEp-2 cells were chosen for this studies as they possess the β_1 integrin receptors that InvA497 uses to mediate the internalization of Yersinia species into eukaryotic cells. Since, Caco-2 cells express these receptors only on the basolateral side, HEp-2 cells will be used as a comparison platform to evaluate the internalization efficiency of Eap *versus* InvA497. Cells were treated with liposomes for two different time points using different Eap concentrations and then flow cytometry BD LSRFortessa™ (Biosciences, Germany) was used to analyze samples and determine the binding and uptake efficiency.

- **HEp-2 cells**

Cells were seeded two days prior the experiment day in 24-well plate, at a density of 2×10^4 cells/ well and incubated in humidifier incubator at 37° C and 5% CO₂. Cells were washed two times with PBS and 0.5 mL of fresh RPMI medium supplemented with 10% FCS and incubated with liposomes (Colistin-loaded liposomes functionalized with 5, 10 and 20 µg/mL Eap and non-functionalized liposomes as a control). After 1 h and 2 h incubation time, cells were washed again with PBS two times and then 0.1 mL of trypsin was added to detach the cells for 10 min at 37° C. A 0.3 mL of flow cytometer buffer (FACS buffer) composed of PBS containing 5% FCS, was added to inhibit trypsin activity and dilute the samples. Cell samples were analyzed freshly with flow cytometry (BD LSRFortessa™ Cell Analyzer Biosciences, Germany) and 10000 events per each sample were analyzed. FlowJo software (FlowJo 7.6.5, FlowJo LLC, USA) was used to analyze the data and uptake values were normalized to untreated cells (blank).

- **Caco-2 monolayer**

Caco-2 cells are the common used model in research for the intestinal epithelial barrier, therefore uptake studies were also performed with this cell line. As a model, Caco-2 cells were cultivated as a monolayer which is characterized by the

formation of tight junctions. Cells were seeded on Transwell inserts of 0.4 μm pore size (Corning Incorporated, USA) at a density of 6×10^4 cells/well in 12-well plate. Cells were supplied with 0.5 mL DMEM supplemented with 10% FCS and 1% NEAA solution on the apical compartment and 1.5 mL on the basolateral compartment, and medium was changed every second day. Cells with TEER values $\geq 500 \Omega \cdot \text{cm}^2$, were washed with PBS two times were incubated with different concentrations of Eap-functionalized liposomes (Eap: 5, 10 and 20 $\mu\text{g}/\text{mL}$) as well as controls including cells without treatment (blank) and non-functionalized liposomes. After incubation time of 2 h and 4 h, cells were washed two times with PBS, trypsinized with 0.1 mL for 10 min at 37°C and 0.4 mL of FACS buffer was added afterwards. Flow cytometer was used to analyze 10000 event per sample each in triplicate. Data were analyzed as described above with HEp-2 cells).

3.6.4 TEER measurements

The barrier integrity of the monolayer was monitored over time via Transepithelial Electrical Resistance (TEER) measurements of cellular monolayer using epithelial volt-ohmmeter (World Precision Instruments, USA) equipped with chopstick electrodes. Electrical resistance measurement is a quantitative method based on the determination of the ohmic resistance by an application of a direct current voltage to the electrodes and measurement of the resulting current using the setup shown in (**Figure 3.8**). Briefly, cellular monolayer cultivated on semipermeable filter inserts which defining the partition for apical and basolateral compartments. The placement of an electrode in the upper compartment and the other in the lower compartment, allows for measuring the tissue resistance expressed in (Ω), where the resistance is inversely proportional to the effective area of the insert membrane expressed in (cm^2). The procedure includes also the blank resistance determined by measuring the semipermeable insert filter without cells. The electrical resistance is then calculated by subtracting the blank inserts value (equal to 110 Ω) from all samples, and further multiplied by the cultivation area of the inserts (equal to 1.12 cm^2) (Haorah et al. 2008; Watson et al. 2013). TEER measurements were taken every second day of the culture over time.

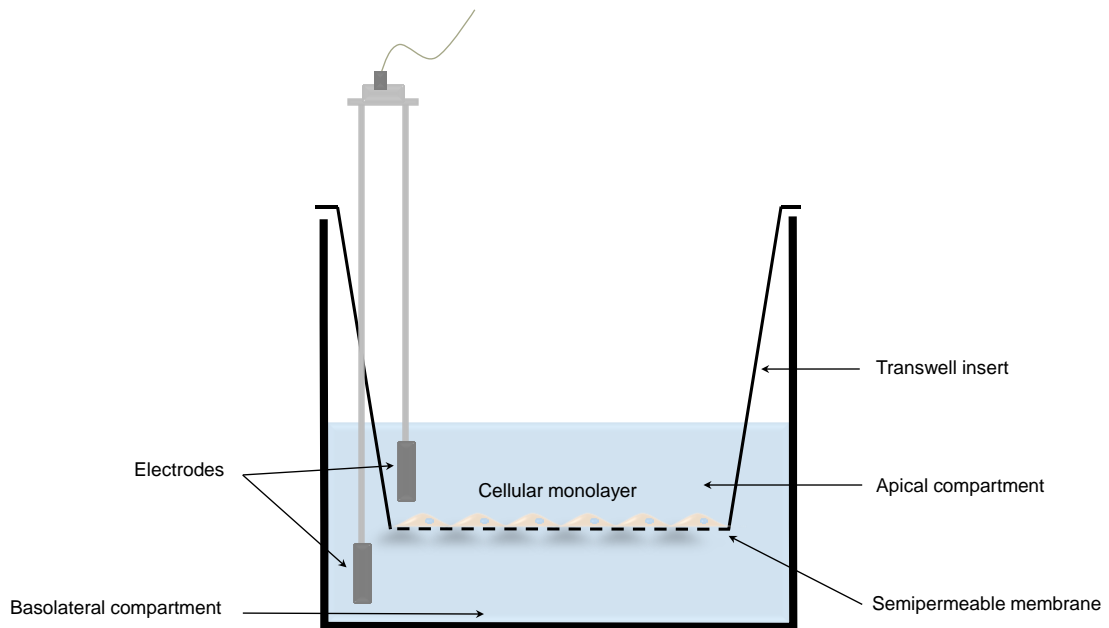


Figure 3.8. TEER measurement setup

Electrical resistance values were measured using chopstick electrodes, placed in the apical and another in the basolateral compartments separated by the cellular monolayer cultured on semipermeable insert filter.

3.6.5 Cell Imaging

For cell imaging, confocal laser scanning microscopy (CLSM Leica TCS SP 8, Leica, Germany) was used. Cells were seeded in 24-well plate with a transparent bottom two days before the experiment. On the experiment day, cells were incubated with liposomes (Eap-functionalized liposomes, non-functionalized liposomes and non-treated cells as a control) for 2 h (HEp-2 cells) and 4 h (Caco-2 cells). Cells were washed with PBS two times and further incubated with 10 $\mu\text{g}/\text{mL}$ fluorescein-labeled wheat germ agglutinin (Flu-WGA) for 15 min at 37° C to stain the cell membrane. Cells were washed with PBS two times and then incubated with 3% of paraformaldehyde (PFA) for 30 min at room temperature for fixation. Cell nucleus was stained with 1 $\mu\text{g}/\text{mL}$ of 4', 6-Diamidin-2-phenylindol (DAPI) for 15 min at room temperature. Cells were washed again to remove excess of DAPI and 0.3 mL of PBS was added to keep cells humidified. Visualization was acquired using either 25x water immersion or 40x oil immersion objectives with excitation wavelengths of 533 nm, 488 nm and 720 nm of

rhodamine-labeled liposomes, Flu-WGA (cell membrane) and DAPI (nucleus) respectively. All images were acquired at 1024 X 1024 resolution and further processed with LAS X software (LAS X 1.8.013370, Leica Microsystems, Germany).

3.6.6 Immunostaining of Caco-2 monolayer

Caco-2 cells used as a model of the GI tract, which under normal conditions it acts as a cellular barrier to prevent the influx of the luminal content. This barrier is reinforced by multiprotein junctional complexes known as zonulae occludentes (ZO) (Anderson and van Itallie 2009). To visualize the integrity and the tightness of Caco-2 monolayer, an immunostaining of ZO-1, a tight junction associated protein, present on the cytoplasmic surface, was performed. Caco-2 monolayer were washed with PBS three times, and then fixed with PFA (3%) for 30 min at room temperature. After removing PFA, cells were incubated with a solution of 50 mM NH₄Cl for 1 h as a quenching solution. Afterwards, a solution of Saponin (0.05%) and bovine albumin serum (BSA) (1%) was added for 1 h at RT after removal of the quenching solution. Cells were washed with PBS again two times then incubated with primary antibody ZO-1, mouse (diluted 1:400 in Saponin / BSA solution) at 4° C overnight. Next day, cells washed three times with PBS, were incubated with a secondary antibody Alexa 488 anti-mouse (1:400 dilution in Saponin/BSA) for 2 h at room temperature. After washing with PBS three times, a nuclear staining using DAPI (as described above) and an actin filament staining using Phalloidin (30 min at RT) were performed. Transwell inserts were mounted on microscopy slides using DAKO mounting medium (Agilent Technologies, USA) and visualized with CLSM.

3.6.7 Uptake mechanism

A preliminary uptake mechanism experiment was performed at 4° C to determine whether HEP-2 and Caco-2 monolayer take up Eap-functionalized liposomes via a passive or an active pathway. Briefly, HEP-2 cells seeded on 24-well plate and Caco-2 monolayer on Transwells inserts exhibiting TEER values $\geq 500 \Omega \cdot \text{cm}^2$ as described previously (**Section 3.6.3**) were incubated with Eap-functionalized

liposomes at 4° C for 2 h and 4 h respectively. Afterwards, cells were washed with PBS three times, trypsinized and further analyzed with flow cytometry.

Further investigation of involved uptake mechanisms was conducted with Caco-2 monolayer in which cells were subjected to an uptake experiment in which pharmacological endocytosis inhibitors were applied. Cells, seeded on Transwells inserts (with TEER values $\geq 500 \Omega \cdot \text{cm}^2$) were washed with PBS three times, and Hank's Balanced Salt Solution (HBSS) was added to apical as well as basolateral compartments containing different inhibitors (**Figure 3.9**) for 1 h at 37° C. Cells were incubated with chlorpromazine (10 $\mu\text{g}/\text{mL}$) to inhibit clathrin-dependent endocytosis, cytochalasin D (1 mg/mL) for the inhibition of macropinocytosis, filipin III (1 $\mu\text{g}/\text{mL}$) to inhibit caveolin-dependent endocytosis and methyl- β -cyclodextrin (M β CD) / lovastatin (10 $\text{mM}/1 \mu\text{g}/\text{mL}$) for the inhibition of clathrin- and caveolin-independent endocytosis pathways (Alexander et al. 2010; Zhang et al. 2014). Afterwards, liposomes were added to the upper compartment in the presence of inhibitors as well for another 2 h at 37° C and 5% CO_2 . Cells were washed with PBS, trypsinized and further analyzed with flow cytometry.

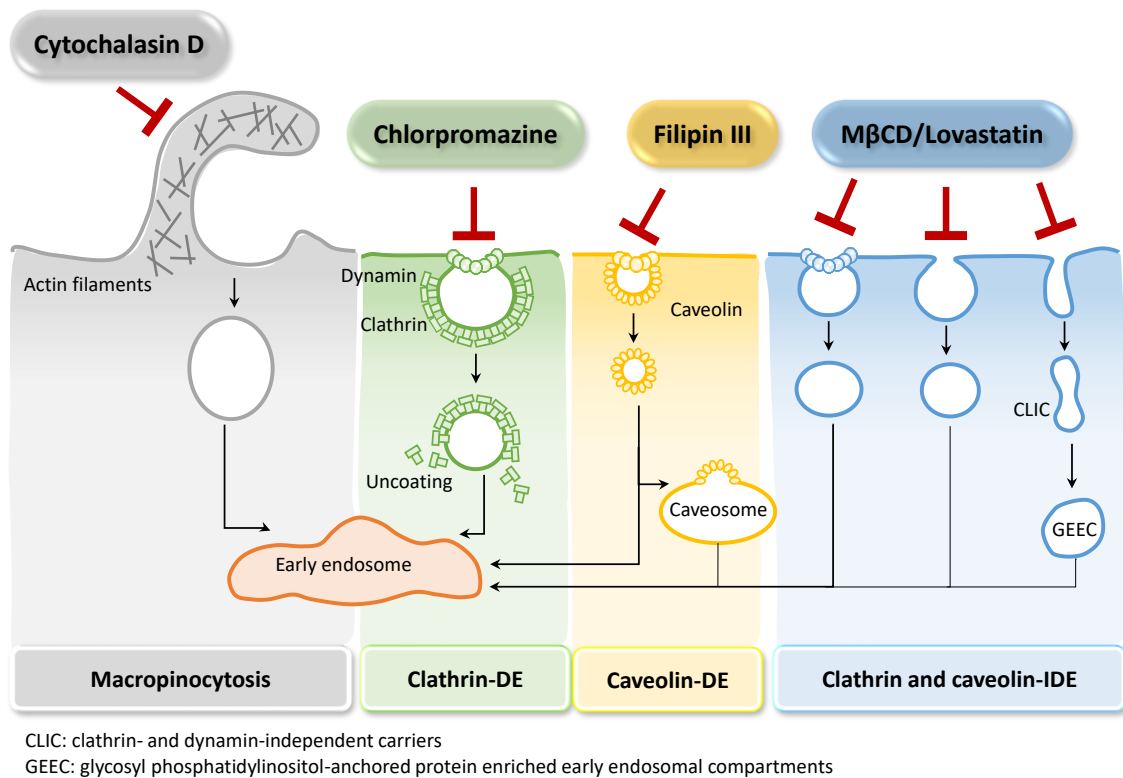


Figure 3.9. Uptake mechanism pathways

Illustration demonstrating different endocytosis pathways including macropinocytosis, clathrin-dependent endocytosis (Clathrin-DE), caveolin-dependent endocytosis (Caveolin-DE) and clathrin- and caveolin-independent pathways (clathrin- and caveolin-IDE), as well as their corresponding inhibitors cytochalasin D, chlorpromazine, filipin III and methyl-β-cyclodextrin (MβCD)/lovastatin respectively.

3.7 *In vitro* infection studies

Bacterial strain *Salmonella enterica* subsp. *enterica* (ex Kauffmann and Edwards) Le Minor and Popoff serovar Typhimurium 14028™ was reconstituted from a lyophilized vial stored at -80° C purchased from (ATCC®, USA). Bacterial cultures were prepared by growing the bacteria in Difco™ Nutrient Broth (BD, USA) for 18 h at 37° C. a stock solution of *S. enterica* was prepared by adding 5% Glycerol (Sigma Aldrich, Germany) to an overnight culture and stored at -80° C.

3.7.1 Bacterial growth curve

A growth study of *S. enterica* was conducted by incubating an optical density (OD) of 0.01 from an overnight culture of single colony in several overnight glass tubes containing 5 mL of Nutrient Broth over 24 h at 37° C. Samples were taken at each time point and their OD was measured and 1 mL from each sample was collected and stored at -20° C. After collections of all time point, samples (stored previously at -20° C, were subjected to a serial dilution in Nutrient Broth to 10, 10², 10³, 10⁴, 10⁵, 10⁶, 10⁷, 10⁸, 10⁹ and 10¹⁰. Afterwards, only dilutions 10⁴, 10⁶, 10⁸, and 10¹⁰ were plated on Nutrient agar plates and incubated overnight at 37° C for 18 h. *Salmonella* colonies were counted for each time point the number was expressed as Colonies Forming Unit (CFU)/mL.

3.7.2 Minimum inhibitory concentration (MIC)

Salmonella was cultured overnight in glass tubes containing 5 mL Nutrient Broth for 18 h at 37° C. A dilution from the overnight culture to an OD₆₀₀ of 0.1 was prepared in 96-well plate, 100 µL in each well. Colistin as free drug, liposomes functionalized and non-functionalized with Eap were diluted to several concentrations separately two times higher than the desired concentration. Afterwards, 100 µL from each sample was added to each well and mixed gently with the pipette up and down. Wells containing Nutrient Broth was used as blank. The OD₆₀₀ of each samples was measured after preparation (T₀) and then incubated at 37° C for 18 h. A measurement of the OD₆₀₀ was performed after the incubation and MIC values were calculated by normalizing samples OD₆₀₀ values to the non-treated samples (only bacteria in Nutrient Broth). IC₅₀ and IC₉₀ values were considered as the lowest concentration of samples, which reduced at least 50% and 90% of the bacterial load respectively were determined using OriginPro software (OriginLab Corporation, USA).

3.7.3 Anti-bacterial efficacy

- **Optimization of the infection assay**

HEp-2 cells were seeded in 24-well plate one day prior the experiment at a density of 1×10^5 cells/well as described previously (Menina et al. 2016). Caco-2 monolayer were seeded on Transwell inserts in 12-well plate at a density of 6×10^4 cells/well for 7 days to reach TEER values of $\geq 500 \Omega \cdot \text{cm}^2$. An overnight culture of *Salmonella* was centrifuged at 350 g for 5 min, Nutrient Broth was aspirated and bacterial pellet was re-suspended in PBS for washing. 2 cycles of washing were performed and bacteria were re-suspended further in the infection buffer composed of either RPMI medium (HEp-2 cells) or DMEM (Caco-2 cells) supplemented with 20 mM Hydroxyethyl-piperazineethane-sulfonic acid buffer (HEPES buffer, Biochrom, Germany) and 0.4% BSA.

HEp-2 and Caco-2 monolayer were washed two times with PBS, and fresh infection buffer was added. Cells were infected with different Multiplicity of infection (MOI) 10, 25, 50, and 100 (number of bacteria per one host cell) and incubated with *Salmonella* for 1 h at 37° C and 5% CO₂. After incubation, cells were washed with PBS two times, and extracellular bacteria were killed by incubating cells for further 2 h with 50 µg/mL of gentamicin solution. Cells were then washed 2 times with PBS and further lysed with ice-cold water for 10 min. Cell lysates were plated on Nutrient agar plates with different dilutions (10^4 , 10^6 , 10^8 , and 10^{10}) (**Figure 3.10**). Plates were incubated at 37° C for 18 h and bacterial colonies were counted, multiplied with dilution factor and expressed as infection percentage using the following formula:

Equation 4. Infection percentage

$$\text{Infection (\%)} = \frac{\text{Number of colonies of cell lysate}}{\text{Number of colonies of inoculum}} \times 100$$

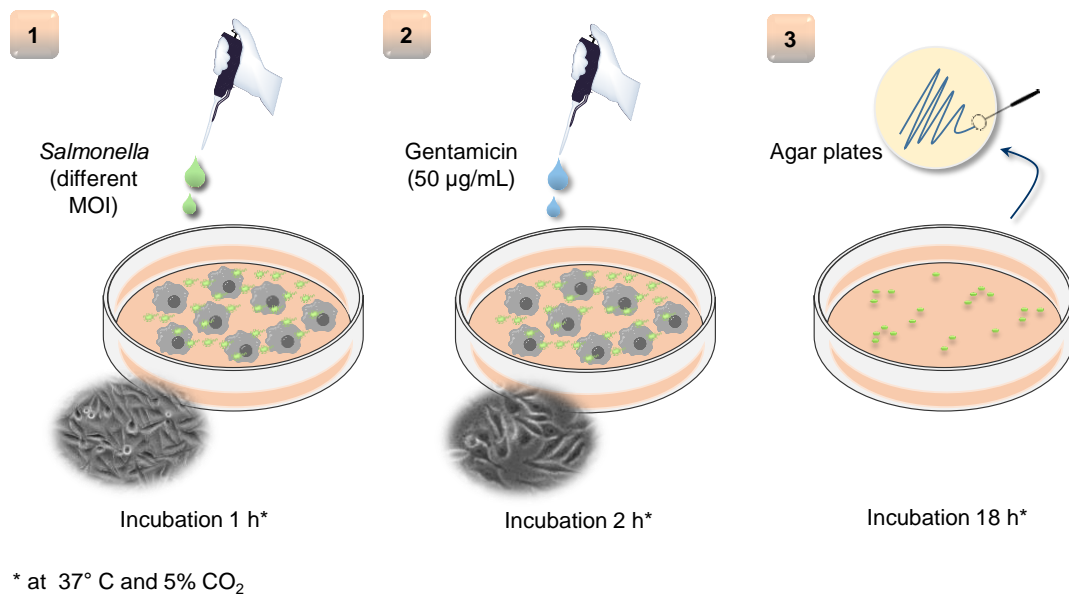


Figure 3.10. Optimization of infection assay

(1) Cells were infected with different MOI of *Salmonella* for 1 h then (2) gentamicin solution (50 µg/mL) was added to kill extracellular bacteria for 2 h. (3) Cells were lysed and the cell lysates containing intracellular *Salmonella* were plated on agar plates and incubated for 18 h at 37° C and 5% CO₂. Light microscope images on (1 and 2) showed HEp-2 cells after washing with PBS and after applying *Salmonella* respectively

▪ Killing efficacy assay

Infection protocol was performed as described above (**Section 3.7.3**). Briefly, after infection of cells with *Salmonella* (MOI of 100) for 1 h and extracellular bacterial killing for 2 h, HEp-2 and Caco-2 monolayer were treated with different liposomal formulations for 2 h and 4 h respectively and incubated at 37° C and 5% CO₂. Unloaded liposomes (Lip-3), colistin-loaded liposomes (Col-Lip-3), Eap-functionalized liposomes containing colistin (EapCol-Lip-3) were used to treat the cells, colistin as free drug (Col) as well as Eap added directly without any functionalization of prior adsorption to colistin as free drug (Col + Eap) and to colistin-loaded liposomes (Col-Lip-3 + Eap) were used as controls. After liposomal treatment, cells were washed with PBS two times, and lysed with ice-cold water for 10 min. Cell lysates were plated on Nutrient agar plates for 18 h

(**Figure 3.11**) and incubated at 37° C and 5% CO₂. Anti-bacterial efficiency was expressed as killing percentage of normalized samples CFU/mL values to the control (untreated sample).

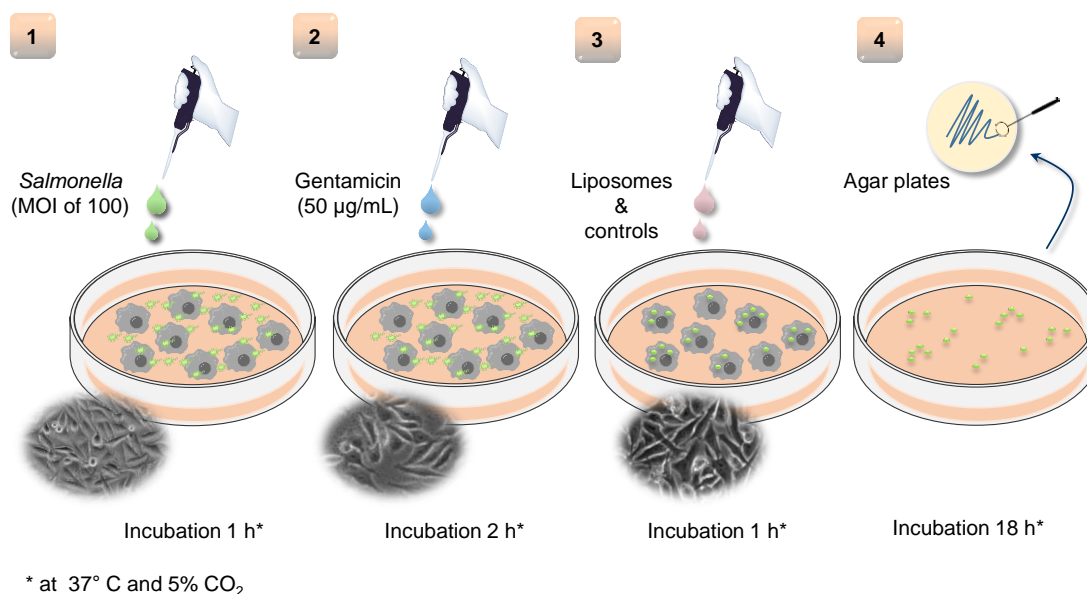


Figure 3.11. Antibacterial efficacy protocol

(1) Cells were infected with *Salmonella* with an MOI of 100, (2) the extracellular *Salmonella* was killed using gentamicin solution of 50 µg/mL. *Salmonella*-infected HEp-2 cells and Caco-2 monolayer were treated with liposomal formulations as well as controls for 2 h or 4h respectively. (4) Cells were lysed to extract intracellular bacteria, which were plated on agar plates and incubated for 18 h at 37°C and 5% CO₂.

3.7.4 Colistin dose-response and Eap titration studies

Colistin dose-response experiment was performed by treating HEp-2 and Caco-2 monolayer with different doses of colistin-loaded liposomes (10, 30, 50, 80, 150 and 200 µg/mL) functionalized initially with 20 µg/mL Eap and loaded with 4 mg/mL colistin (as described previously in **Section 4.2**). Eap titration study was conducted by incubation HEp-2 cells and Caco-2 monolayer with colistin-loaded liposomes containing 30 µg/mL of colistin dose and functionalized with different concentrations of Eap (7, 12, 20, and 40 µg/mL). Cells were incubated for 2 h at

37°C and 5% CO₂. The infection and treatment protocols were performed as previously described in **Section 3.7.3**.

3.8 *In vivo* assessment of anti-infective efficacy

A pilot study was carried out by the group of Prof. Dr. Till Strowig at the Microbial Immune Regulation Department, Helmholtz Centre for Infection Research (HZI) in Braunschweig. The aim of this *in vivo* study was to investigate the efficacy of the developed system; Eap-functionalized liposomes containing colistin to eradicate the enteroinvasive bacterium *Salmonella enterica* in a mouse model (

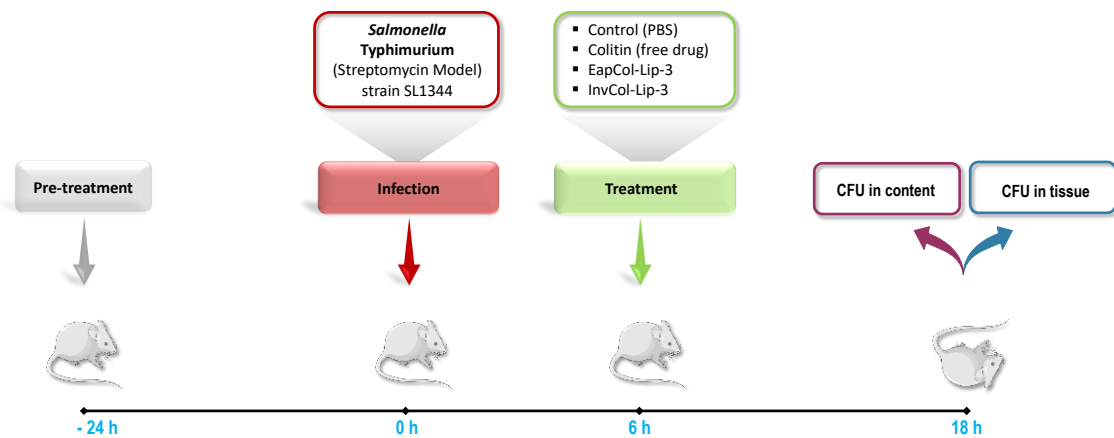


Figure 3.12). Briefly, mice were divided into four groups each group consists of five mice treated prior the infection day with streptomycin to decrease the colonization resistance. *Salmonella* Typhimurium strain SL1344, was used to infect the mice. After 6 h animals were treated with 1 mg dose of colistin either encapsulated into EapCol-Lip-3 or InvCol-Lip-3; or as free drug via oral gavage, PBS was used as control. After 18 h, the mice were weighed and then sacrificed. Small intestine and cecum were recovered, washed and the resulted suspension was plated on agar plates to obtain CFU in content, and then the tissues were homogenized and plated on agar plates to obtain CFU in tissue. Results were expressed as CFU/g.

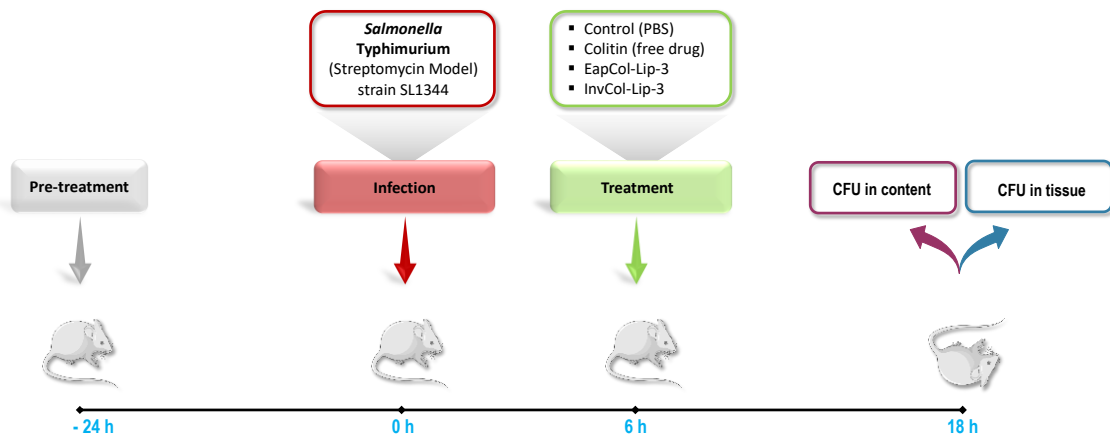


Figure 3.12. Experimental plan of the in vivo study

Animals were subjected to a pre-treatment with antibiotics 24 h prior the infection, afterwards, they were infected using *S. Typhimurium* strain SL1344 for a period of 6 h. Liposomal treatment was administrated via oral gavage (EapCol-Lip-3 and InvCol-Lip-3) as well as free colistin free and PBS as controls. CFU in content and in tissue were counted after 18 h from the treatment.

3.9 Statistical analysis

All data are shown as mean \pm standard error of the mean (SEM) from at least three independent experiments. One-way Anova followed by post hoc analysis was used to calculate the statistical significance using OriginPro software (OriginLab Corporation, USA). Differences were considered to be significant at P-value < 0.05 (*), < 0.01 (**) and < 0.001 (***)).

4 Results

Parts of these results section were published in *Advanced Healthcare Materials Journal*, in 2018 (<https://doi.org/10.1002/adhm.201900564>), included in the following chapters: Colistin-loaded liposomes characterization and Morphology, Stability studies for oral route, Eap-functionalized liposomes containing colistin, Eap mediates the binding/internalization of liposomes into epithelial cells and antibacterial efficacy of EapCol-Lip-3.

4.1 Unloaded liposomes

4.1.1 Colloidal characterization

Three liposomal formulations were prepared using DPPC, DSPC and DPPC:DSPC separately as main phospholipids. These formulations contained also cholesterol for rigidity and DPPE-GA to provide the liposomal surface with carboxylic group for facilitating their functionalization. For better understanding of liposomal internalization and tracking their delivery pathways, Rhod-DPPE was implemented into liposomal composition which label them with a red fluorescence. All three formulations exhibited a size of approximately 200 nm, with a homogeneous distribution reflected by PDI values lower than 0.1 (**Figure 4.1 a, b**). Moreover, a negative charge of -28 mV and -25 mV for DPPC-(Lip-1) and DSPC-containing liposomes (Lip-2) respectively was measured, while a less negative ζ -potential value (-19 mV) was measured with DPPC/DSPC formulation (Lip-3) (**Figure 4.1 c**).

4.1.2 Unloaded liposomes stability

Lip-1, Lip-2 and Lip-3 were subjected to different stability studies, in which colloidal parameters size, PDI and surface charge were monitored in various conditions including storage, impact of pH and impact of bile salts/phospholipids presence on their integrity over time. Samples were taken from prepared liposomes stored at 4° C every one week during one month period. Results showed that Lip-1, Lip-2 and Lip-3 were stable in suspension at 4° C and no

notable changes were seen in all parameters (**Figure 4.2 a, b, c**). Incubation of liposomes in PBS (pH 7.4) as buffer control (B), buffer of pH 6.5 and a buffer of pH 1.6 as well as in simulated media FaSSGF and FaSSIF at 37° C for 5 h period, resulted in a stable size of approximately 200 nm except in FaSSIF –where the size of all liposomes decreased to approximately 100 nm (**Figure 4.2 d**).

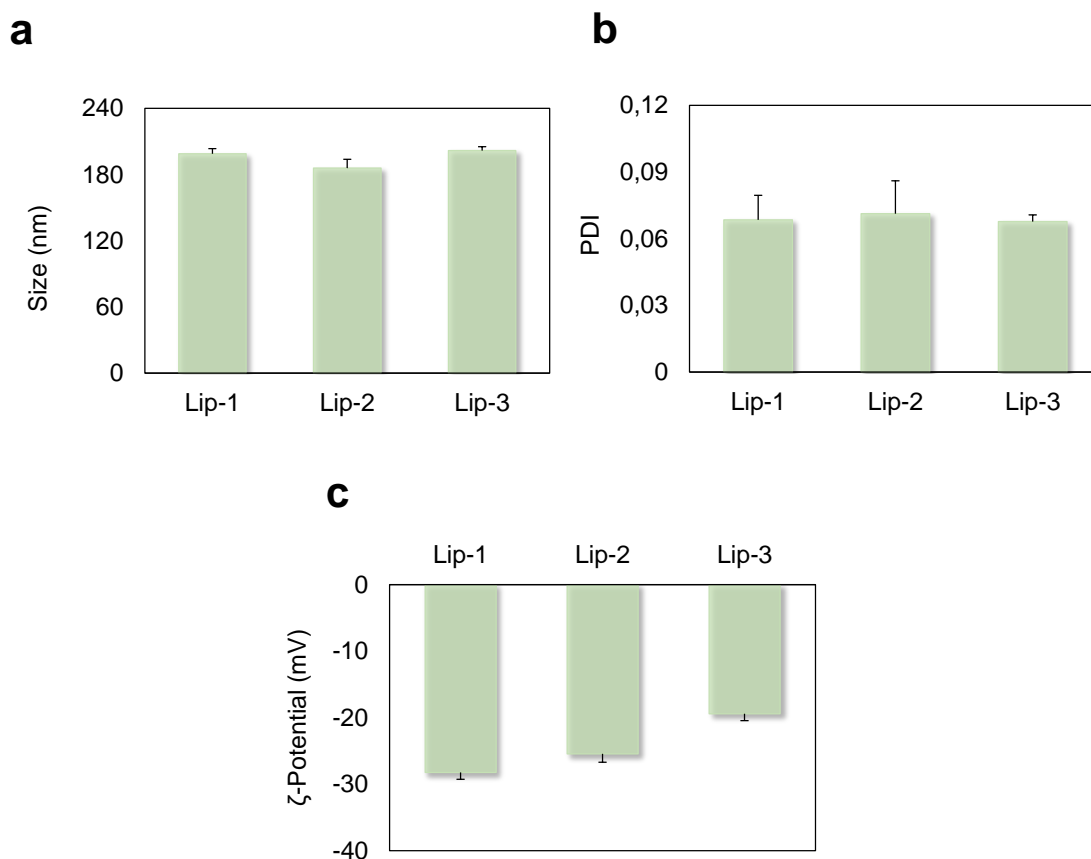


Figure 4.1. Colloidal characteristics of unloaded liposomes

(a) Size, (b) PDI and (c) ζ-potential of unloaded liposomes Lip-1 (DPPC:CHOL:DPPE-GA), Lip-2 (DSPC:CHOL:DPPE-GA) and Lip-3 (DPPC:DSPC:CHOL:DPPE-GA) measured after preparation (day 0). Data are shown as mean \pm SEM from three independent experiments ($n=3$, $N=9$, as “ n ” is number of independent experiments and “ N ” is number of repetitions).

A slight increase of PDI was observed in pH 1.6 buffer and in FaSSGF, while a decrease to <0.03 was seen in FaSSIF (**Figure 4.2 e**). A charge values of -30 mV

to -20 mV were measured in all media; however lower values with all three formulations were observed in FaSSIF (-27 to -28 mV) (**Figure 4.2 f**).

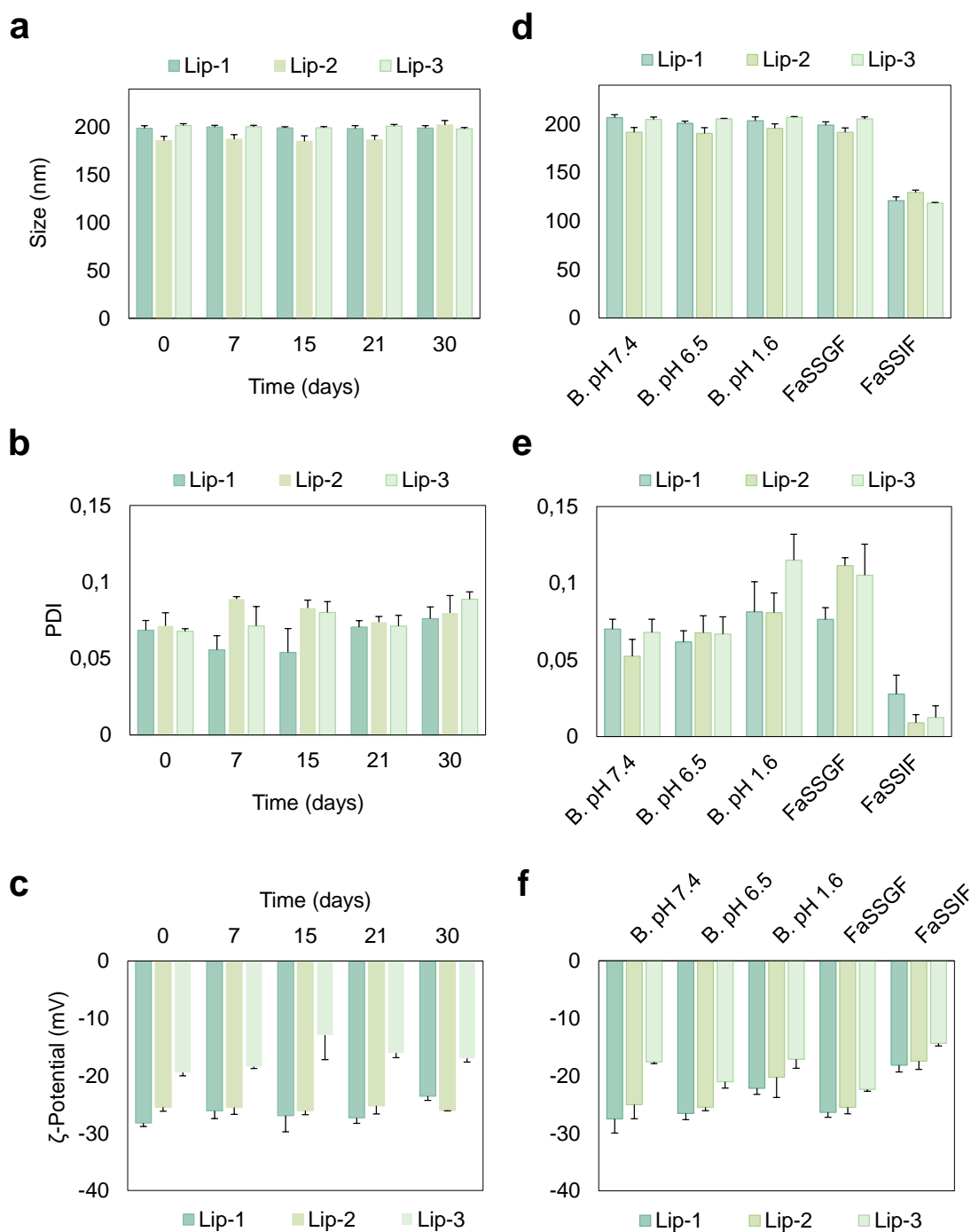


Figure 4.2. Unloaded liposomes stability

(a) Size, (b) PDI and (c) ζ -potential of unloaded liposomes Lip-1, Lip-2 and Lip-3 at storage conditions (4° C in suspension) during one month. (d) Size, (e) PDI

and (f) ζ -potential of liposomal formulation after incubation for 5 h in PBS (pH 7.4, B) buffer pH 6.5, buffer pH 1.6, gastric (FaSSGF) and intestinal simulated media (FaSSIF) at 37° C. Data are shown as mean \pm SEM from three independent experiments (n= 3, N= 9).

4.2 Colistin-loaded liposomes

Colistin was encapsulated into the above formulated liposomes Lip-1, Lip-2 and Lip-3 since no major differences were observed between the formulations after stability studies. Preparation of colistin-loaded liposomes Col-Lip-1, Col-Lip-2 and Col-Lip-3 was conducted using lipid film hydration method, in which the hydration of the lipid film was done with colistin solution in PBS using different concentrations (1, 2, 3, 4, 5, 10 mg/mL) aiming to obtain an optimum liposomal formulation which exhibits a high entrapment efficiency as well as an optimum loading capacity.

4.2.1 Colloidal characterization

Col-Lip-1, Col-Lip-2 and Col-Lip-3 were characterized in terms of size, PDI and surface charge. Results did not show significant changes in size and PDI compared to unloaded liposomes. Homogeneously distributed spherical-shaped vesicles of 200 nm (**Figure 4.3 a**) were observed except Col-Lip-1 prepared with 10 mg/mL of colistin showed a PDI of 0.15 (**Figure 4.3 b**). Regarding liposomal surface charge, a decrease of ζ -potential values in a range of -12 mV to -23 mV was observed, which was expected as colistin exhibits a positive charge. Col-Lip-2 exhibited higher negative charge compared to the other two formulations (**Figure 4.3 c**).

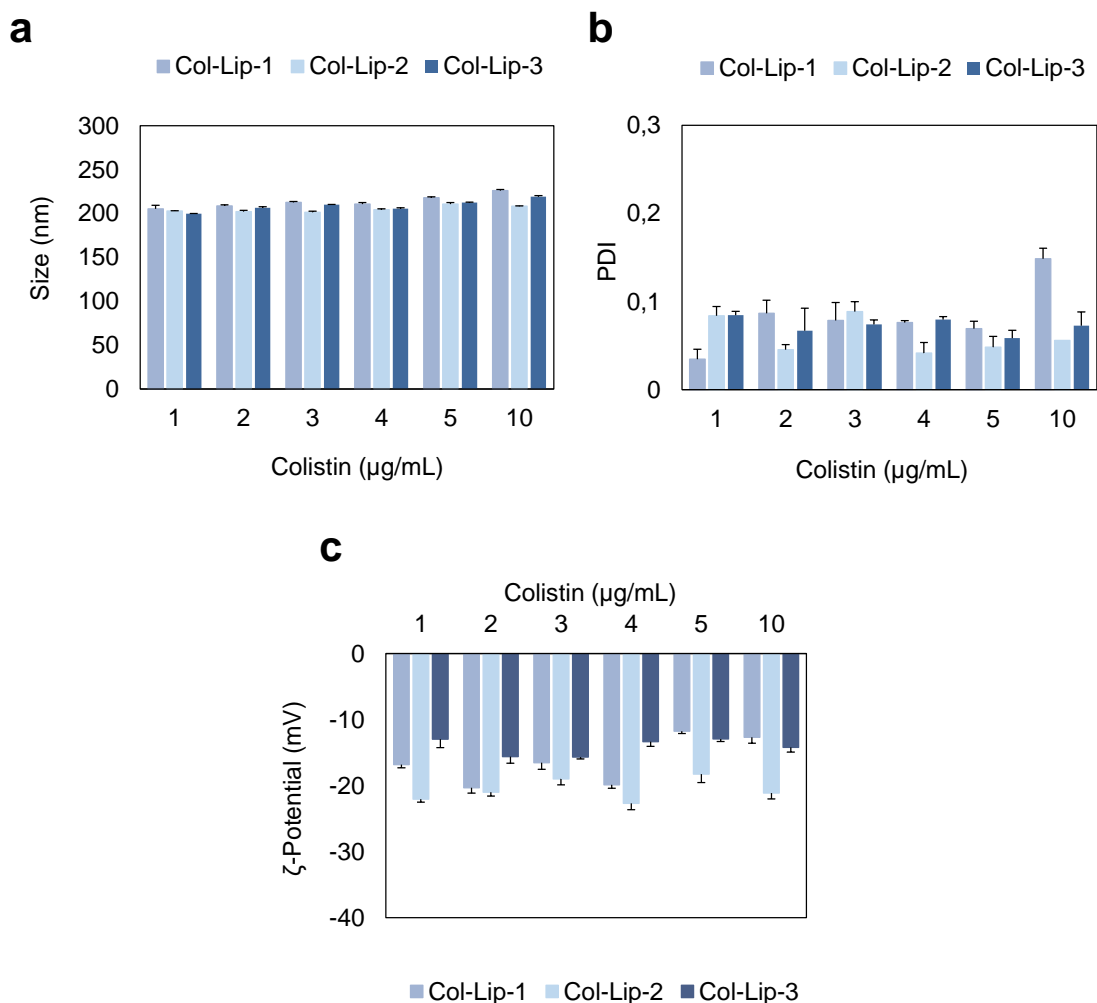


Figure 4.3. Colloidal parameters of colistin-loaded liposomes

(a) Size, (b) PDI and (c) ζ -potential of Col-Lip-1, Col-Lip-2 and Col-Lip-3 loaded with 1, 2, 3, 4, 5 and 10 $\mu\text{g/mL}$ of colistin. Samples were measured immediately after preparation. Data are shown as mean \pm SEM from three independent experiments ($n=3$, $N=9$).

4.2.2 Liposomes morphology

Electron microscopy imaging was conducted to investigate liposomal morphology of Col-Lip-1, Col-Lip-2 and Col-Lip-3. SEM image of Col-Lip-1 showed a homogenous distribution of 200 nm spherical vesicles (**Figure 4.4 a**). No difference was detected between formulations in all imaging techniques; therefore, only one formulation was shown for each technique as a representative

image. TEM imaging also showed a spherical-shaped liposomes with a presence of small impurities in the background, which could be due to the staining solution which was used to increase the contrast of the electron beam and enhance the imaging (**Figure 4.4 b**). The advantage of Cryo-TEM imaging is that the sample needs no pre-treatment like staining, washing of buffer salts, drying, which both SEM and TEM require. Col-Lip-3 image showed nicely spherical vesicles of about 200 nm (**Figure 4.4 c**).

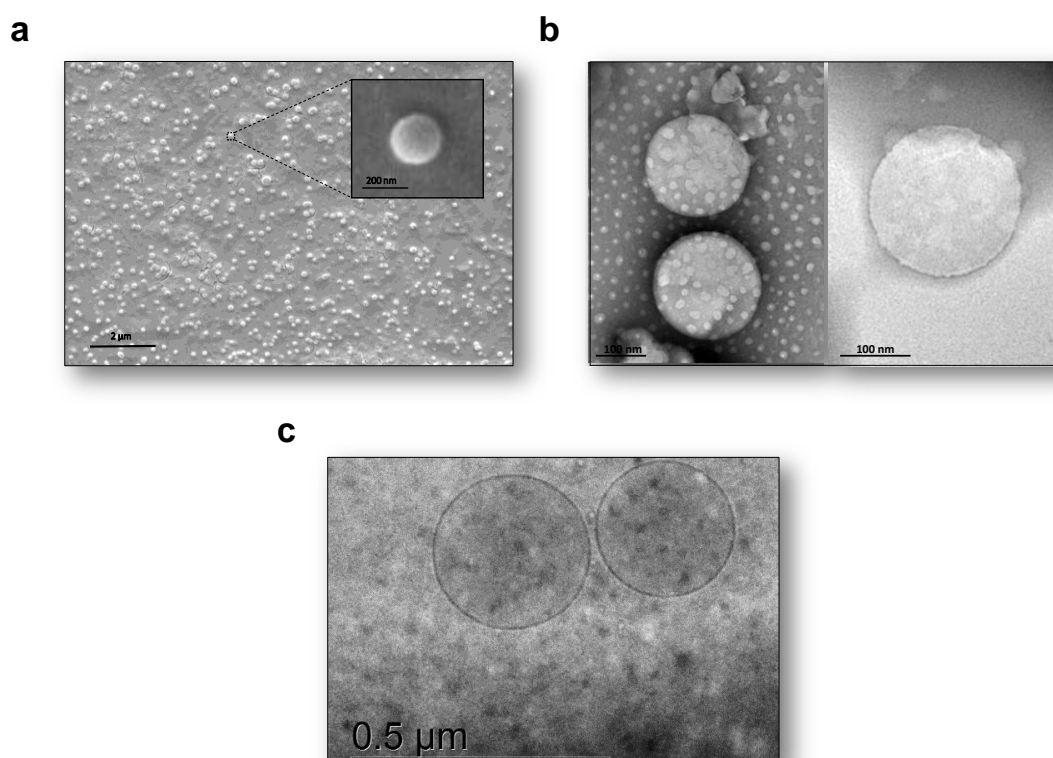


Figure 4.4. Liposomes morphology

Representative microscopy images of Col-Lip-1 visualized using SEM (a) and TEM (b) techniques and of Col-Lip-3 using Cryo-TEM (c), indicating the presence of spherical liposomes with homogeneous size distribution as shown in SEM image.

4.2.3 Colistin loading

Col-Lip-1, Col-Lip-2 and Col-Lip-3 were subjected to further characterization including determination of the encapsulation efficiency and loading capacity. The

amount of colistin encapsulated into liposomes was approximately 60% using 1 mg/mL of colistin for the three liposomal formulations. However, the EE% values decreased by increasing colistin concentration with also differences between the different formulations where the lower value was 20%, obtained using 10 mg/mL colistin loaded into Col-Lip-1 (**Figure 4.5 a**). On the other hand, the loading capacity increased by increasing colistin concentrations, starting with 20% in the three liposomes and increased to 80% using 10 mg/mL of colistin (**Figure 4.5 b**).

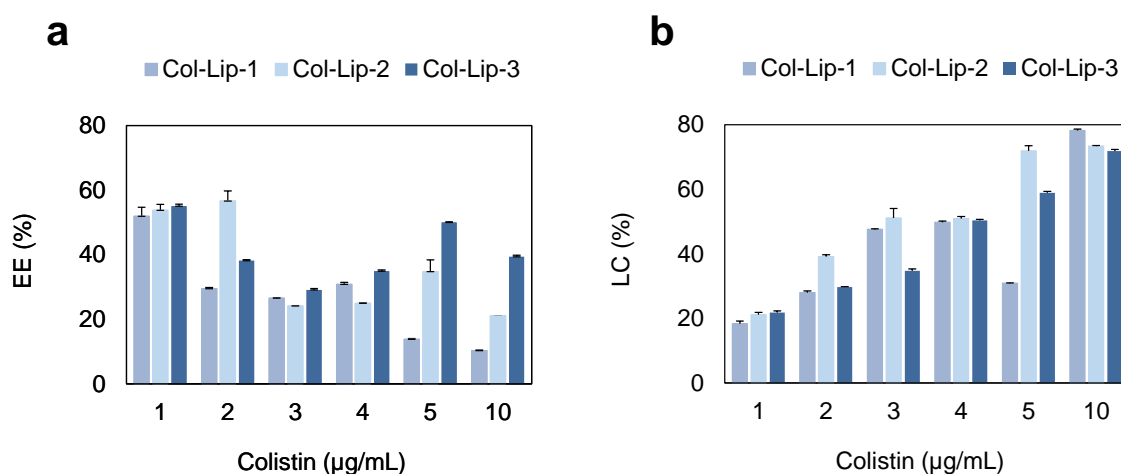


Figure 4.5. Colistin-loaded liposomes properties

The entrapment efficiency (a), loading capacity (b) of Col-Lip-1, Col-Lip-2 and Col-Lip-3 loaded with different concentrations of colistin (1, 2, 3, 4, 5 and 10 mg/mL). Data are shown as mean \pm SEM from three independent experiments ($n=3$, $N=9$).

After comparison of the obtained data for each formulation (Col-Lip-1, Col-Lip-2 and Col-Lip-3) with each concentration (1, 2, 3, 4, 5 and 10 mg/mL), we decide to use 4 mg/mL as standard colistin concentration for the three liposomal formulations. This decision was based on the fact that 4 mg/mL was the optimal compromise between the EE and LC. Moreover, it showed no-to-low differences between the three formulations. Afterwards, an optimization of the preparation process was performed in order to achieve higher entrapment efficiency and loading capacity values (**Table 4**).

Table 4. Characteristics of colistin-loaded liposomes (4 mg/mL) after optimization

Liposomes	Size (nm)	PDI	ζ-Potential (mV)	EE (%)	LC (%)
<i>Col-Lip-1</i>	211.8 ± 1.7	0.05 ± 0.1	-21.0 ± 0.6	55.3 ± 5.2	49.8 ± 0.4
<i>Col-Lip-2</i>	201.3 ± 1.0	0.05 ± 0.1	-17.3 ± 0.3	61.7 ± 5.7	50.9 ± 0.7
<i>Col-Lip-3</i>	202.7 ± 1.4	0.03 ± 0.1	-15.3 ± 1.2	59.3 ± 4.3	50.4 ± 0.3

4.3 Stability studies for the oral route

Stability of liposomes in storage conditions (at 4° C) over time did not show major changes in terms of colloidal properties for all liposomes, except Col-Lip-1 containing 2 mg/mL and 10 mg/mL of colistin, showed an increase in size to 300 nm after 15 days (**Figure 4.6 a**). However, the size decreased to 200 nm during the two following weeks. The increase in size of the two formulations was accompanied with an increase in PDI from 0.08 and 0.12 to 0.25 and 0.24 respectively, and a PDI values ranging from 0.03 to 0.15 were observed with other concentrations (**Figure 4.6 b**). Similar pattern was observed with Col-Lip-2 loaded with 3 mg/mL of colistin after one week and loaded with 2 mg/mL after 3 weeks (**Figure 4.6 d, e**). While, Col-Lip-3 containing 3 mg/mL of colistin exhibited a size of 300 nm after preparation and showed some size fluctuations each week to reach approximately 200 nm in the fourth week (**Figure 4.6 g, h**). In all cases, no notable changes in surface charge were seen during the tested period (**Figure 4.6 c, f, I** for Col-Lip-1, Col-Lip-2 and Col-Lip-3 respectively).

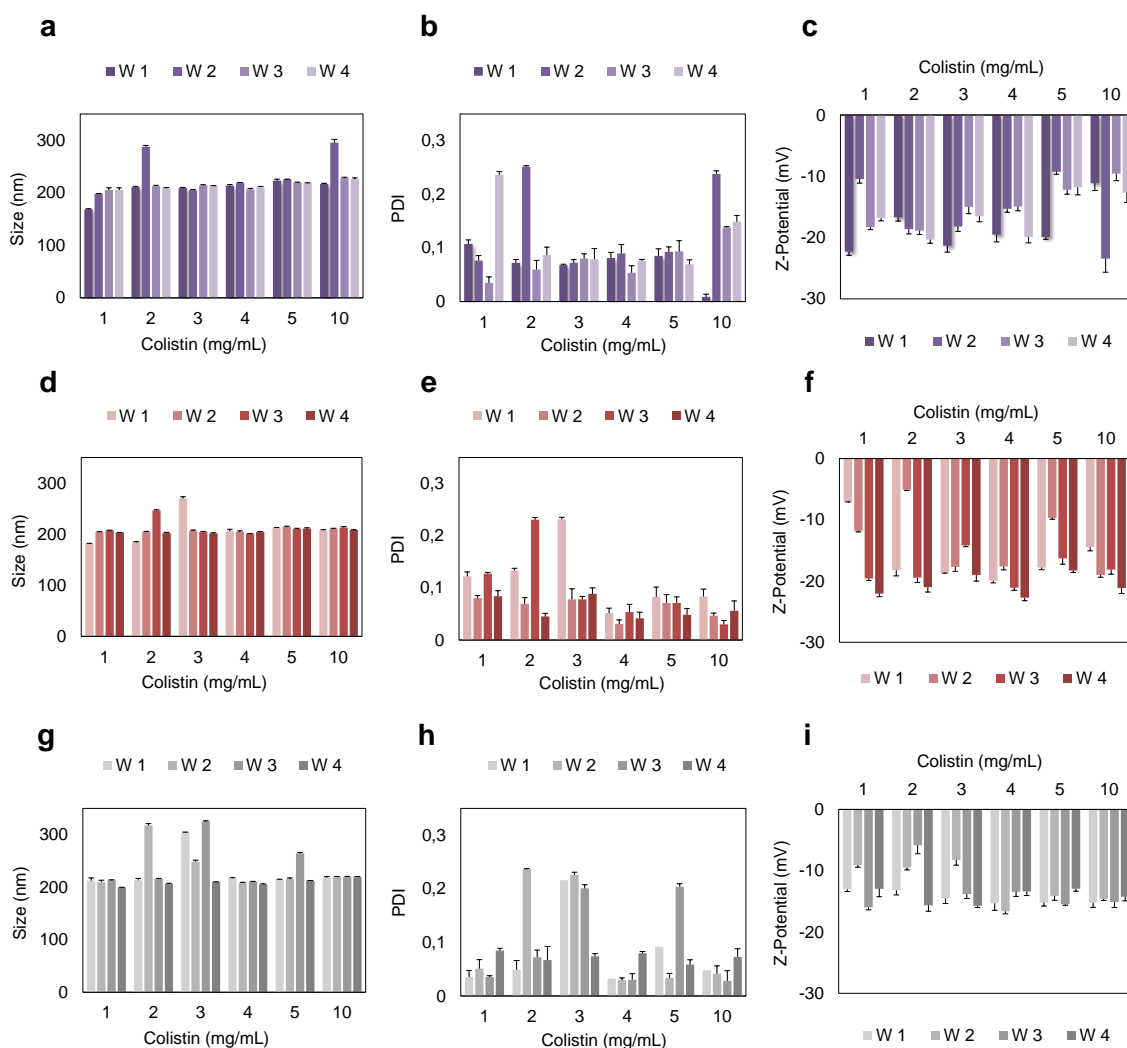


Figure 4.6. Stability characteristics of colistin-loaded liposomes

Size, PDI and ζ -potential values of Col-Lip-1 (a, b and c), Col-Lip-2 (d, e and f) and Col-Lip-3 (g, h and i) loaded with 1, 2, 3, 4, 5 and 10 mg/mL of colistin. Measurements were taken every week after preparation over 4 weeks. Data are shown as mean \pm SEM from three independent experiments ($n=3$, $N=9$).

Colloidal parameters of Col-Lip-1, Col-Lip-2, and Col-Lip-3 after incubation in FaSSGF and FaSSIF showed an optimum stability after 5 h in terms of size and PDI without major changes between both simulated media compared to the control (PBS) (**Figure 4.7**). While, their incubation in FaSSIF_{Enz} (which contains lipase, protease and amylase) resulted in a dramatic increase in size (>600 nm) (**Figure 4.7 a**) with heterogeneous size distribution indicated by PDI values ≥ 0.4 (**Figure 4.7 b**). Incubation of Col-Lip-1, Col-Lip-2 and Col-Lip-3 in FeSSIF

resulted in particles with a slight increase of size compared to control of approximately 250 nm, 210 nm and 350 nm respectively. Moreover, a polydispersity of particles was also observed especially with Col-Lip-1 and Col-Lip-3 ($PDI \geq 0.4$), while a PDI of 0.3 was measured for Col-Lip-2. Regarding the surface charge, in FaSSGF, an increase from -12 mV to -23 mV (Col-Lip-1), from -18 mV to -22 mV (Col-Lip-2) and from -9 mV to -18 mV (Col-Lip-3) was observed. However, these values followed a decreasing pattern in FaSSIF and FaSSIF_{Enz} reaching values below -10 mV for all the formulations (**Figure 4.7 c**). On the other hand, ζ -potential values for all the liposomes increased to -30 mV after incubation in FeSSIF. These results indicate that the lower pH of FaSSGF had mainly effect on the ζ -potential; enzymes addition to intestinal simulated fluid caused the largest change in size/size distribution. While, high concentration of salts and phospholipids in FeSSIF had an effect on size distribution and charge.

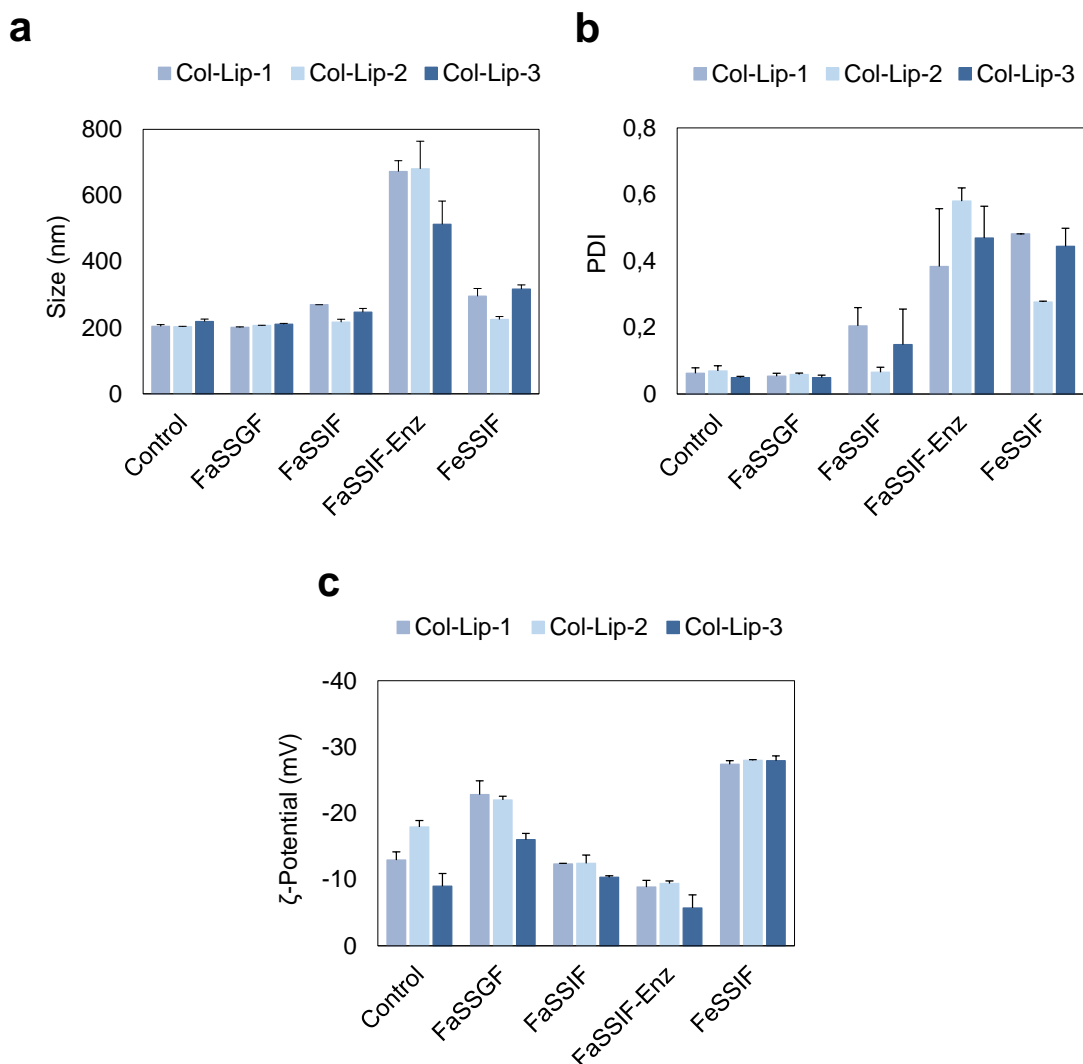


Figure 4.7. Colloidal characteristics in simulated media

(a) Size, (b) PDI, and (c) ζ -potential of Col-Lip-1, Col-Lip-2 and Col-Lip-3 after incubation in different simulated media (FaSSGF, FaSSIF, FaSSIF_{Enz} and FeSSIF) and PBS as a control. The experiment was conducted at 37° C for 5 h. Data are shown as mean \pm SEM from three independent experiments ($n=3$, $N=9$).

Colistin retention results over 5 h incubation in simulated media are shown in **Figure 4.8**. All liposomal formulations showed a release of less than 4 % in PBS. However, a burst release reaching a maximum of 20% was detected after incubation of Col-Lip-1 in all biorelevant media with a colistin retention of approximately 75% in FaSSGF, FaSSIF, and FaSSIF_{Enz} after the 5 h. While, a

release of $\leq 60\%$ was detected in FeSSIF (**Figure 4.8 a**). While, a retention of $\geq 80\%$ of colistin was seen after incubation of Col-Lip-2 (**Figure 4.8 b**) and Col-Lip-3 (**Figure 4.8 c**) in all simulated media characterized with a slower release compared to Col-Lip-1. After analysis and comparison of the obtained data, only Col-Lip-2 and Col-Lip-3 were carried for further experiments due to the instability of Col-Lip-1.

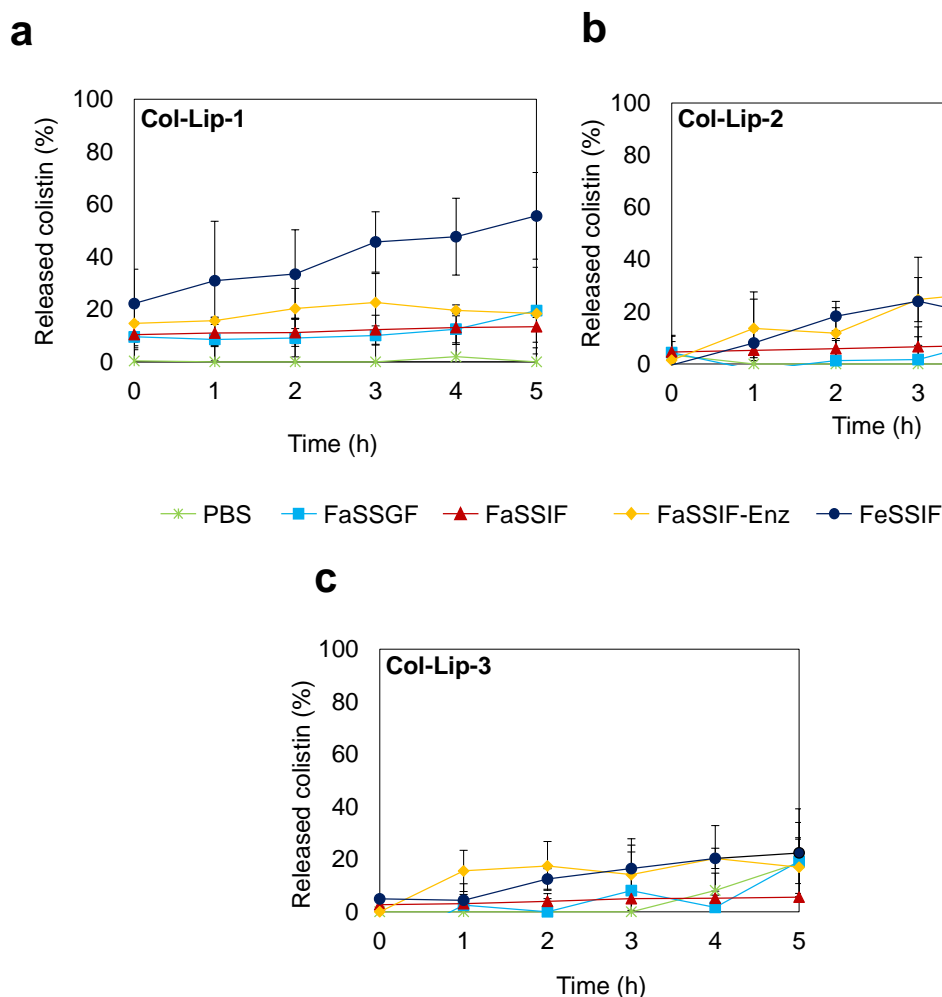


Figure 4.8. Colistin release kinetics in simulated media

Released amount of colistin from Col-Lip-1 (a), Col-Lip-2 (b) and Col-Lip-3 (c) after incubation in different media (FaSSGF, FaSSIF, FaSSIF_{Enz} and FeSSIF) in comparison to control (PBS) after 5 h test period and incubation at physiological temperature (37° C). Released amount at each time point was normalized to the total amount of colistin encapsulated in each formulation and determined before

the incubation. Data are shown as mean \pm SEM from three independent experiments (n= 3, N= 9).

4.4 Eap-functionalized liposomes containing colistin

Liposomes loaded with colistin (Col-Lip-2 and Col-Lip-3) were functionalized with Eap using different methods, including covalent coupling (Cov) using either EDC/NHS or DMTMM reagents or physical adsorption (Phy) achieved by a direct incubation of liposomes with Eap. Quantification of coupled and/or adsorbed Eap on liposomal surface was not possible using common proteins quantification assays such as BCA assay or Bradford assay due to the interference of polypeptide “colistin”, therefore SDS-PAGE was used to estimate the approximate amount of Eap on liposomal surface. Results showed clear Eap bands around 55 kDa with all Eap-functionalized liposomes and no detectible bands with non-functionalized liposomes, indicating the successful coupling and/or adsorption of Eap on liposomal surface (**Figure 4.9 a**). Regarding the functionalization efficiency, covalent linking using EDC/NHS lead only to 37% of functionalization efficiency for EapCol-Lip-2 and 44% for EapCol-lip-3 (**Figure 4.9 b**). Covalent coupling using DMTMM reagent lead to approximately 39% and 57% functionalization efficiency for EapCol-Lip-2 and EapCol-Lip-3 respectively, while incubation of Eap with liposomes for physical surface adsorption lead to a FE of approximately 53% for EapCol-Lip-2 and 74% for EapCol-Lip-3 (**Figure 4.9 b**).

Eap coupled via surface adsorption on EapCol-Lip-3 surface showed the highest FE; therefore, only this formulation was carried further to investigate uptake kinetics and antibacterial efficacy.

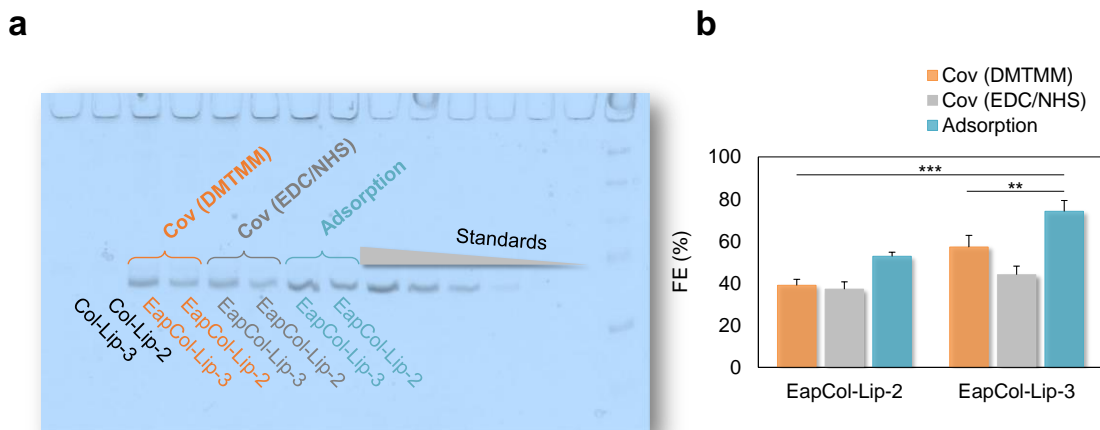


Figure 4.9. Functionalization efficiency

(a) SDS-PAGE of Eap standards (5, 10, 20, 30, 40 and 50 $\mu\text{g/mL}$), non-functionalized liposomes (Col-Lip-2 and Col-Lip-3) and Eap-functionalized liposomes (EapCol-Lip-2 and EapCol-Lip-3). (b) Functionalization efficiency of EapCol-Lip-2 and EapCol-Lip-3 calculated using Image J. Liposomes were functionalized with Eap either covalently [Cov (DMTMM) and Cov (EDC/NHS)] or physically via adsorption on liposomal surface (adsorption). Data are shown as mean \pm SEM from three independent experiments ($n=3$, $N=9$).

Eap-functionalized liposomes were characterized also in terms of colloidal parameters, after functionalization. Results showed that the size as well as the PDI increased dramatically to ≥ 1000 nm and ≥ 0.7 respectively using both functionalization methods; covalent coupling [Eap (Cov)] or surface adsorption [Eap (Ads)] (**Figure 4.10 a, b**). This increase is caused by the aggregation of liposomes once interacting with Eap, since Eap is characterized with its adhesive properties (clear flakes were detected by eye after incubation of liposomes with Eap). Therefore, liposomes were subjected after functionalization to a sonication cycle, which lead to restoration of their initial size of approximately 200 nm with a PDI below 0.2. All liposomal formulations showed a surface charge of about -20 mV after sonication (**Figure 4.10 c**).

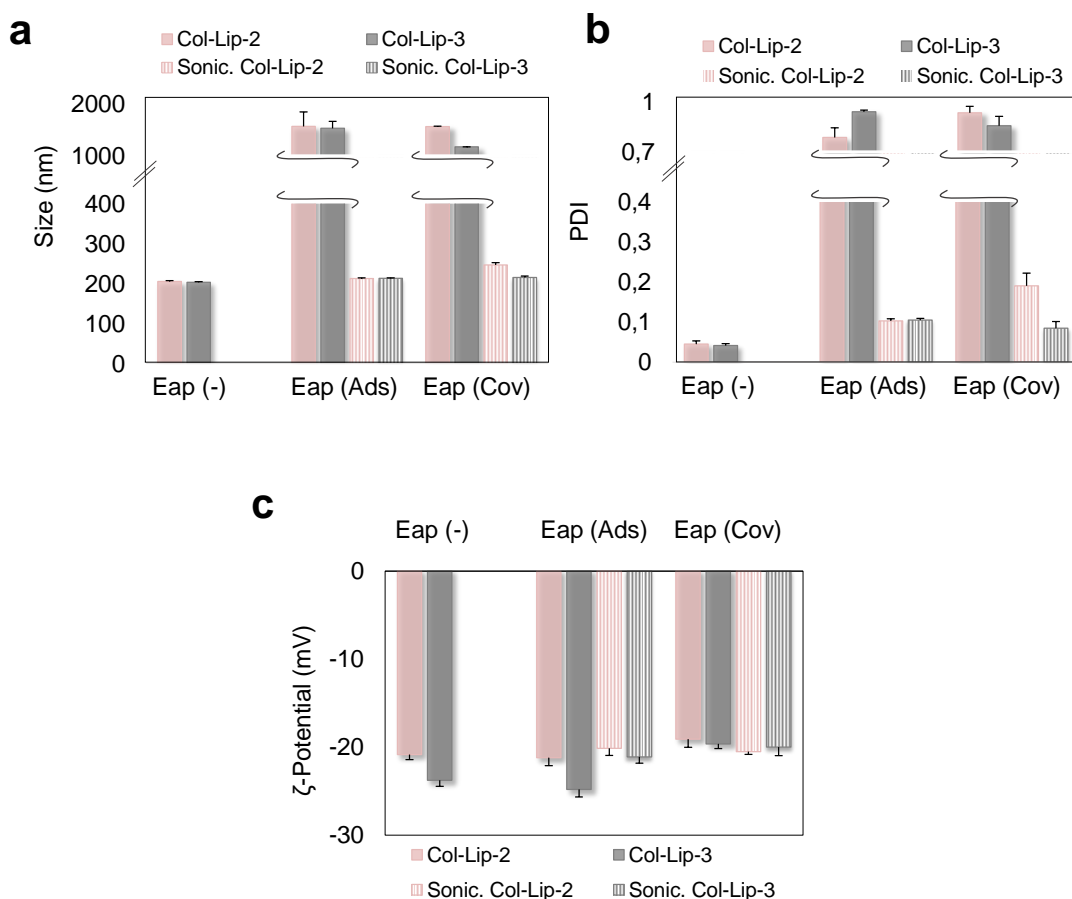


Figure 4.10. Colloidal characteristics of Eap-functionalized liposomes

(a) Size, (b) PDI and (c) ζ -potential of colistin-loaded liposomes (Col-Lip-2 and Col-Lip-3) and sonicated-colistin-loaded liposomes (Sonic. Col-Lip-2 and Sonic Col-Lip-3) without functionalization [Eap (-)], Eap-functionalized via surface adsorption [Eap (Ads)] and Eap-functionalized via covalent coupling [Eap (Cov)]. Data are shown as mean \pm SEM from three independent experiments ($n=3$, $N=9$).

Stability of sonicated liposomes was monitored over a short time period to ensure the stable state of particles after sonication process and investigate whether the presence of Eap will lead to a reversible aggregation effect (**Figure 4.11**). Results showed that liposomes were stable in terms of colloidal properties after sonication during the tested period and no major changes in size or PDI were detected (**Figure 4.11 a, b**). Regarding ζ -potential, the negative surface charge did not shift much with all the samples except EapCol-Lip-3, where a decrease from -25

mV to -20 mV after sonication but only with liposomes functionalized via surface adsorption was observed (**Figure 4.11 c**). Despite, the stability of Eap-functionalized liposomes after sonication, it has been decided to use liposomes freshly functionalized and sonicated for further studies.

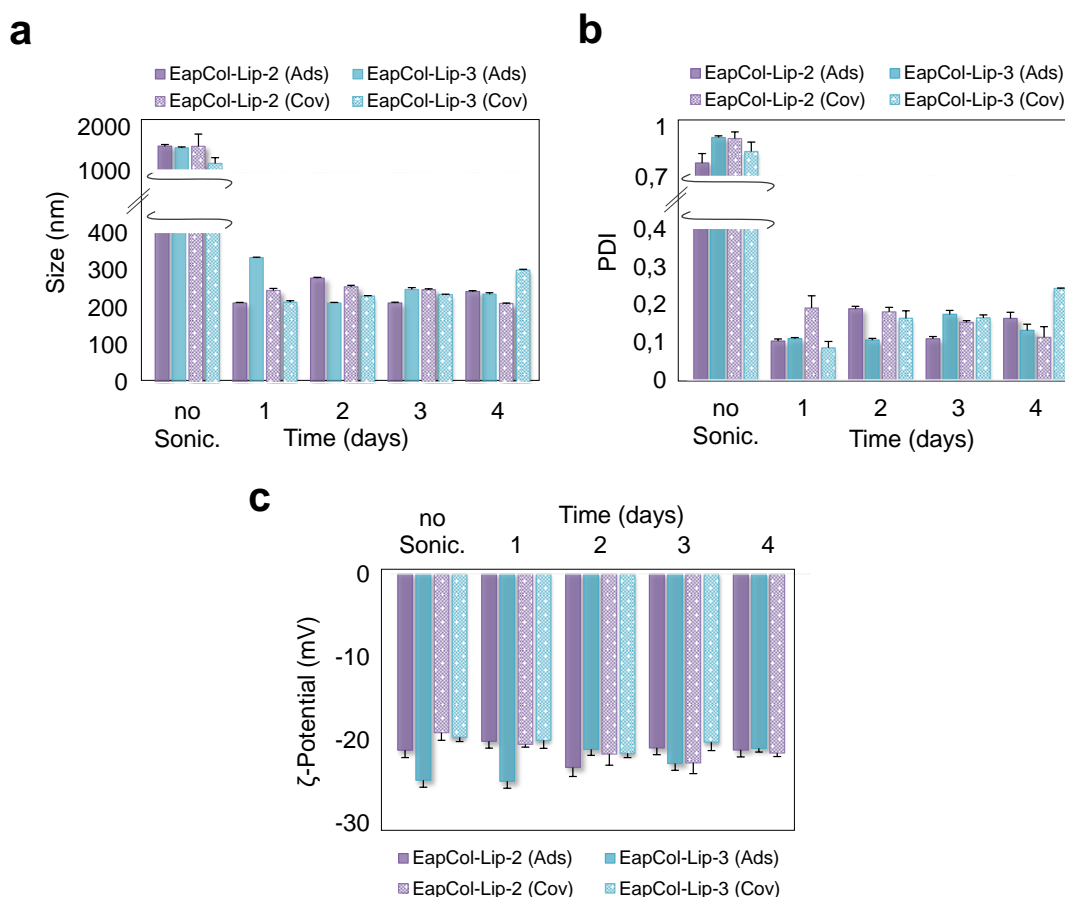


Figure 4.11. Stability of Eap-functionalized liposomes

(a) Size, (b) PDI and (c) ζ -potential of colistin-loaded liposomes functionalized with Eap subjected to two cycles of sonication using 50% amplitude for 30 seconds each with an interval of 2 min (EapCol-Lip-2 and EapCol-Lip-3) in comparison to non-sonicated Eap-functionalized liposomes (no Sonic.). Functionalization was performed either via adsorption (Ads) or covalently coupled (Cov). Data are shown as mean \pm SEM from three independent experiments ($n=3$, $N=9$).

4.5 *In vitro* cellular studies

4.5.1 Intestinal barrier model

Epithelial cells of the Caco-2 cell line, were used as a model for the intestinal cellular barrier. Cells were cultured on Transwells inserts with a semipermeable filters for 7 days to form tight junctions. TEER measurements taken every second day showed values $< 200 \Omega \cdot \text{cm}^2$ during the first 5 days followed by an increase of the transepithelial resistance to reach $2000 \Omega \cdot \text{cm}^2$ on day 8 (**Figure 4.12 a**). Values $\geq 500 \Omega \cdot \text{cm}^2$ were considered as an indication of barrier formation. This barrier is characterized by the formation of tight junctions which was confirmed using an immunostaining of Zonula occludens-1 (ZO-1) at day 7. ZO-1 as a scaffold protein, called also tight junction protein-1, is a 220 kDa peripheral membrane protein that cross-links tight junction strand proteins located within lipid bilayer to the actin cytoskeleton. Immunofluorescence image showed nice formed tight junctions stained in green with red actin filaments (**Figure 4.12 b**).

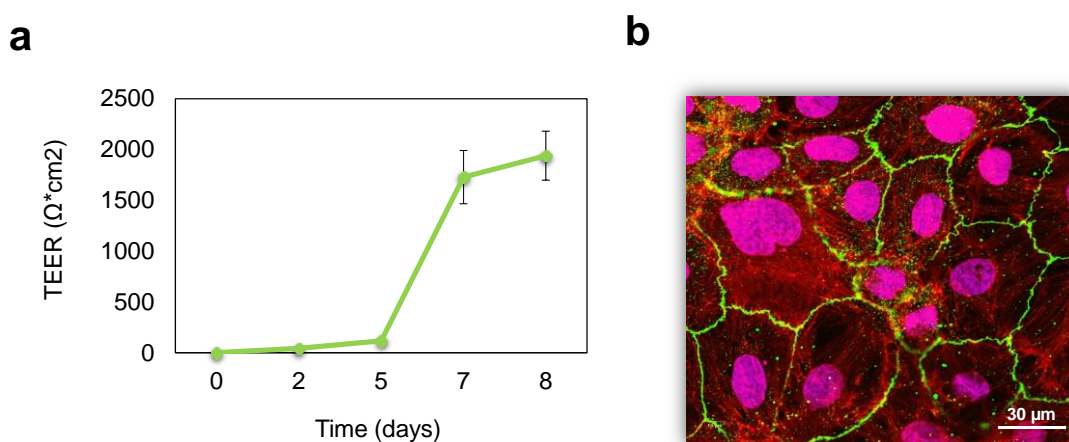


Figure 4.12. Caco-2 monolayer properties

(a) Development of TEER for Caco-2 grown on Transwell inserts equipped with semipermeable filters. TEER measurements were taken every second day for a period of 8 days. Data are shown as mean \pm SEM from three independent experiments ($n=3$, $N=9$). (b) Immunofluorescence staining of Caco-2 monolayer showing clear cell to cell contact ZO-1 stained in green using Alexa 488, actin

filament stained in red using Phalloidin and nucleus in purple (red and blue) using DAPI.

4.5.2 Cytotoxicity assessment

The effect of liposomes application of on cell viability was investigated using MTT assay. Unloaded liposomes, colistin-loaded liposomes or Eap-functionalized liposomes containing colistin were tested using three different liposome concentrations (15, 120 and 750 $\mu\text{g}/\text{mL}$) which covers the concentrations of liposomes used for all cell-based assays. Colistin as free drug as well as Eap were also tested on HEp-2 cells and Caco-2 monolayer as controls and incubation was defined as 4 h for all samples. Colistin concentrations from 1 $\mu\text{g}/\text{mL}$ to 500 $\mu\text{g}/\text{mL}$ did not show any toxicity on HEp-2 cells (**Figure 4.13 a**) neither on Caco-2 monolayer (**Figure 4.13 b**), except the 1 mg/mL colistin concentration showed a 50% cell death of HEp-2 cells whereas no effect was seen with Caco-2 monolayer using same concentration. On the other hand, incubation of HEp-2 cells (**Figure 4.13 c, e**) and Caco-2 monolayer (**Figure 4.13 d, f**) with Lip-2, Lip-3, Col-Lip-2, Col-Lip-3, EapCol-Lip-2 and EapCol-Lip-3 did not show any notable cytotoxicity within tested range of concentrations.

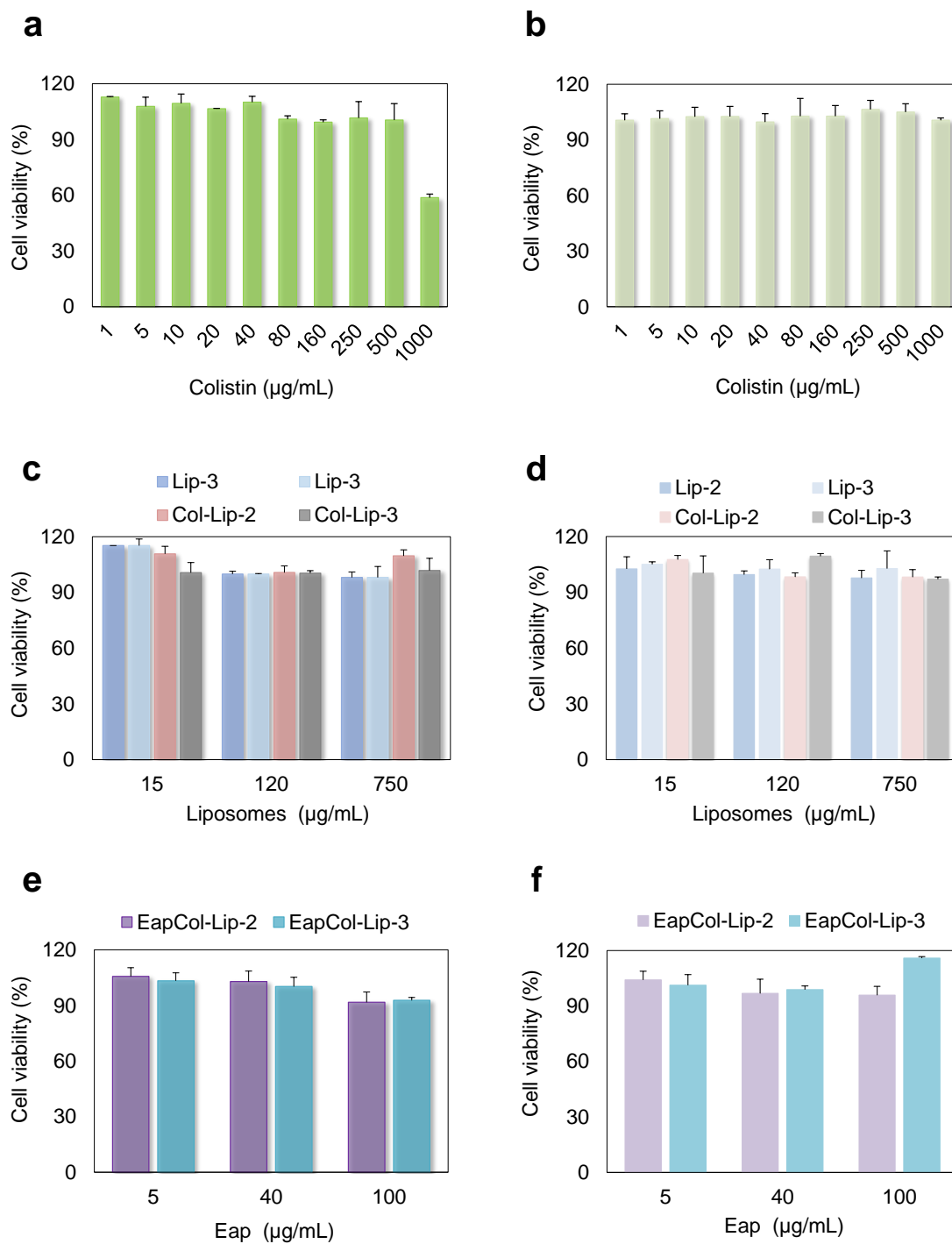


Figure 4.13. Cytotoxicity results

HEp-2 cells and Caco-2 cells were incubated with colistin (a, b), unloaded liposomes (Lip-2 and Lip-3), Colistin-loaded liposomes (Col-Lip-2 and Col-Lip-3) (c, d) and Eap-functionalized liposomes containing colistin (EapCol-Lip-2 and EapCol-Lip-3) respectively. Cells were incubated with samples for 4 h at 37°C

and 5% CO₂. Data are shown as mean \pm SEM from three independent experiments ($n=3$, $N=9$).

4.5.3 Eap mediates the binding/internalization of liposomes into epithelial cells

HEp-2 cells and Caco-2 monolayer were employed in this experiment to assess the ability of Eap to mediate the binding and the internalization of liposomes into the cells. Col-Lip-3 was used for the following studies and Eap functionalization was conducted using surface adsorption. Uptake of Col-Lip-3 by HEp-2 cells was negligible while incubation of Caco-2 monolayer with Col-Lip-3 induced 35% uptake (rhodamine-positive cells percentage determined using flow cytometry) of these nanocarriers (**Figure 4.14 a, c** respectively). On the other hand, application of EapCol-Lip-3 on HEp-2 cells as well as on Caco-2 monolayer, functionalized with different concentrations of Eap (5, 10 and 20 $\mu\text{g/mL}$) showed a concentration- and time-dependent uptake. After 1 h incubation of cells with EapCol-Lip-3 (5 $\mu\text{g/mL}$), only 5% of HEp-2 cells and 12% of Caco-2 cells showed a positive-rhodamine fluorescence, however increasing the incubation time to 2 h showed a significant increase of the uptake efficiency of approximately 47% and 42% respectively (**Figure 4.14 a, c**). The use of 10 $\mu\text{g/mL}$ Eap-functionalized Col-Lip-3 showed an uptake of 32% (and 45% by HEp-2 cells (1 h) and Caco-2 cells (2 h) respectively, further incubation induced a significant increase of rhodamine-positive HEp-2 cells (2 h) and Caco-2 monolayer (4 h) to 99% and 83% respectively as shown in **Figure 4.14 a, b**. Utilization of 20 $\mu\text{g/mL}$ of Eap to functionalize liposomes showed an improvement of the uptake efficiency from 88% to 99% by HEp-2 cells after 1 h and 2 h respectively, and from 76% to 97% by Caco-2 cells after 2 h and 4 h respectively. However, 2 h incubation time of Eap-Col-Lip-3 either with 10 $\mu\text{g/mL}$ or 20 $\mu\text{g/mL}$ by HEp-2 cells showed a saturation achieving almost 100% of rhodamine-positive cells. Flow cytometry histograms showed a clear gradually shift of EapCol-Lip-3 (with a concentration-dependence) on the red fluorescence channel (PE) with both cell types HEp-2 cells (2 h) and Caco-2 monolayer (4 h) compared to the control (without liposomes) (**Figure 4.14 b, d**).

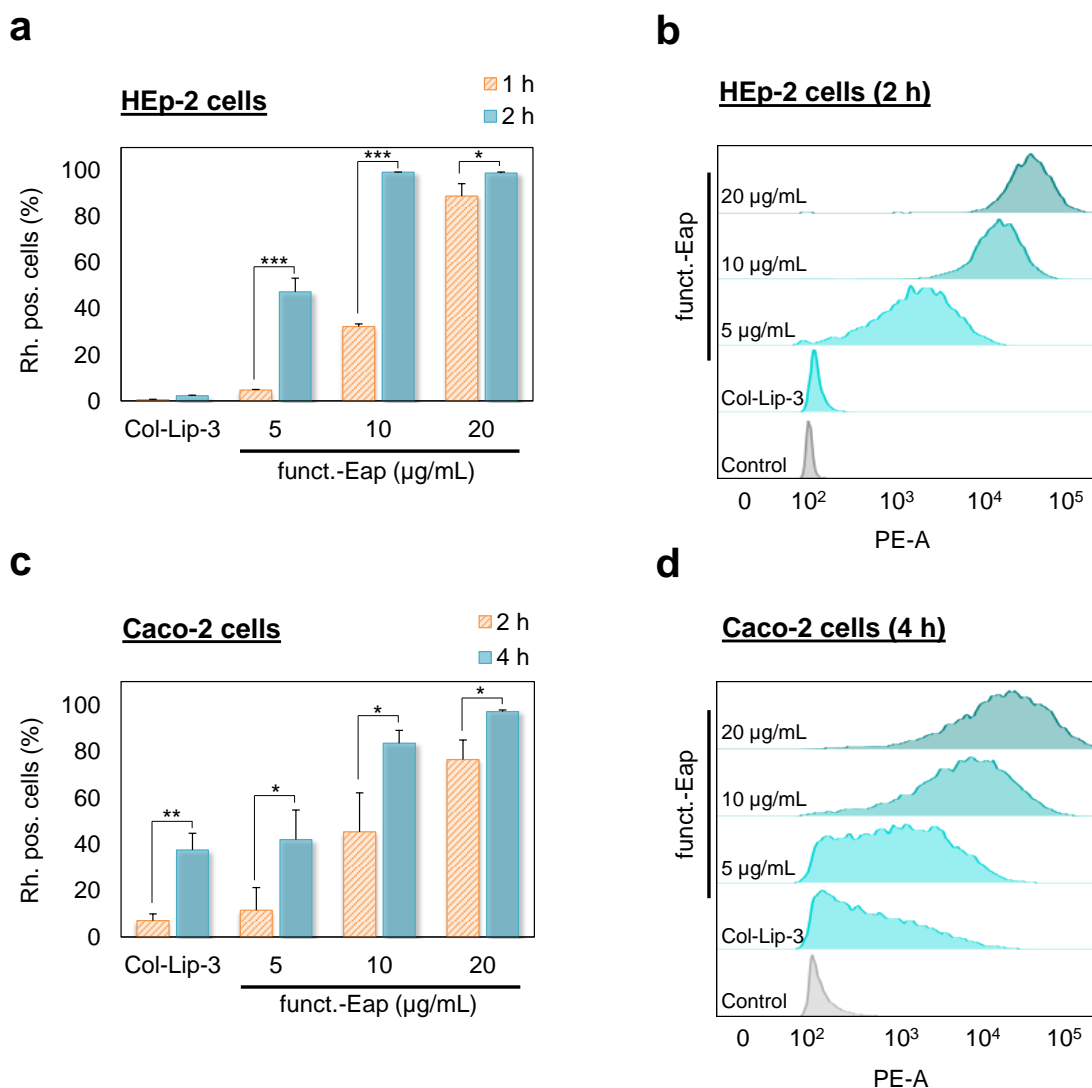


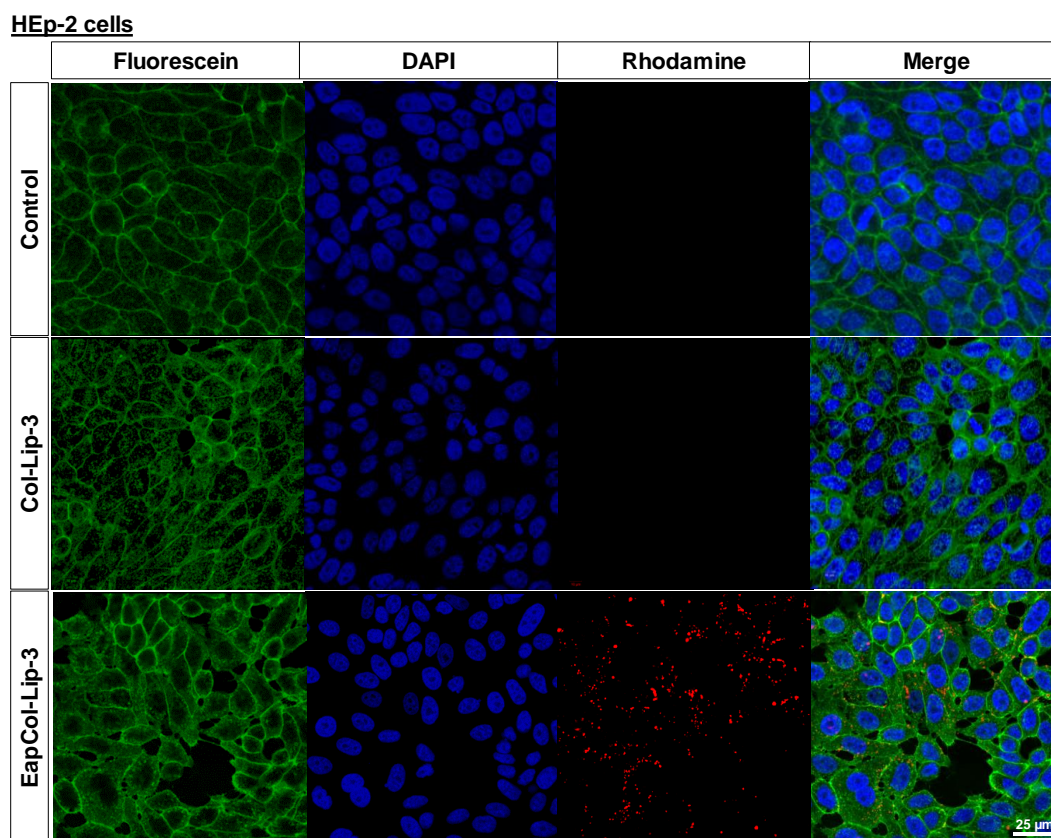
Figure 4.14. Uptake efficiency

Percentage of rhodamine-positive HEP-2 cells (a) and Caco-2 cells (c) as well as a representative flow cytometry histograms of HEP-2 cells (2 h, b) and Caco-2 cells (4 h, d) after incubation with non-functionalized Col-Lip-3 and EapCol-Lip-3 functionalized with either 5, 10 or 20 $\mu\text{g/mL}$ of Eap. Non-treated cells were used as a control. Data are shown as mean \pm SEM from three independent experiments ($n=3$, $N=9$). Statistical difference is considered significant with P-value < 0.05 (*), < 0.01 (**) and < 0.001 (***).

Imaging of liposomal internalization into HEP-2 cells and Caco-2 monolayer was performed using CLSM. Cells were cultured either on 24-well plate with transparent bottom or cover slips (HEP-2 cells) and on Transwells insert mounted

afterwards on microscope slides (Caco-2 cells). Uptake study was performed as described in flow cytometry setup, in addition cell membrane was stained with Flu-WGA (green), nucleus with DAPI (blue) after fixation with paraformaldehyde and liposomes were labeled covalently with rhodamine (red) during preparation. Images showed no noticeable red fluorescent on HEp-2 cells after incubation with Col-Lip-3 (**Figure 4.15 a**), while, a detectable red fluorescence in Caco-2 cells indicating an uptake of Col-Lip-3 at some extent (**Figure 4.15 b**), which support the data obtained from the flow cytometry. On the other hand, application of EapCol-Lip-3 on HEp-2 cells (for 2 h, **Figure 4.15 a**) and Caco-2 cells (for 4 h, **Figure 4.15 b**), showed a high red fluorescence indicating higher uptake in comparison to non-functionalized liposomes or to the control (non-treated cells).

a



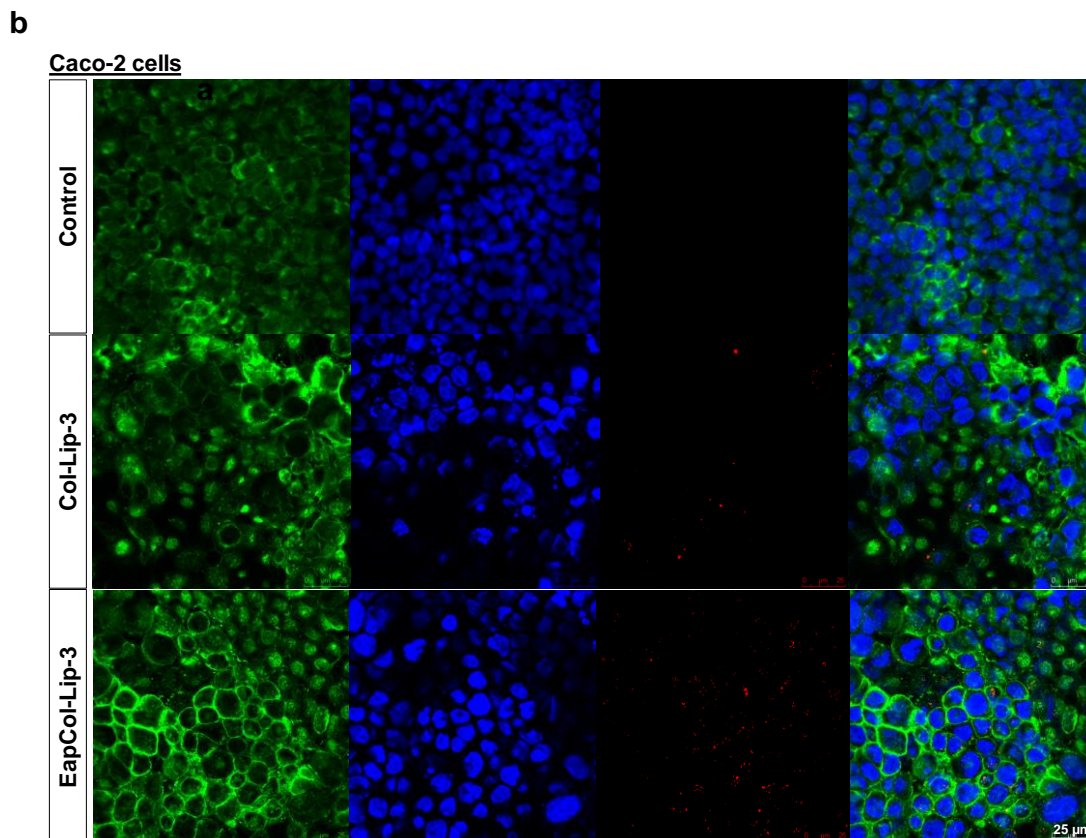


Figure 4.15. Uptake imaging

Representative confocal images of Col-Lip-3 and EapCol-Lip-3 (functionalized with 20 $\mu\text{g}/\text{mL}$ Eap) uptake by (a) HEP-2 cells (2 h) and (b) Caco-2 cells (4 h) in comparison to non-treated cells. Cell membrane was stained in green (Fluorescein), nucleus in blue (DAPI) and liposomes in red (rhodamine). Images were taken with 25x water immersion, using 533 nm, 488 nm and 720 nm excitation wavelengths for rhodamine-labeled liposomes, fluorescein (cell membrane) and DAPI (nucleus) respectively.

A 3D imaging of uptake of EapCol-Lip-3 (functionalized with 20 $\mu\text{g}/\text{mL}$ Eap) using HEP-2 and Caco-2 cells after 2 h and 4 h respectively was conducted (**Figure S3** in supplement), and results supported the 2D images taken in **Figure 4.15** showing a dominant red fluorescence in the red channel which can be also visible in merge picture. An Orth-view imaging with same setup was performed in order to visualize the localization of liposomes into the cells and investigate closely whether liposomes were attached or taken up. Results showed a red

fluorescence in the same level as nucleus rather than on the level of cell membrane indicating that indeed liposomes were internalized into HEP-2 and Caco-2 cells (**Figure S4**).

In order to understand the mechanism behind the internalization of Eap-functionalized liposomes by HEP-2 cells and Caco-2 cells, an uptake experiment at 4° C was performed. The results of EapCol-Lip-3 uptake by HEP-2 cells showed a similar tendency to the uptake performed at 37° C (**Figure 4.16 a**). While, uptake of EapCol-Lip-3 by Caco-2 cells showed a significant decrease in rhodamine-positive cells percentage of approximately 18% compared to uptake at 37° C (**Figure 4.16 a**). Flow cytometry histograms showed a complete peak shift in PE channel (rhodamine/red fluorescence) in HEP-2 cells at 4° C, comparable to 37° C uptake kinetics. While, only a slight shift was seen in case of Caco-2 cells indicating an inhibition process of the uptake was accrued at 4° C in comparison to 37° C (**Figure 4.16 b**). These results indicated that the uptake mechanism of Eap in Caco-2 cells is an energy-dependent process whereas a passive pathway was the main characteristic of EapCol-Lip-3 uptake in HEP-2 cells.

A following experiment investigating deeply the mechanism of uptake in Caco-2 cells using pharmacological endocytosis inhibitors was conducted. The results showed a decrease in the uptake efficiency of approximately 8% after using cytochalasin D, and a decrease of 17% using either chlorpromazine or M β CD + lovastatin. While, 40% of the uptake was inhibited in the presence of caveolin-dependent endocytosis inhibitor "Filipin III" (**Figure 4.16 c**).

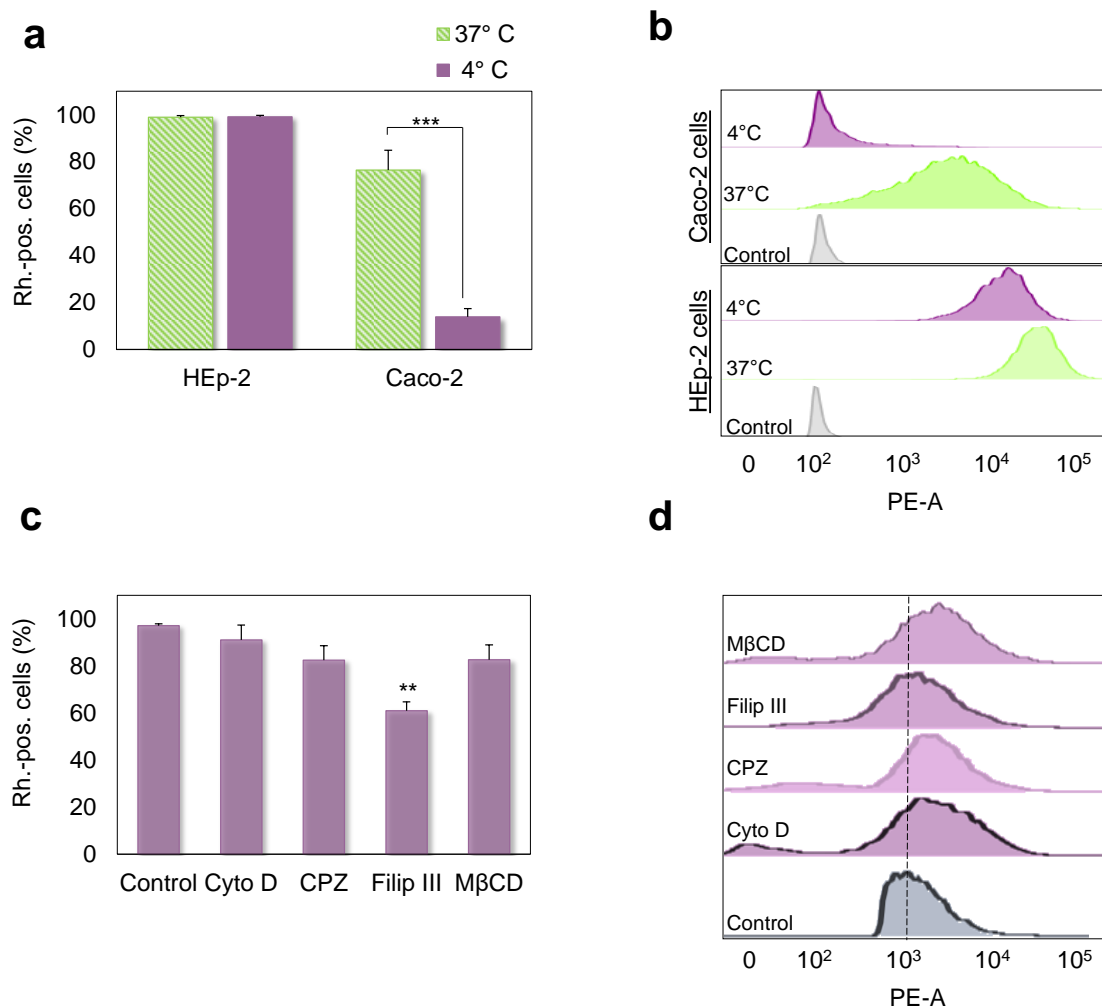


Figure 4.16. Uptake mechanism kinetics

(a) *EapCol-Lip-3* uptake mechanism study on HEp-2 (2 h) and Caco-2 (4 h) cells at 4° C in comparison to uptake at 37° C showed in Figure 4-14 and the corresponding flow cytometry histograms (b). (c) Uptake mechanism study of *EapCol-Lip-3* by Caco-2 cells in presence of endocytosis inhibitors, cytochalasin D (Cyto D), chlorpromazine (CPZ), Filipin III and MβCD in combination with lovastatin. Data are shown as mean \pm SEM from three independent experiments ($n=3$, $N=9$). Statistical difference is considered significant with P -value < 0.05 (*), < 0.01 (**) and < 0.001 (***).

4.6 *Salmonella enterica* growth curve and MIC determination

Salmonella was cultured over time from a single colony of an overnight culture. The OD₆₀₀ of each time point culture was measured and plated on agar plates to be counted colonies. The obtained data set expressing the bacterial growth, was plotted as time versus OD₆₀₀ and bacterial count per mL (CFU/mL) as shown in **Figure 4.17 a**. Growth curve showed a typical bacterial growth characterized by an initial lag phase of 2 h, where bacteria go through an increase of their size and adapting to the environment. Afterwards, *Salmonella* started to divide indicated by the increase of the bacterial count over 2 h defined as exponential growth phase to reach approximately 2×10^{13} CFU/mL. Finally, the bacterial growth went to a stationary phase, in which cellular division was stopped due to a nutrient exhaustion and leading to cellular death. In order to ensure an optimal viability and pathogenicity of bacteria during anti-bacterial efficacy studies, bacterial cultures were all used during their exponential phase. From an overnight culture of *Salmonella*, an OD of 0.7 was inoculated further in fresh Nutrient Broth for 2.5 h at 37° C before use. A morphological identification of *Salmonella's colonies* was conducted using phase contrast microscopy from an overnight culture inoculated in fresh culture medium and plated to microscope slide. *Salmonella* colonies were characterized by a frizzy circular shape with a smoother appearance (**Figure 4.17 b**). However, colonies of *Salmonella* plated on agar plates exhibited the same shape with raised surfaces (**Figure 4.17 c**).

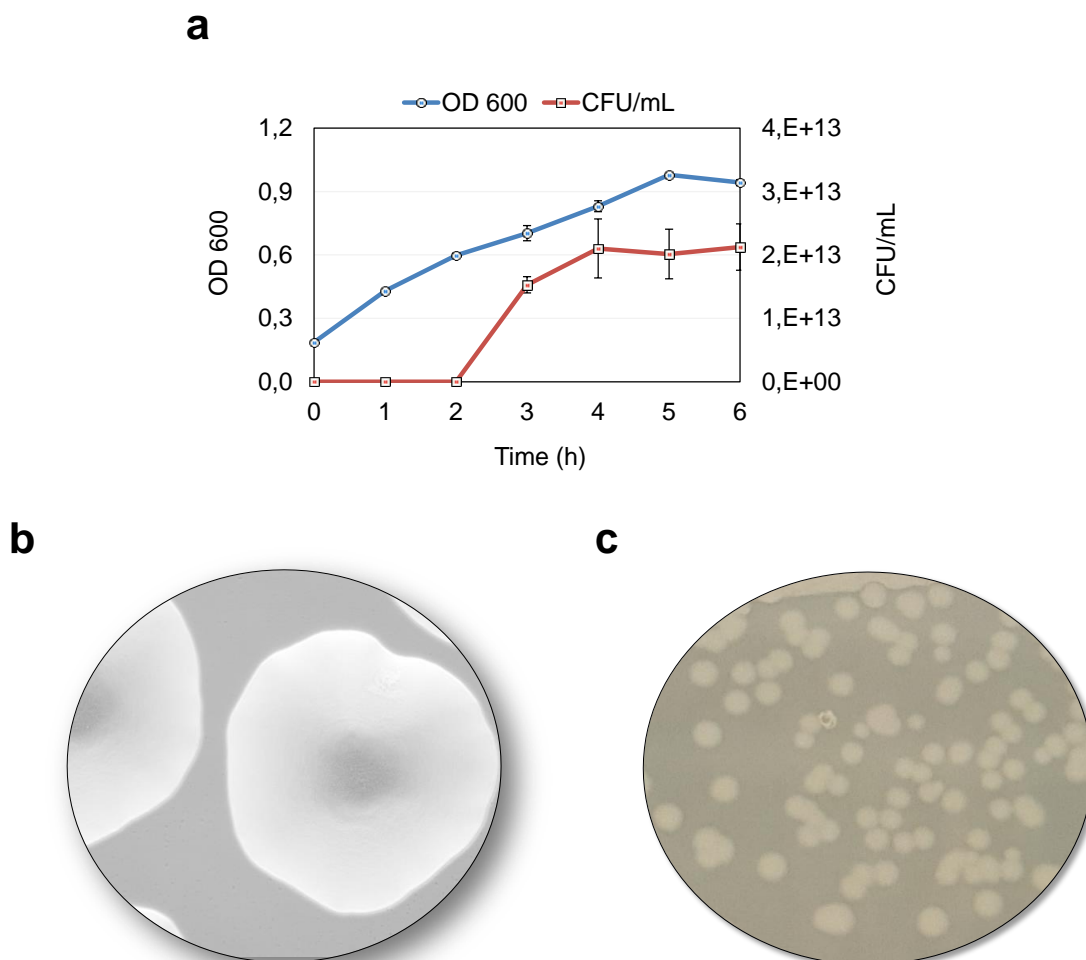


Figure 4.17. Salmonella characteristics

(a) Growth curve expressed as optical density measured at 600 nm (OD_{600}) and number of bacterial colonies (CFU/mL) versus time. (b, c) Images of *Salmonella* colonies in suspension plated on microscopic slide and colonies grown on agar plate respectively.

The minimum inhibitory concentrations were determined after incubation of bacterial cultures of an OD of 0.1 with different treatments including colistin as free drug, Col-Lip-3 and EapCol-Lip-3 using different concentrations between the ranges of 0.125 $\mu\text{g/mL}$ to 128 $\mu\text{g/mL}$. Fitting curves and IC_{50} as well as IC_{90} values are showed in **Figure 4.18**. Results indicated that colistin as free drug had an IC_{50} of 2.63 $\mu\text{g/mL}$ and IC_{90} of 4.14 $\mu\text{g/mL}$ after 18 h incubation period. While, 50% of the bacterial growth was inhibited by 3.10 $\mu\text{g/mL}$ and 3.35 $\mu\text{g/mL}$ using Col-Lip-3 and EapCol-Lip-3 respectively. Moreover, 5.34 $\mu\text{g/mL}$ of Col-Lip-3 and

5.53 $\mu\text{g/mL}$ of EapCol-Lip-3 were required to reach 90% of bacterial growth inhibition. The values for liposomes formulations were higher than colistin drug which was expected as colistin encapsulated into liposomes would require more time to be released, however no significant difference was observed between non-functionalized liposomes and colistin-loaded liposomes functionalized with Eap **Figure 4.18 d**.

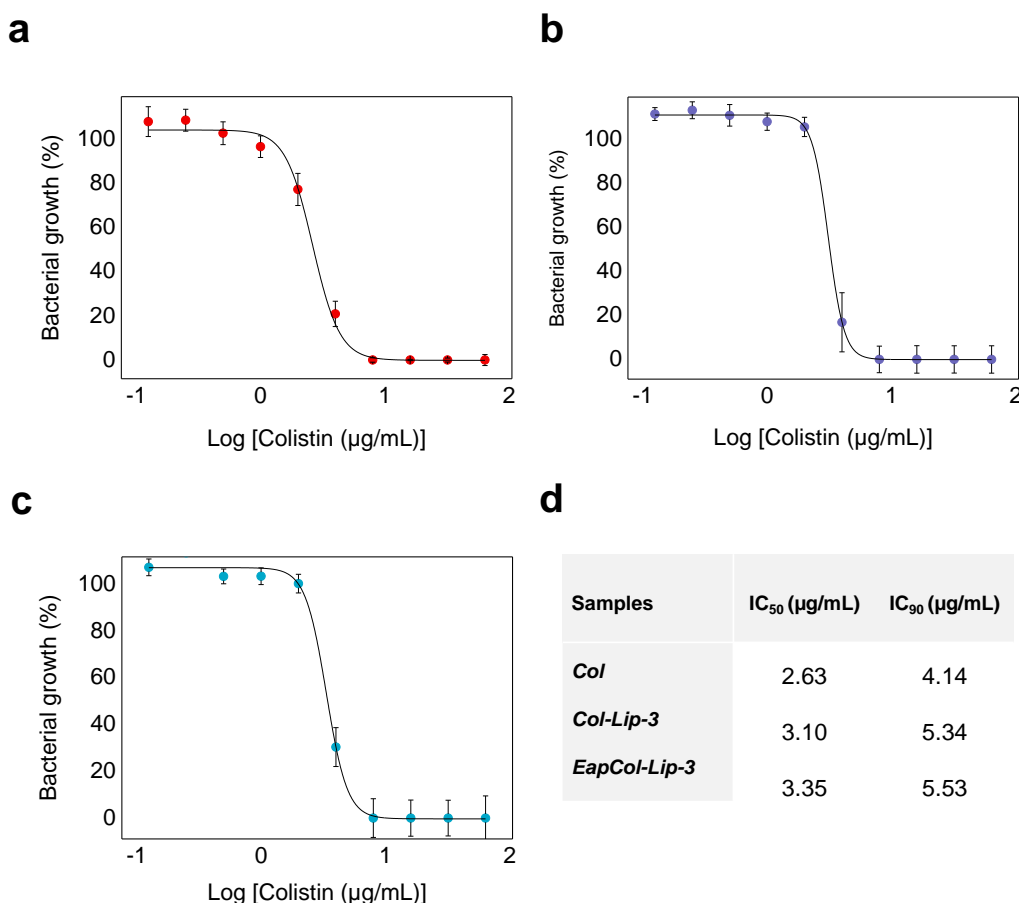


Figure 4.18. *Salmonella* minimum inhibitory concentrations

MIC fitting curves of *Salmonella* treated with colistin in red (*Col*, a), colistin-loaded liposomes in purple (*Col-Lip-3*, b) and Eap-functionalized liposomes, containing colistin in blue (*EapCol-Lip-3*, c) -treated *Salmonella*'s cultured samples over 18 h at 37° C. (d) IC₅₀ and IC₉₀ values of *Col*, *Col-Lip-3* and *EapCol-Lip-3*. Data are shown as mean \pm SEM from three independent experiments (n= 3, N= 9).

4.7 Impact of Eap-functionalized liposomes on infected cells

4.7.1 Infection parameters determination

In order to evaluate the antibacterial efficacy of Eap-functionalized liposomes, loaded with colistin on intracellular *Salmonella*, establishment of an optimal infection settings are required for better interpretation of the efficacy as well as toxicity. HEP-2 cells and Caco-2 monolayer were infected with different MOI (10, 25, 50 and 100) during 1 h incubation time at 37° C. Further treatment of the cells with gentamicin solution to eradicate extracellular *Salmonella* was conducted and cells were then, lysed to count bacterial colonies. Cells morphology was monitored during the study at each stage in order to ensure their viability and well-state after each treatment and treatment duration. Results showed that number of colonies reflecting intracellular *Salmonella* count (CFU/mL) in HEP-2 cells, increased by increasing number of bacteria per cell in following x2 profile with each MOI reaching an maximum of approximately 3 million bacteria/ mL using an MOI of 100 (**Figure 4.19a**).

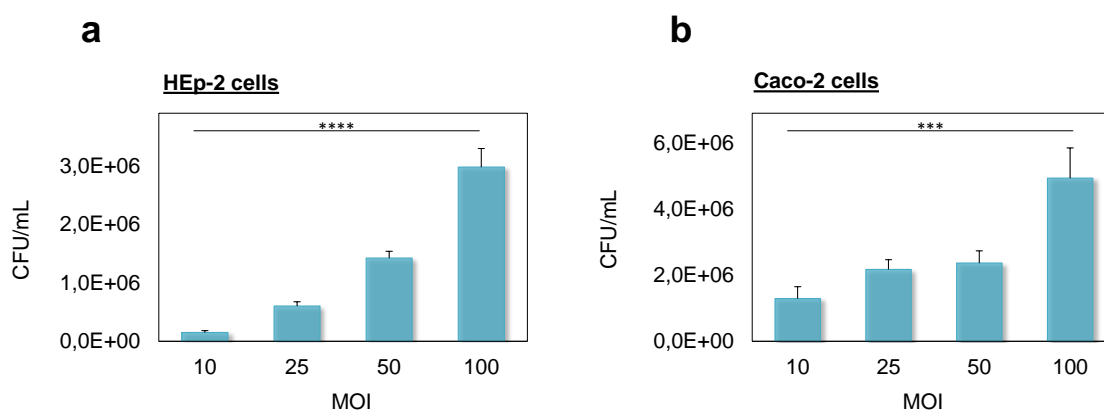


Figure 4.19. Intracellular infection optimization

(a) HEP-2 cells and (b) Caco-2 monolayer infected with MOI of 10, 25, 50 and 100 for 1 h, and further treated with gentamicin solution (50 µg/mL) for 2 h. Cells were lysed and cell lysate was plated on agar plates. Bacterial colonies were counted and expressed as CFU/mL. Data are shown as mean \pm SEM from three

independent experiments ($n= 3$, $N= 9$).). Statistical difference is considered significant with P -value < 0.0001 (****).

On the other hand, number of bacteria which were able to invade Caco-2 monolayer increased slightly by increasing MOI from 10 to 25, and no notable change was observed by using an MOI of 50. However, these values were higher than the values obtained with HEP-2 cells, especially with an MOI of 100, more than 4 million colonies/mL were capable to infect Caco-2 cells (**Figure 4.19 b**). Images of HEP-2 cells after each step were taken to ensure cell viability based on the morphology, no major observation were seen that could indicate cell death or damage except of small number of round-shaped cells which could be seen in all images (**Figure 8.8**). However, imaging of Caco-2 cells was not possible due to Transwells inserts setup.

4.7.2 Antibacterial efficacy of EapCol-Lip-3

HEP-2 cells and Caco-2 monolayer were treated with different liposomal formulations as well as colistin as free drug. A dose of 30 $\mu\text{g/mL}$ colistin was used for the study and 20 $\mu\text{g/mL}$ of Eap was used for functionalization. Colistin as free drug as well as Col-Lip-3 mixed separately with Eap immediately prior treating cells with liposomes were used as controls to evaluate binding affinity of Eap. Results showed that EapCol-Lip-3 were able to reduce significantly the infection load of *Salmonella*-infected HEP-2 cells by 36% compared to Col, Lip-3, Col-Lip-3, as well as to Col and Col-Lip-3 mixed with Eap (**Figure 4.20 a**). Results using Caco-2 monolayer showed a similar tendency of a significant infection reduction; approximately 30% after application of EapCol-Lip-3 in comparison to samples and controls. However, as shown previously in uptake studies that non-functionalized liposomes (Col-Lip-3) were able to be taken up by Caco-2 cells, which was confirmed in this experiment by a decrease of the infection load by 11% after treating Caco-2 cells with Col-Lip-3 (**Figure 4.20 b**). On the other hand, Eap-mixed Col and Eap-Mixed Col-Lip-3, showed a reduction of less than 9% in both cell setups (**Figure 4.20 a, b**).

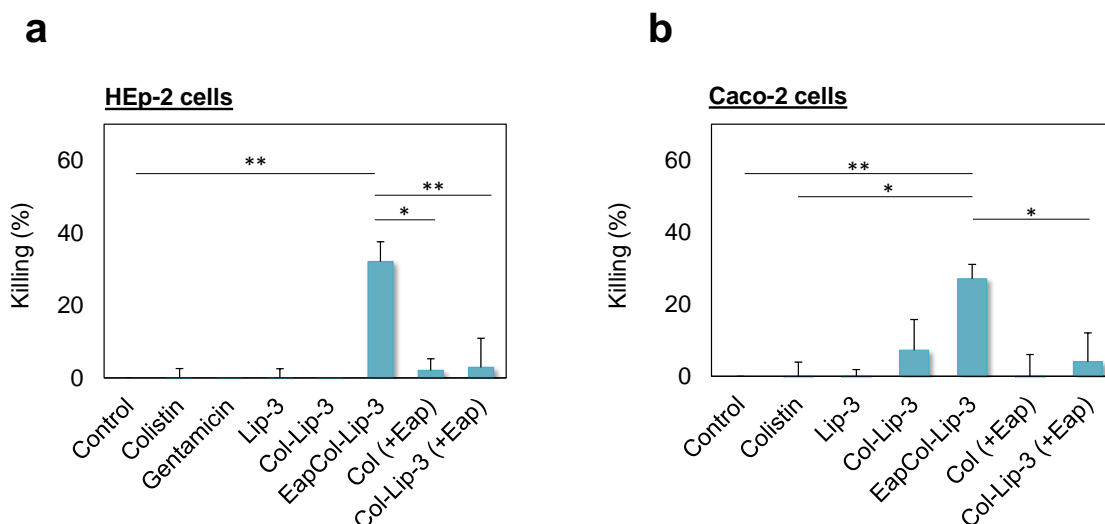


Figure 4.20. Antibacterial efficacy

Killing percentage of Col, Lip-3, Col-Lip-3, EapCol-Lip-3 and Col, Col-Lip-3 mixed with Eap of *Salmonella*-infected HEP-2 cells (a) and *Salmonella*-infected Caco-2 monolayer (b). HEP-2 cells and Caco-2 cells were incubated with all samples and controls (non-treated, infected cells) for 2 h and 4 h respectively at 37° C and 5 % CO₂. Data are shown as mean ± SEM from three independent experiments (n= 4, -N= 12). Statistical difference is considered significant with P-value < 0.05 (*), < 0.01 (**).

4.7.3 Cell viability during infection studies

A cell viability assessment was conducted in order to evaluate the state of infected cells after treatment with liposomes and after several incubation periods during the study. Both cell lines were subjected to a Live/Dead staining after the gentamicin killing of extracellular bacteria. Cells were stained with Live/Dead kit and measured using flow cytometry. Results showed that using liposomal formulations (Lip-3, Col-Lip-3 and EapCol-Lip-3) as well as colistin as free drug (Col) did not cause any cellular death, in which a similar percentage of live cells was obtained with all samples comparable to the control (+) (non-infected and non-treated cells) in both cell lines (**Figure 4.21**). Approximately 10% of dead cells was obtained which reflect the number of lost cells during multiple washing steps, as seen also for the control (+). Cells treated with heat at 50° C used as

control (-) were used to gate the flow cytometer parameters in two areas, live cells with optimal size and optimal granulation situated in the middle of plotted cell dots as forward Scattering (FSC) versus Side scattering (SSC), while dead cells were located on left vertical middle to upper area indicating lower size (debris).

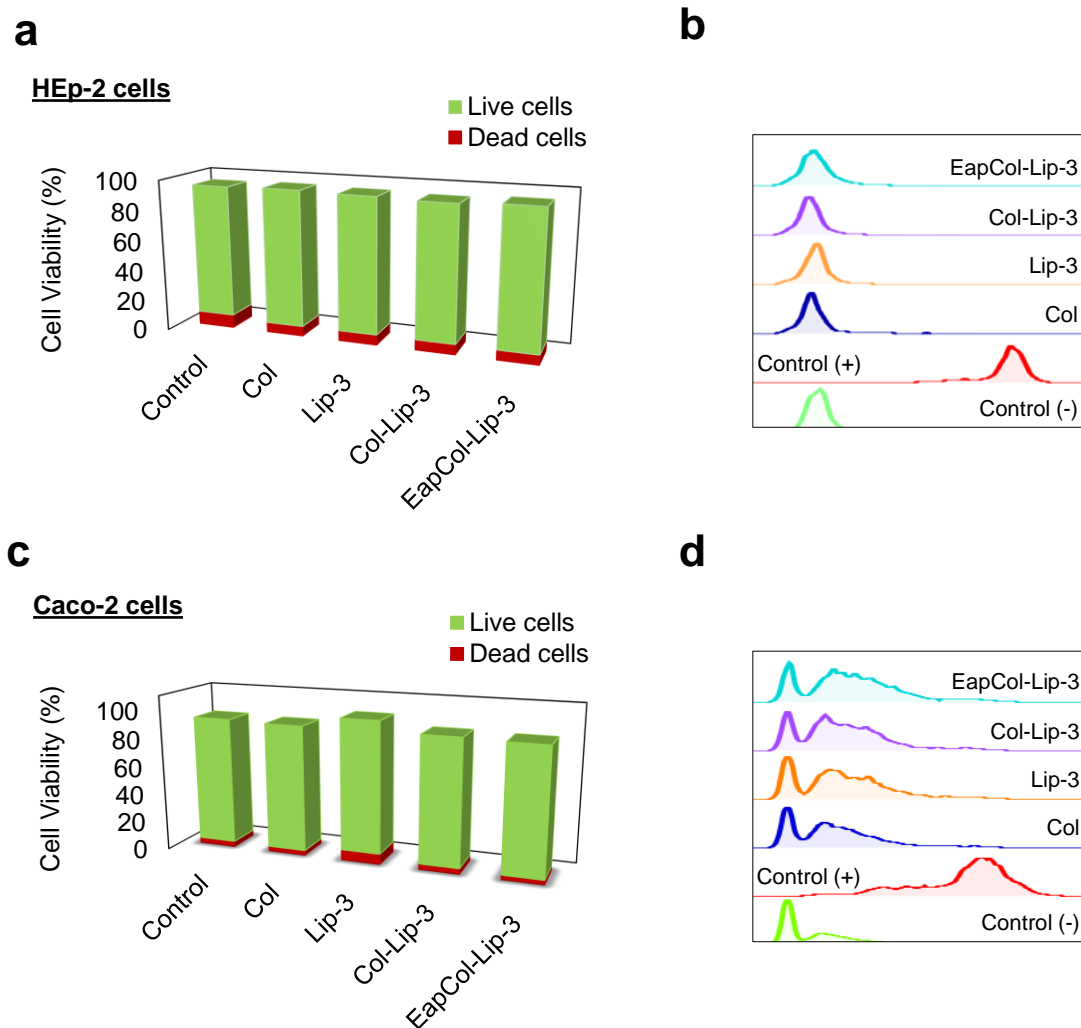


Figure 4.21. Cell viability after infection studies

Viable cells percentage of HEp-2 cells (a) and Caco-2 monolayer (c) using Live/Dead after treatment of Salmonella-infected cells with liposomal formulations Lip-3, Col-Lip-3 and EapCol-Lip-3 as well as colistin as free drug (col). Corresponding flow cytometry histograms of HEp-2 cells (b) and Caco-2 monolayer (d) compared to controls; un-treated cells as control (-) and heat-killed

cells as control (+) as dead cells. Data are shown as mean \pm SEM from three independent experiments ($n=4$, $-N=12$).

4.7.4 Eap dose titration

Liposomes containing 30 $\mu\text{g/mL}$ of colistin were functionalized with different Eap concentrations, to evaluate the potency of Eap to induce liposomal internalization and therefore lead to the highest killing percentage. Results showed an increase of the killing percentage from 17% to approximately 50% by increasing the Eap concentration from 7 $\mu\text{g/mL}$ to 20 $\mu\text{g/mL}$ in HEP-2 cells. However, using 40 $\mu\text{g/mL}$ of Eap did not show any significant increase of the antibacterial effect of liposomes (**Figure 4.22 a**). On the other hand, results of Caco-2 cells, showed a 22 % decrease of infection load using Col-Lip-3 functionalized with 7 $\mu\text{g/mL}$ of Eap, an increase of Eap concentration did not show any significant improvement of the bacterial killing (**Figure 4.22 b**).

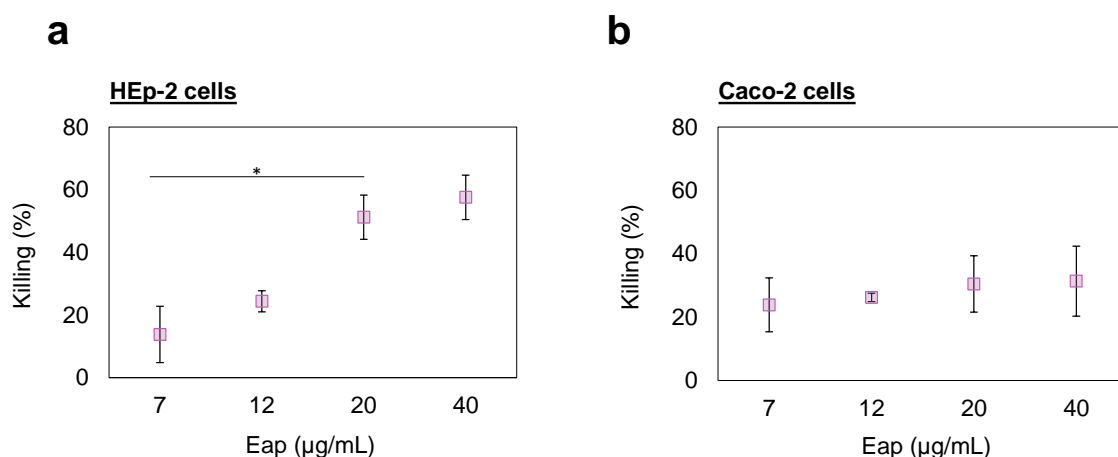


Figure 4.22. Eap-dose titration

HEP-2 cells (a) and Caco-2 cells (b) were incubated with Col-Lip-3 functionalized with 7, 12, 20 and 40 $\mu\text{g/mL}$ of Eap for 2 h and 4 h respectively at 37°C and 5% CO₂. Data are shown as mean \pm SEM from three independent experiments ($N=4$, $n=12$). Statistical difference is considered significant with P-value < 0.05 (*).

4.7.5 Colistin-dose response

Salmonella-infected cells were treated with liposomes functionalized with 20 $\mu\text{g}/\text{mL}$ of Eap and titrated with different colistin concentrations ranged from 30 $\mu\text{g}/\text{mL}$ to 200 $\mu\text{g}/\text{mL}$. Results showed that the killing percentage increased from 36% to almost 60% by increasing colistin dose on *Salmonella*-infected HEp-2 cells (**Figure 4.23 a**). While, an increase from 20% to only 40% was observed after treatment of Caco-2-infected monolayer with EapCol-lip-3 containing colistin dose up to 200 $\mu\text{g}/\text{mL}$ (**Figure 4.23 b**).

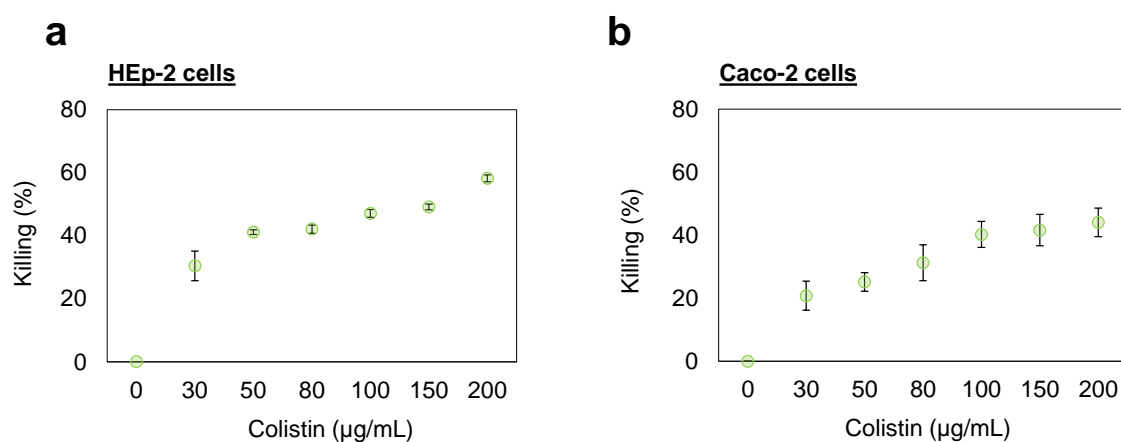


Figure 4.23. Colistin-dose response

Percentage of killing after treatment of HEp-2 cells (a) and Caco-2 cells (b) with EapCol-Lip-3 in different colistin doses 30, 50, 80, 100, 150, 200 $\mu\text{g}/\text{mL}$. Liposomes were functionalized with 20 $\mu\text{g}/\text{mL}$ of Eap and cells were incubated for 2 h (HEp-2 cells) and 4 h (Caco-2 monolayer) at 37° C and 5% CO₂. Data are shown as mean \pm SEM from three independent experiments (N= 4, n= 12).

4.8 *In vivo* pilot study

In vivo experiment was conducted using mice infected with *Salmonella* Typhimurium, and treated with EapCol-Lip-3 as well as InvCol-Lip-3 to compare the two therapeutic strategies. Colistin as free drug was used beside PBS as controls. Results were divided in two parts, CFU in content of the small intestine and cecum to evaluate the impact of treatment on extracellular bacteria, and CFU in tissue of the aforementioned organs, to evaluate the intracellular killing efficiency (**Figure 4.24 a - d**). Body weight was monitored during the study (**Figure 4.24 e**). Results of both small intestine and cecum content showed that colistin (as free drug) had a significant antimicrobial effect in comparison to the untreated group (PBS) as well as to the liposomal-based formulations. This is expected as different time points for such read-out is required for liposomal formulations due to the slow release of colistin from the liposomal compartment. InvCol-Lip-3 showed a significant reduction of the infection in the cecum content but not in the small intestine compared to untreated group. In the tissue colistin again had the most potent effect on *Salmonella*'s infection compared to EapCol-Lip-3 and InvCol-Lip-3, which was not expected as colistin cannot penetrate into the GI tract cellular membranes. Regarding the body weight, results showed approximately 4% decrease of animals' body weight upon treatment with EapCol-Lip-3 (**Figure 4.24 e**), while <3% was observed with InvCol-Lip-3 and no major changes with colistin and PBS.

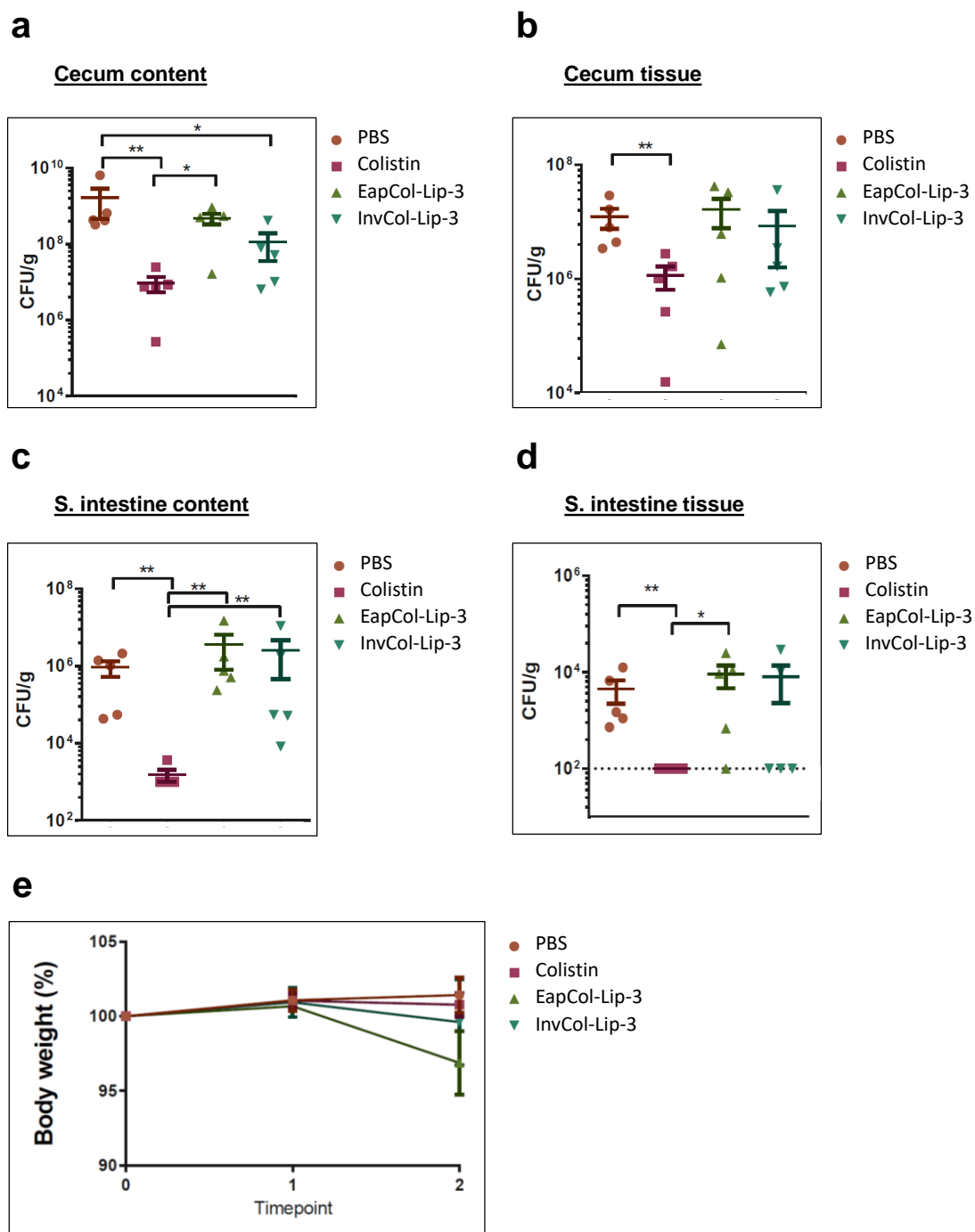


Figure 4.24. Liposomal treatment of *Salmonella*-mouse model

Bacterial counts (CFU/g) in cecum content (a), cecum tissue (b), small intestine content (c) and small intestine tissue (d) of mice treated with EapCol-Lip-3, InvCol-Lip-3, colistin and PBS after 18 h. (e) Body weight monitoring over the study duration. Data are shown as median \pm SEM from five mice (P -value < 0.05 (*), < 0.01 (**)).

5 Discussion

5.1 Colistin-loaded liposomes for oral delivery

Liposomes as lipid-based nanocarriers are commonly used in the pharmaceutical and cosmetic industries. Since their discovery in 1964, this particular field in nanotechnology has known successful progress and achievements. These include Doxil[®], a formulation consisting of 80 - 90 nm PEGylated liposomes containing doxorubicin for treatment of Kaposi's sarcoma and recurrent ovarian cancer, and Abelcet[®], a 250 nm sized liposomal formulation encapsulating amphotericin B to treat fungal infections (Working et al. 2008; Weissig et al. 2014). These represent a breakthrough in nanomedicine evolution. However, most of the FDA-approved lipid-based formulations are designed for parenteral administration routes. Administration by the highly convenient oral route presents several challenges, particularly for liposomes, due to their inherent instability in the GI tract as well the presence of different biological barriers including mucus layer and the epithelial cellular barrier. Therefore, numerous efforts are being focused on achieving efficient liposomal drug delivery via the oral route. Utilization of long chain phospholipids together with cholesterol has proven to stabilize orally administered liposomes. Liposomes composed of DPPC and DSPC, phospholipids which exhibit high transition temperatures (T_m) of 41 °C and 55 °C respectively, have shown an ability in previous studies to protect their payload in simulated gastric and intestinal media such as in low pH medium and in the presence of enzymes (Kokkona et al. 2000b; Rowland and Woodley 1980a; Mannock et al. 2006). Therefore in the current work, different liposomal formulations were prepared using DPPC and DSPC as main phospholipids in addition to 30% (w/w) cholesterol [Lip-1 (DPPC:CHOL), Lip-2 (DSPC:CHOL) and Lip-3 (DPPC:DSPC:CHOL)]. These liposomal formulations shared similar colloidal parameters: a mean diameter of 200 nm, a monodisperse size distribution and a negative surface charge (**Figure 4.1**). Colistin, a polypeptide anti-infective, was then selected to be loaded into these formulations, due to the recent attention it has attracted as a last resort anti-infective in light of the uncontrollable increase in bacterial resistance and lack of new antibiotic

alternatives (Falagas and Kasiakou 2005; Li et al. 2006; Li et al. 2005). Colistin is effective against most Gram negative bacteria especially MDR strains such as *Pseudomonas aeruginosa*, however in practice it is mainly used as parenteral or inhalable forms (Gurjar 2015; Li et al. 2005). Therefore, there is considerable interest in the optimization of colistin use. Different concentrations of colistin were loaded into all three liposomal formulations, in order to determine the optimum loading conditions. A loading concentration of 4 mg/mL was chosen as this resulted in optimal entrapment efficiency and loading capacity in comparison to the other tested concentrations. Moreover, it showed less differences between the three formulations and therefore an optimal choice for comparison (**Figure 4.5**). Further optimization steps such as an increase of shaking speed during lipid film hydration and short sonication cycles before extrusion, led to an increase in EE (**Table 4**). The achieved EE is considered to be quite high as lipid film hydration method is mostly known for lower capacity of encapsulating hydrophilic molecules when compared to remote loading (Muppidi et al. 2012; Colletier et al. 2002). This EE could be due to the fact that colistin possesses a lipid tail which could interact with the liposomal bilayers. Such a high EE was also observed by Wallace and his colleagues who encapsulated CMS in DOPC : CHOL (2:1) liposomes (Wallace et al. 2012). Moreover, the obtained LC (~ 50%) in the current work, is also considered high as the loading of water soluble drugs into other nanocarriers, such as polymeric nanoparticles, is generally lower than 10% (Barichello et al. 1999; Cai et al. 2015; Qin et al. 2017; Zheng et al. 2014).

Thermal characterization of Col-Lip-1, Col-Lip-2 and Col-Lip-3 (corresponding to Lip-1, Lip-2 and Lip-3 formulations loaded with colistin) using DSC showed an abolishment of the phase transition temperature of liposome components – namely, DPPC (41 °C) and DSPC (55 °C) – in the range of 0 °C to 80 °C. This is likely due to the incorporation of 30% cholesterol into the liposomal bilayer, which would positively affect the stability of these liposomes and has been widely documented previously to abolish phase transition temperatures (Mannock et al. 2006; Fritzsching et al. 2013).

As mentioned before, the aim of the current work was to develop a liposomal formulation able to deliver colistin orally. This represents a significant challenge

in terms of formulating such a system capable of withstanding the harsh GI tract conditions. To characterize liposome integrity under such conditions, stability studies in GI-biorelevant media simulating stomach and intestinal environments were performed. Incubation in FaSSGF and FaSSIF, characterized by a low pH (pH=1.6) and the presence of bile salts/phospholipids respectively, did not affect the colloidal parameters of any of the three liposomal formulations compared to the control. Moreover, no major effect on the integrity of these liposomes was observed, as only 10 to 15% of colistin was released from the formulations during the incubation time. However, no colistin release was observed in PBS as a control, indicating that presence of bile salts and the lower pH challenge the formulations. Incubation in FeSSIF, showed no major changes in the size of the three formulations with an increase of the PDI to 0.4. On the other hand, incubation of liposomes in FaSSIF containing enzymes (lipase) resulted in a huge size increase in all the formulations accompanied by an increase in PDI. This result was contrary to what was expected, as any liposome degradation was rather anticipated to result in a decrease in particle size (**Figure 4.7**). Therefore, in order to further investigate the effect of FaSSIF containing enzymes medium on colistin-loaded liposomes, cryo-TEM was utilized to visually examine liposomes after incubation with media. Surprisingly intact spherical-shaped liposomes were observed, but additional different colloidal structures were observed which were also present in the medium alone (**Figure 8.5**). The presence of such colloidal assemblies ranging from micelles to larger structures including vesicles and discs has been widely investigated and proven to be a very important factor in the solubility of hydrophobic drugs in the GI tract (Hjelm et al. 1995; Nawroth et al. 2011; Müllertz et al. 2015; Riethorst et al. 2016; Elvang et al. 2016; Clulow et al. 2017). The presence of these colloidal assemblies could explain the increase in liposome size and PDI as measured by DLS. This suggests that colloidal characterization in conjunction with the use of complex media including FeSSIF should be conducted carefully with optimal techniques, and should also be accompanied by microscopic evaluation. No major changes in the size upon the incubation in FeSSIF with all formulation, while PDI values indicated a heterogeneous size distribution, as indicated above due to the presence of other colloidal structures such as micelles. Regarding the surface

charge, an increase in zeta-potential values was observed in the FaSSGF and FeSSIF due to high pH and high salts concentrations in the media respectively which plays a major role in the electrostatic interactions (Yan and Huang 2009). In terms of colistin retention, Col-Lip-1 released almost 60% in FeSSIF, and less than 20% from Col-Lip-2 and Col-Lip-3 (**Figure 4.8**). This difference in behavior in FeSSIF is due to the presence of DSPC in Col-Lip-2 and Col-Lip-3. The long chain fatty acids of DSPC compared to the shorter chains of DPPC were able to enhance the stability of both Col-Lip-2 and Col-Lip-3 liposomal formulations and prevent the high leakage of colistin. This finding align with previous study results in which saturated phospholipids with long carbon chains such as DSPC ($T_m = 55\text{ }^\circ\text{C}$) with cholesterol showed better stability in the presence of bile salts or enzymes compared to DMPC-containing liposomes (Kokkona et al. 2000a; Rowland and Woodley 1980b). In contrast to DSPC, liposomes composed of phospholipids with lower T_m such as dimyristoyl phosphatidylcholine (DMPC) are susceptible to a disruption of lipid bilayers in the presence of bile salts and to the effect of lipases, and are therefore unable to maintain intact structures (Kokkona et al. 2000a; Liu et al. 2015; Shukla et al. 2016). This affects more hydrophilic drugs and causes their leakage from liposomes, while poorly soluble drugs remain encapsulated in mixed micelles formed as a result of liposome degradation (Wu et al. 2015; Tian et al. 2016). Due to the observation that Col-Lip-1 released more than 50% of its loaded colistin in FeSSIF in 5 h time period, further studies were carried out only with Col-Lip-2 and Col-Lip-3.

5.2 Eap mediates the internalization of liposomes

Oral delivery of liposomes is impeded by different barriers including the instability in the GI tract as discussed in **Section 5.1**, as well as to the difficulties to cross biological membranes (Wu et al. 2015; He et al. 2019). Therefore, different strategies have been developed to facilitate penetration across the enteric epithelium. One example is the incorporation of permeation enhancers into liposomes, which interferes with tight junctions or increases the liposomal fusion with cell membranes (Ganem-Quintanar et al. 1997; Parmentier et al. 2010; Maher et al. 2016). As another approach, coating of liposomal surfaces with permeation enhancing polymers has been also widely investigated and reported

to be efficient to some extent – this includes polymers such as chitosan, which has the ability to interfere with tight junction proteins and initiate paracellular transport (Thanou et al. 2001; Zambito et al. 2006; Kowapradit et al. 2012; Chen et al. 2012). Furthermore, to achieve more specific targeting by mimicking the way nutrients are absorbed, or the process by which pathogens are internalized into epithelial cells of the GI tract, liposomal surfaces have been functionalized with nutritional ligands (Wang et al. 2014; Zhang, X. et al. 2014; Anderson et al. 2001; Anderson et al. 1999) or invasive moieties (Werle et al. 2010; i, K. et al. 2011; Labouta et al. 2015; Menina et al. 2016). InvA497, a well characterized bacterial-derived protein, interacts with $\alpha_5\beta_1$ integrin receptors and promotes the internalization of *Yersinia* spp. into mammalian cells (Dersch and Isberg 1999, 2000; Bühler et al. 2006; Uliczka et al. 2011). This protein has been coupled to several nanocarriers such as latex nanoparticles (Hussain and Florence 1998), polylactide-co-glycolide (PLGA) nanoparticles (G. F. Dawson and G. W. Halbert 2000), microparticles (S. E. Autenrieth and I. B. Autenrieth 2008) and liposomes (Menina et al. 2016; Labouta et al. 2015), to enhance their uptake by eukaryotic cells. The promising results of these studies have opened a way to the use of bacteria-derived proteins as invasive moieties and the mimicking of pathogen invasion by adopting some of their strategies. *S. aureus*, classified as an extracellular bacteria, has been shown to possess the ability to invade eukaryotic cells using different types of proteins (Lowy 2000; Josse et al. 2017). Eap, a virulence factor secreted by *S. aureus*, which can re-bind again to the bacteria itself, mediates its binding and internalization. It is also not well understood to date how Eap mediates the binding and the invasion of *S. aureus* into eukaryotic cells. Josse and his colleagues gathered all published research investigating *S. aureus* internalization mechanisms in a recent review, in which two suggestions of Eap mechanism as known to-date were stated: (I) Eap interacts with $\alpha_5\beta_1$ integrin receptors after binding to fibronectin (Fn), or (II) Eap triggers actin-dependent phagocytosis (Josse et al. 2017). Therefore, the novelty of this work is based on functionalization of liposomes containing colistin with Eap, to further demonstrate the ability of this protein to promote invasion and also to investigate its mechanism of internalization. Coupling of ligands on liposomes is mostly performed via a covalent linking using either common coupling reagents such as

carbodiimides (EDC) (Sheehan and Hlavka 1956), triazines (DMTMM) (Kamiński et al. 2005) or more sophisticated methods (Dunetz et al. 2016). Besides, the covalent coupling which offers more control of the ligands orientation and also the amount, Eap in this case was functionalized via a physical adsorption on the liposomal surface due to its adhesive properties. The high percentage of FE obtained using surface adsorption confirms clearly that Eap possess a strong adhesion properties which allow Eap to stick to liposomal surface (**Figure 4.9**). These adhesion properties have been investigated previously by Haggar et al. showing that Eap mutant *S. aureus* (Newman mAH12) were found to have a reduced ability to internalize into fibroblasts as well as epithelial cells when compared to wild-type Eap gene. They also showed in their study that by adding Eap to the mutant strain, internalization role of Eap was restored and resulted in an increase of the uptake of these pathogens by the tested cells (Haggar et al. 2003). This high adhesion properties of Eap have affected negatively liposomes in a ways that after functionalization, liposomes tend to form aggregates. This observation is in agreement with previous findings that Eap has the ability to spontaneously aggregate *S. aureus* in concentration-dependent manner (Palma et al. 1999; Hussain et al. 2008; Thompson et al. 2010). However, sonication of Eap-functionalized liposomes lead to restoration of liposomal size and no major changes were observed during consecutive 4 days (**Figure 4.10**, **Figure 4.11**). The sonication protocol was applied for short time as recommended by Zhu et.al to ensure that the structure as well as the functionality of Eap would not be compromised (Zhu et al. 2018).

In the current work, the ability of Eap to promote the binding and internalization of liposomes was first evaluated by performing uptake studies. Subsequent to cytotoxicity assessment, which showed no adverse effects of colistin, Eap or liposomal components at defined dose range (**Figure 4.13**), uptake of liposome formulations in epithelial cells of the HEP-2 cell line and in Caco-2 monolayers as a GI epithelial cell model was assessed. The uptake studies were carried out only with Col-Lip-3 as functionalization study showed that only this formulation functionalized via surface adsorption exhibited the highest functionalization efficiency. The outcomes of the uptake study showed, for the first time, that

functionalization of liposomes with Eap promoted significantly the uptake of colistin-loaded liposomes (EapCol-Lip-3) in HEP-2 cells compared to non-functionalized liposomes. Uptake results of non-functionalized liposomes (Col-Lip-3) in HEP-2 cells showed no-to-low uptake efficiency after 1 h and 2 h. While, using 5 µg/mL of Eap to functionalize these liposomes induced approximately 50 % of uptake after 2 h, and by increasing the Eap concentrations to either 10 µg/mL or 20 µg/mL, the uptake efficiency increased to > 95%. On the other hand, similar uptake efficiency was observed with Col-Lip-3 and EapCol-Lip-3 functionalized with 5 µg/mL in Caco-2 monolayer (<10% and ~40% after 2 h and 4 h respectively). Whereas, increasing Eap concentration lead to increased uptake efficiency in a concentration-dependent manner (**Figure 4.14**). Functionalizing liposomes with 20 µg/ml Eap was sufficient to promote almost 100% uptake of liposomes into both cell types. This concentration is comparable to that used in a study by Bur and his colleagues, where it was shown that pre-incubation of HaCaT cells with 10 µg/mL of Eap was sufficient to mediate the cellular uptake of *S. aureus* (Eap-mutant starin SA113), whereas 40 µg/mL induced a saturation of its internalization. Moreover, pre-incubation of HaCaT cells with Eap promoted the uptake of *S. epidermidis* and *S. lugdunensis* as well as *Escherichia coli* (Bur et al. 2013). The method of Col-Lip-3 functionalization with Eap either covalently or via surface adsorption did not affect the efficiency of the uptake (**Figure 8.6**). This suggests that Eap does not require a specific orientation or specific functional group to promote the binding as well as the internalization. This is in direct contrast to InvA497 – we have previously shown that coupling InvA497 to DPPC-based liposomes requires a covalent coupling, in which the free C terminal group plays an important role in mediating the uptake of these liposomes (Labouta et al. 2015). Moreover, an InvA497 derivative (InvA197) was not able to promote the internalization of latex beads efficiently compared to InvA497 (Dersch and Isberg 1999).

The ability of Eap to promote liposomal binding and/or internalization into HEP-2 cells was further compared to InvA497-functionalized Col-Lip-3 after 1 h incubation time. Results indicated that Eap was more efficient in achieving >75% Rhod-positive cells with all tested concentrations compared to InvA497, where

only 40% of Rhod-positive cells was achieved with the highest used concentration (**Figure 8.7**). However, it is difficult to make an appropriate comparison as the two proteins differ in their mechanism of action, several aspects need to be considered such as concentration, coupling method and incubation time, e. g. InvA497 requires higher concentration to be used to functionalize liposomes (15 times Eap concentration to achieve 95% positive signal in 1 h, **Figure 8.7**).

The exact mechanism by which Eap mediates binding and uptake is not yet well understood, and therefore further investigations into this aspect would be valuable. To understand how Eap enhances the uptake of liposomes by HEP-2 cells and Caco-2 cells, one should look first at the non-functionalized liposomes. As mentioned before, in contrast to HEP-2 cells, 35% of Caco-2 cells were able to take up non-functionalized liposomes after 4 h indicating differences in their uptake mechanism (**Figure 4.14**). Despite the enormous amount of research on liposomes that has been conducted, the uptake mechanism of liposomes has not been clarified completely (Düzgüneş and Nir 1999). Most of the reports on liposomal internalization showed that these nanocarriers are taken up via clathrin-dependent endocytosis (Ziello et al. 2010; Rejman et al. 2005; Andar et al. 2014), whereas other studies demonstrated that caveolae-mediated pathway plays an essential role in the uptake of liposomes (Andar et al. 2014; Kheirloom and Ferrara 2007; Fiandaca et al. 2011; Alshehri et al. 2018). On the other hand, it has been shown also in early studies that internalization of liposomes could be achieved passively. Papahadjopoulos et al. found that liposomes can fuse with cell membranes and release therefore their payload into the cell (Papahadjopoulos et al. 1973). However, the internalization of liposomes or nanocarriers in general is influenced by several factors, such as size, surface charge, shape, composition, and surface chemistry (Rejman et al. 2004; Gratton et al. 2008; Nangia and Sureshkumar 2012; Ernsting et al. 2013). Functionalizing liposomes with Eap resulted in almost 100% uptake. However, lowering the incubation temperature from 37 °C to 4 °C inhibited the uptake only in Caco-2 cells but not in HEP-2 cells, indicating that the uptake in Caco-2 cells is energy-dependent, while in HEP-2 cells passive uptake is likely to be occurring (**Figure 4.16 a, b**).

Several pathways are involved in energy-mediated uptake (pinocytosis), however the study of these various pathways is still an evolving domain (Kuhn et al. 2014). One of the well-investigated mechanisms is clathrin-dependent endocytosis, via which it has been shown that nanocarriers with a size <200 nm may be taken up. The binding arrangement of clathrin-coated pits to envelop the cargo leads to the formation of clathrin-coated vesicles and further to cargo internalization (Chen et al. 2018). Transferrin is considered as a marker for this pathway as it binds to the transferrin receptor and initiates uptake via clathrin-mediated endocytosis (Ivanov 2008). Caveolin-dependent endocytosis on the other hand, is characterized by small flask-shaped invaginations of the cell membrane with an enrichment of caveolin-1 (Nabi and Le 2003) This pathway is involved in particular for the uptake of some pathogens such as SV40 virus and cholera toxin and in which this latter is usually selected as marker for caveolin-mediated endocytosis (Ivanov 2008). Macropinocytosis, by contrast, is considered an unspecific endocytosis pathway, characterized by the engulfment of liquid macromolecules, in which the macropinosomes have a size of up to 5 μm (Jones 2007). There is also a class of clathrin- and caveolin-independent endocytosis, in which various sub-pathways are involved such as dynamin-mediated endocytosis, lipid rafting and the flotillin-dependent pathway (Mayor and Pagano 2007). Over the years, several studies have utilized various pharmacological inhibitors to identify a specific pathway for uptake of different molecules, pathogens and also nanocarriers. However, there are a number of studies which have highlighted the lack of specificity of these inhibitors (Vercauteren et al. 2010; dos Santos et al. 2011). Chlorpromazine as a cationic amphiphilic drug is known to interfere in the binding of clathrin and its proteins leading to inhibition of clathrin-coated pits formation and thereby, inhibition of clathrin-mediated endocytosis in a reversible manner (Chen et al. 2018). Methyl β -cyclodextrin, is a cyclic oligomer of glucopyranoside which extracts steroids from the cell membrane in a reversible manner leading to cholesterol inhibition and therefore, is utilized as a clathrin and caveolin-independent pathway inhibitors (Vercauteren et al. 2010). Macropinocytosis is known as an actin-driven pathway that forms protrusions, engulfing large fragments in a suspended environment. Through the de-polymerization of actin filaments, cytochalasin D is utilized to inhibit

macropinocytosis (Kanlaya et al. 2013). Filipin III is an antibiotic which binds to the cholesterol present in cell membranes and induces formation of aggregates that interfere with the caveolin-dependent uptake mechanism (Schnitzer et al. 1994). While a large number of inhibitors are therefore available, it is important to state that toxicity of these inhibitors play a major role in their function, and requires an optimization of the used concentrations which varies between different cell types (Dutta and Donaldson 2012).

To dissect the type of energy-mediated pathway involved in liposomal internalization in Caco-2 cells, cells were incubated with EapCol-Lip-3 in the presence of endocytosis inhibitors. Results showed that all inhibitors had (varying) inhibitory potential on the uptake of liposomes (**Figure 4.16**). This strongly suggests that Eap-induced liposomal uptake depends on several pathways, but that this mainly occurs via caveolae-mediated endocytosis. Those results represent a starting point in elucidating the Eap-mediated mechanism of internalization, however further studies using several cell types are required to draw a complete picture of how it works.

5.3 Impact of Eap-functionalized liposomes containing colistin on intracellular infection

Targeting intracellular bacteria using liposomes or other nanocarriers such as polymeric or solid lipid nanoparticles has been widely investigated. However, their efficacy has mainly been studied in phagocytic cells such as macrophages, in which the delivery of the nanoparticle system and/or the payload is not limited due to the ability of these cells to engulf foreign particulates (Salouti and Ahangari 2014). In contrast, achieving an intracellular killing effect within non-phagocytic cells requires more effort such as functionalization of nanocarrier systems with invasive moieties (Goes and Fuhrmann 2018). As mentioned above, the current work showed that Eap is able to mediate liposome internalization in HEP-2 cells and Caco-2 monolayers; however their ability to release colistin intracellularly remained to be seen. Therefore, the efficacy of Eap-functionalized liposomes containing colistin (EapCol-Lip-3) to deliver colistin intracellularly was evaluated by their ability to kill intracellularly-located pathogens. For this purpose, HEP-2

cells and Caco-2 cells were infected with enteroinvasive *Salmonella enterica*. After killing extracellular bacteria using gentamicin, cells were treated with different liposomal formulations as well as free colistin as a control. EapCol-Lip-3 was able to reduce the infection load in HEp-2 cells and Caco-2 cells by 32% and 30% respectively. Interestingly, Col-Lip-3 without Eap functionalization reduced the infection load by 11% in Caco-2 cells, but had no effect on the infection load in HEp-2 cells (**Figure 4.20**). This aligns with the above results of uptake studies which showed that Caco-2 cells had a basal liposome uptake ability in the absence of Eap (**Figure 4.14**). In addition, the anti-infective efficacy of Eap-functionalized liposomes was Eap and colistin dose-dependent, with uptake into HEp-2 cells reaching almost 60% following a 2 h incubation with liposomes containing 40 $\mu\text{g/ml}$ Eap / 30 $\mu\text{g/ml}$ colistin or 200 $\mu\text{g/ml}$ colistin / 20 $\mu\text{g/ml}$ Eap (**Figure 4.22**, **Figure 4.23**). In a previous study, we could show a similar intracellular killing effect on *Y. pseudotuberculosis* and *S. enterica* using a different bio-inspired delivery system, which was based on targeting $\alpha_5\beta_1$ integrin receptors of the GI tract (Labouta et al. 2015; Menina et al. 2016). However invasin-based nanoparticles are able only to target specific cell types expressing $\alpha_5\beta_1$ integrin receptors in the GI tract. Eap on the other hand is able to interact with a wider variety of cell types and thereby offers a broader coverage to eradicate intracellular pathogens.

In vivo testing of such a system requires an established model. The conducted pilot study tried to establish *Salmonella*-infection mouse model to test liposomes. This model was not conclusive in a way that colistin was able to kill intracellular bacteria (in tissue). The fact that colistin lack the ability to penetrate through biological membranes raised a critical question: whether these results indeed indicate the anti-bacterial effect on intracellularly-located *Salmonella* or also includes extracellularly and/or bounded- bacterial counts. Due to the complexity of such model, various factors should be taken in consideration while designing the study in the future, such as the administrated dose, the treatment duration and more important optimal read-outs and/or tests to address each aspect of such an investigation.

However, the use of this bacteria-derived protein as an invasive moiety to facilitate the intracellular delivery of nanocarriers would require deeper investigations, in order to fully understand the function and optimize the system towards different targets and/or different administration routes. Moreover, *in vivo* studies and/or complex cell models could be considered as further steps to be performed, as *in vitro* studies show only the proof of concept, which needs to be investigated further in more sophisticated systems.

6 Conclusion

A lipid-based nanoparticulate system encapsulating colistin, a hydrophilic polypeptide antibiotic, was first formulated to deliver colistin orally. Withstanding the GI tract environment including acidic medium and enzymatic degradation was achieved by the assembly of liposomes containing long chain phospholipids together with cholesterol, which led to improving the liposomal stability. In order to facilitate the intracellular delivery of colistin, which is poorly permeable through cellular membranes, a subsequent functionalization of the liposomal surface with the bacteria-derived protein, Eap, was performed. The presence of Eap on liposomal surfaces enabled the internalization of these liposomes into epithelial cells, resulting in a substantial killing of intracellular *S. enterica*. As the internalization pathway mediated by Eap has not been well understood to date, the study provided valuable insight into the fact that depending on cell type, Eap-mediated liposome internalization occurred in either an energy-dependent manner involving several pathways or in an energy-independent manner. Further investigations are required to characterize in detail the mechanisms by which Eap binds to and penetrates into cells. The importance of this work is to show that bacterial-derived invasion factors are a strategy to achieve higher accumulation of poorly-permeable drugs in non-phagocytic cells. For Eap, this was to our knowledge the first time to demonstrate enhanced uptake of a functional drug carrier. The principle of such bio-inspired invasion factors would be transferable to other topical application routes (e.g. urinary tract infections) and poorly accumulating anti-infectives. However, it would be important to investigate as such an invasion molecule; which directly derived from a rather abundant bacterium like *S. aureus*, can be used without modifications, or is would be a target for antibodies opsonization.

7 References

1. Aburahma MH. Bile salts-containing vesicles: promising pharmaceutical carriers for oral delivery of poorly water-soluble drugs and peptide/protein-based therapeutics or vaccines. *Drug Deliv.* 2016;23(6):1847–67. doi:10.3109/10717544.2014.976892.
2. Adler-Moore J, Proffitt RT. AmBisome: liposomal formulation, structure, mechanism of action and pre-clinical experience. *J. Antimicrob. Chemother.* 2002;49 Suppl 1:21–30.
3. Alexander LM, Pernagallo S, Livigni A, Sánchez-Martín RM, Brickman JM, Bradley M. Investigation of microsphere-mediated cellular delivery by chemical, microscopic and gene expression analysis. *Mol Biosyst.* 2010;6(2):399–409. doi:10.1039/b914428e.
4. Ali MH, Moghaddam B, Kirby DJ, Mohammed AR, Perrie Y. The role of lipid geometry in designing liposomes for the solubilisation of poorly water soluble drugs. *Int J Pharm.* 2013;453(1):225–32. doi:10.1016/j.ijpharm.2012.06.056.
5. Alshehri A, Grabowska A, Stolnik S. Pathways of cellular internalisation of liposomes delivered siRNA and effects on siRNA engagement with target mRNA and silencing in cancer cells. *Sci Rep.* 2018;8(1):3748. doi:10.1038/s41598-018-22166-3.
6. Alshraim MO, Sangi S, Harisa GI, Alomrani AH, Yusuf O, Badran MM. Chitosan-Coated Flexible Liposomes Magnify the Anticancer Activity and Bioavailability of Docetaxel: Impact on Composition. *Molecules* 2019. doi:10.3390/molecules24020250.
7. amr-bioMérieux. A lack of antibiotics: are new antibiotics being developed. 2019. <https://amr.biomerieux.com/en/challenges/a-lack-of-antibiotics/>.
8. Andar AU, Hood RR, Vreeland WN, Devoe DL, Swaan PW. Microfluidic preparation of liposomes to determine particle size influence on cellular uptake mechanisms. *Pharm. Res.* 2014;31(2):401–13. doi:10.1007/s11095-013-1171-8.

9. Anderson KE, Stevenson BR, Rogers JA. Folic acid–PEO-labeled liposomes to improve gastrointestinal absorption of encapsulated agents. *Journal of Controlled Release*. 1999;60(2-3):189–98. doi:10.1016/S0168-3659(99)00072-3.
10. Anderson KE, Eliot LA, Stevenson BR, Rogers JA. Formulation and evaluation of a folic acid receptor-targeted oral vancomycin liposomal dosage form. *Pharm. Res*. 2001;18(3):316–22.
11. Anderson JM, van Itallie CM. Physiology and function of the tight junction. *Cold Spring Harb Perspect Biol*. 2009;1(2):a002584. doi:10.1101/cshperspect.a002584.
12. Aslam B, Wang W, Arshad MI, Khurshid M, Muzammil S, Rasool MH, et al. Antibiotic resistance: a rundown of a global crisis. *Infect Drug Resist*. 2018;11:1645–58. doi:10.2147/IDR.S173867.
13. Bai L, Ma Z, Yang G, Yang J, Cheng J. A simple HPLC method for the separation of colistimethate sodium and colistin sulfate. *journal of chromatography and separation techniques* 2011. doi:10.4172/2157-7064.1000105.
14. Bangham AD, Standish MM, Watkins JC. Diffusion of univalent ions across the lamellae of swollen phospholipids. *J. Mol. Biol*. 1965;13(1):238–52.
15. Barea MJ, Jenkins MJ, Gaber MH, Bridson RH. Evaluation of liposomes coated with a pH responsive polymer. *Int J Pharm*. 2010;402(1-2):89–94. doi:10.1016/j.ijpharm.2010.09.028.
16. Barea MJ, Jenkins MJ, Lee YS, Johnson P, Bridson RH. Encapsulation of Liposomes within pH Responsive Microspheres for Oral Colonic Drug Delivery. *Int J Biomater*. 2012;2012:458712. doi:10.1155/2012/458712.
17. Barenholz Y. Doxil®--the first FDA-approved nano-drug: lessons learned. *J Control Release*. 2012;160(2):117–34. doi:10.1016/j.jconrel.2012.03.020.
18. Barichello JM, Morishita M, Takayama K, Nagai T. Encapsulation of hydrophilic and lipophilic drugs in PLGA nanoparticles by the

- nanoprecipitation method. *Drug Dev Ind Pharm.* 1999;25(4):471–6. doi:10.1081/DDC-100102197.
19. Bbosa GS, Mwebaza N, Odda J, Kyegombe DB, Ntale M. Antibiotics/antibacterial drug use, their marketing and promotion during the post-antibiotic golden age and their role in emergence of bacterial resistance. *Health.* 2014;06(05):410–25. doi:10.4236/health.2014.65059.
 20. Bhuyan AK. On the mechanism of SDS-induced protein denaturation. *Biopolymers.* 2010;93(2):186–99. doi:10.1002/bip.21318.
 21. Bialvaei AZ, Samadi K. H. Colistin, mechanisms and prevalence of resistance. *Curr Med Res Opin.* 2015;31(4):707–21. doi:10.1185/03007995.2015.1018989.
 22. Bies C, Lehr C-M, Woodley JF. Lectin-mediated drug targeting: history and applications. *Adv. Drug Deliv. Rev.* 2004;56(4):425–35. doi:10.1016/j.addr.2003.10.030.
 23. Biswas S, Brunel J-M, Dubus J-C, Reynaudt GM, Rolain J-M. Colistin: An update on the antibiotic of the 21st century. *Expert Rev Anti Infect Ther.* 2012;10(8):917–34. doi:10.1586/eri.12.78.
 24. Briuglia M-L, Rotella C, McFarlane A, Lamprou DA. Influence of cholesterol on liposome stability and on in vitro drug release. *Drug Deliv Transl Res.* 2015;5(3):231–42. doi:10.1007/s13346-015-0220-8.
 25. Bühler OT, Wiedig CA, Schmid Y, Grassl GA, Bohn E, Autenrieth IB. The *Yersinia enterocolitica* Invasin Protein Promotes Major Histocompatibility Complex Class I- and Class II-Restricted T-Cell Responses. *Infect. Immun.* 2006;74(7):4322–9.
 26. Bulbake U, Doppalapudi S, Kommineni N, Khan W. Liposomal Formulations in Clinical Use: An Updated Review. *Pharmaceutics* 2017. doi:10.3390/pharmaceutics9020012.
 27. Bur S, Preissner KT, Herrmann M, Bischoff M. The *Staphylococcus aureus* extracellular adherence protein promotes bacterial internalization by
-

- keratinocytes independent of fibronectin-binding proteins. *J Invest Dermatol.* 2013;133(8):2004–12. doi:10.1038/jid.2013.87.
28. Cai K, He X, Song Z, Yin Q, Zhang Y, Uckun FM, et al. Dimeric drug polymeric nanoparticles with exceptionally high drug loading and quantitative loading efficiency. *J Am Chem Soc.* 2015;137(10):3458–61. doi:10.1021/ja513034e.
 29. Carafa M, Marianecchi C, Annibaldi V, Di Stefano A, Sozio P, Santucci E. Novel O-palmitoylscleroglucan-coated liposomes as drug carriers: development, characterization and interaction with leuprolide. *Int J Pharm.* 2006;325(1-2):155–62. doi:10.1016/j.ijpharm.2006.06.040.
 30. Chavakis T, Hussain M, Kanse SM, Peters G, Bretzel RG, Flock J-I, et al. Staphylococcus aureus extracellular adherence protein serves as anti-inflammatory factor by inhibiting the recruitment of host leukocytes. *Nat Med.* 2002;8(7):687–93. doi:10.1038/nm728.
 31. Chen H, Wu J, Sun M, Guo C, Yu A, Cao F, et al. N-trimethyl chitosan chloride-coated liposomes for the oral delivery of curcumin. *Journal of Liposome Research.* 2012;22(2):100–9. doi:10.3109/08982104.2011.621127.
 32. Chen F, Zhu L, Zhang Y, Kumar D, Cao G, Hu X, et al. Clathrin-mediated endocytosis is a candidate entry sorting mechanism for Bombyx mori cypovirus. *Sci Rep.* 2018;8(1):7268. doi:10.1038/s41598-018-25677-1.
 33. Choonara BF, Choonara YE, Kumar P, Bijukumar D, Du Toit LC, Pillay V. A review of advanced oral drug delivery technologies facilitating the protection and absorption of protein and peptide molecules. *Biotechnol Adv.* 2014;32(7):1269–82. doi:10.1016/j.biotechadv.2014.07.006.
 34. Clardy J, Fischbach M, Currie C. The natural history of antibiotics. *Curr Biol.* 2009;19(11):R437-41. doi:10.1016/j.cub.2009.04.001.
 35. Clulow AJ, Parrow A, Hawley A, Khan J, Pham AC, Larsson P, et al. Characterization of Solubilizing Nanoaggregates Present in Different
-

- Versions of Simulated Intestinal Fluid. *J Phys Chem B*. 2017;121(48):10869–81. doi:10.1021/acs.jpcc.7b08622.
36. Coates A, Hu Y, Bax R, Page C. The future challenges facing the development of new antimicrobial drugs. *Nat Rev Drug Discov*. 2002;1(11):895–910. doi:10.1038/nrd940.
 37. Coates ARM, Halls G, Hu Y. Novel classes of antibiotics or more of the same? *Br J Pharmacol*. 2011;163(1):184–94. doi:10.1111/j.1476-5381.2011.01250.x.
 38. Colletier J-P, Chaize B, Winterhalter M, Fournier D. Protein encapsulation in liposomes: efficiency depends on interactions between protein and phospholipid bilayer. *BMC Biotechnol*. 2002;2(1):9. doi:10.1186/1472-6750-2-9.
 39. Cossart P, Sansonetti PJ. Bacterial invasion: the paradigms of enteroinvasive pathogens. *Science*. 2004;304(5668):242–8. doi:10.1126/science.1090124.
 40. Cossart P, Roy CR. Manipulation of host membrane machinery by bacterial pathogens. *Curr Opin Cell Biol*. 2010;22(4):547–54. doi:10.1016/j.ceb.2010.05.006.
 41. Cui M, Wu W, Hovgaard L, Lu Y, Chen D, Qi J. Liposomes containing cholesterol analogues of botanical origin as drug delivery systems to enhance the oral absorption of insulin. *Int J Pharm*. 2015;489(1-2):277–84. doi:10.1016/j.ijpharm.2015.05.006.
 42. Dahal RH, Chaudhary DK. Microbial Infections and Antimicrobial Resistance in Nepal: Current Trends and Recommendations. *Open Microbiol J*. 2018;12:230–42. doi:10.2174/1874285801812010230.
 43. Dersch P, Isberg RR. A region of the *Yersinia pseudotuberculosis* invasin protein enhances integrin-mediated uptake into mammalian cells and promotes self-association. *EMBO J*. 1999;18(5):1199–213. doi:10.1093/emboj/18.5.1199.
-

44. Dersch P, Isberg RR. An immunoglobulin superfamily-like domain unique to the *Yersinia pseudotuberculosis* invasin protein is required for stimulation of bacterial uptake via integrin receptors. *Infect. Immun.* 2000;68(5):2930–8.
45. Dorrington G, Chmel NP, Norton SR, Wemyss AM, Lloyd K, Praveen Amarasinghe D, Rodger A. Light scattering corrections to linear dichroism spectroscopy for liposomes in shear flow using calcein fluorescence and modified Rayleigh-Gans-Debye-Mie scattering. *Biophys Rev.* 2018;10(5):1385–99. doi:10.1007/s12551-018-0458-8.
46. dos Santos T, Varela J, Lynch I, Salvati A, Dawson KA. Effects of transport inhibitors on the cellular uptake of carboxylated polystyrene nanoparticles in different cell lines. *PLoS ONE.* 2011;6(9):e24438. doi:10.1371/journal.pone.0024438.
47. Dunetz JR, Magano J, Weisenburger GA. Large-Scale Applications of Amide Coupling Reagents for the Synthesis of Pharmaceuticals. *Org. Process Res. Dev.* 2016;20(2):140–77. doi:10.1021/op500305s.
48. Dutta D, Donaldson JG. Search for inhibitors of endocytosis: Intended specificity and unintended consequences. *Cell Logist.* 2012;2(4):203–8. doi:10.4161/cl.23967.
49. Düzgüneş N, Gregoriadis G. Introduction: The Origins of Liposomes: Alec Bangham at Babraham. 2005;391:1–3. doi:10.1016/S0076-6879(05)91029-X.
50. Düzgüneş N, Nir S. Mechanisms and kinetics of liposome–cell interactions. *Adv. Drug Deliv. Rev.* 1999;40(1-2):3–18. doi:10.1016/S0169-409X(99)00037-X.
51. Dwivedi N, Arunagirinathan MA, Sharma S, Bellare J. Silica-Coated Liposomes for Insulin Delivery. *Journal of Nanomaterials.* 2010;2010(33):1–8. doi:10.1155/2010/652048.

52. Ebato Y, Kato Y, Onishi H, Nagai T, Machida Y. In vivo efficacy of a novel double liposome as an oral dosage form of salmon calcitonin. *Drug Dev. Res.* 2003;58(3):253–7. doi:10.1002/ddr.10162.
53. Elsayed MMA, Abdallah OY, Naggar VF, Khalafallah NM. Deformable liposomes and ethosomes: mechanism of enhanced skin delivery. *Int J Pharm.* 2006;322(1-2):60–6. doi:10.1016/j.ijpharm.2006.05.027.
54. Elvang PA, Hinna, A. H., Brouwers, J., Hens, B., Augustijns P, Brandl M. Bile Salt Micelles and Phospholipid Vesicles Present in Simulated and Human Intestinal Fluids: Structural Analysis by Flow Field-Flow Fractionation/Multiangle Laser Light Scattering. *J Pharm Sci.* 2016;105(9):2832–9. doi:10.1016/j.xphs.2016.03.005.
55. Ensign LM, Cone R, Hanes J. Oral drug delivery with polymeric nanoparticles: the gastrointestinal mucus barriers. *Adv. Drug Deliv. Rev.* 2012;64(6):557–70. doi:10.1016/j.addr.2011.12.009.
56. Ernsting MJ, Murakami M, Roy A, Li S-D. Factors Controlling the Pharmacokinetics, Biodistribution and Intratumoral Penetration of Nanoparticles. *J Control Release.* 2013;172(3):782–94. doi:10.1016/j.jconrel.2013.09.013.
57. Falagas ME, Kasiakou SK. Colistin: The revival of polymyxins for the management of multidrug-resistant gram-negative bacterial infections. *Clinical Infectious Diseases.* 2005;40(9):1333–41. doi:10.1086/429323.
58. Fällman M, Deleuil F, McGee K. Resistance to phagocytosis by *Yersinia*. *International Journal of Medical Microbiology.* 2001;291(6-7):501–9. doi:10.1078/1438-4221-00159.
59. Fiandaca MS, Berger MS, Bankiewicz KS. The use of convection-enhanced delivery with liposomal toxins in neurooncology. *Toxins (Basel).* 2011;3(4):369–97. doi:10.3390/toxins3040369.
60. Fritzsching KJ, Kim J, Holland GP. Probing lipid-cholesterol interactions in DOPC/eSM/Chol and DOPC/DPPC/Chol model lipid rafts with DSC and

- (13)C solid-state NMR. *Biochim Biophys Acta*. 2013;1828(8):1889–98. doi:10.1016/j.bbame.2013.03.028.
61. G. F. Dawson and G. W. Halbert. The in vitro cell association of invasin coated polylactide-co-glycolide nanoparticles. *Pharm. Res.* 2000;17(11):1420–5.
62. Gal-Mor O, Boyle EC, Grassl GA. Same species, different diseases: How and why typhoidal and non-typhoidal *Salmonella enterica* serovars differ. *Front Microbiol.* 2014;5:391. doi:10.3389/fmicb.2014.00391.
63. Ganem-Quintanar A, Kalia YN, Falson-Rieg F, Buri P. Mechanisms of oral permeation enhancement. *Int J Pharm.* 1997;156(2):127–42. doi:10.1016/S0378-5173(97)00193-2.
64. Gao L, Liu G, Ma J, Wang X, Zhou L, Li X, Wang F. Application of drug nanocrystal technologies on oral drug delivery of poorly soluble drugs. *Pharm. Res.* 2013;30(2):307–24. doi:10.1007/s11095-012-0889-z.
65. Garg T, Kumar A, Rath G, Goyal AK. Gastroretentive drug delivery systems for therapeutic management of peptic ulcer. *Crit Rev Ther Drug Carrier Syst.* 2014;31(6):531–57. doi:10.1615/critrevtherdrugcarriersyst.2014011104.
66. Goes A, Fuhrmann G. Biogenic and Biomimetic Carriers as Versatile Transporters To Treat Infections. *ACS Infect Dis.* 2018;4(6):881–92. doi:10.1021/acsinfecdis.8b00030.
67. Gradauer K, Barthelmes J, Vonach C, Almer G, Mangge H, Teubl B, et al. Liposomes coated with thiolated chitosan enhance oral peptide delivery to rats. *J Control Release.* 2013;172(3):872–8. doi:10.1016/j.jconrel.2013.10.011.
68. Gratton SEA, Ropp PA, Pohlhaus PD, Luft JC, Madden VJ, Napier ME, DeSimone JM. The effect of particle design on cellular internalization pathways. *Proc. Natl. Acad. Sci. U.S.A.* 2008;105(33):11613–8. doi:10.1073/pnas.0801763105.

69. Guan P, Lu Y, Qi J, Niu M, Lian R, Hu F, Wu W. Enhanced oral bioavailability of cyclosporine A by liposomes containing a bile salt. *Int J Nanomedicine*. 2011;6:965–74. doi:10.2147/IJN.S19259.
70. Gurjar M. Colistin for lung infection: An update. *J Intensive Care*. 2015;3(1):3. doi:10.1186/s40560-015-0072-9.
71. Hagggar A, Hussain M, Lönnies H, Herrmann M, Norrby-Teglund A, Flock JI. Extracellular Adherence Protein from *Staphylococcus aureus* Enhances Internalization into Eukaryotic Cells. *Infect. Immun*. 2003;71(5):2310–7. doi:10.1128/IAI.71.5.2310-2317.2003.
72. Ham H, Sreelatha A, Orth K. Manipulation of host membranes by bacterial effectors. *Nat Rev Microbiol*. 2011;9(9):635–46. doi:10.1038/nrmicro2602.
73. Hamman JH, Enslin GM, Kotzé AF. Oral delivery of peptide drugs: barriers and developments. *BioDrugs*. 2005;19(3):165–77. doi:10.2165/00063030-200519030-00003.
74. Hammel M, Němeček, D., Keightley JA, Thomas GJ, Geisbrecht BV. The *Staphylococcus aureus* extracellular adherence protein (Eap) adopts an elongated but structured conformation in solution. *Protein Science*. 2007;16(12):2605–17. doi:10.1110/ps.073170807.
75. Haorah J, Schall K, Ramirez SH, Persidsky Y. Activation of protein tyrosine kinases and matrix metalloproteinases causes blood-brain barrier injury: Novel mechanism for neurodegeneration associated with alcohol abuse. *Glia*. 2008;56(1):78–88. doi:10.1002/glia.20596.
76. Harraghy N, Hussain M, Hagggar A, Chavakis T, Sinha, B., Herrmann, M., Flock J-I. The adhesive and immunomodulating properties of the multifunctional *Staphylococcus aureus* protein Eap. *Microbiology*. 2003;149(Pt 10):2701–7. doi:10.1099/mic.0.26465-0.
77. Hassett DJ, Cohen MS. Bacterial adaptation to oxidative stress: Implications for pathogenesis and interaction with phagocytic cells. *FASEB J*. 1989;3(14):2574–82.

78. He H, Lu Y, Qi J, Zhu Q, Chen Z, Wu W. Adapting liposomes for oral drug delivery. *Acta Pharm Sin B*. 2019;9(1):36–48. doi:10.1016/j.apsb.2018.06.005.
79. Higgins PG, Fluit AC, Schmitz FJ. Fluoroquinolones: structure and target sites. *Curr Drug Targets*. 2003;4(2):181–90.
80. Hjelm RP, Schteingart C, Hofmann AS, Sivia DS. Form and structure of self-assembling particles in monoolein-bile salt mixtures. *The Journal of Physical Chemistry*. 1995;99(44):16395–406. doi:10.1021/j100044a030.
81. Hoegen P von. Synthetic biomimetic supra molecular Biovector™ (SMBV™) particles for nasal vaccine delivery. *Adv. Drug Deliv. Rev.* 2001;51(1-3):113–25. doi:10.1016/S0169-409X(01)00175-2.
82. Hosny KM, Ahmed OAA, Al-Abdali RT. Enteric-coated alendronate sodium nanoliposomes: a novel formula to overcome barriers for the treatment of osteoporosis. *Expert Opin Drug Deliv.* 2013;10(6):741–6. doi:10.1517/17425247.2013.799136.
83. Huang Y-B, Tsai M-J, Wu P-C, Tsai Y-H, Wu Y-H, Fang J-Y. Elastic liposomes as carriers for oral delivery and the brain distribution of (+)-catechin. *J Drug Target.* 2011;19(8):709–18. doi:10.3109/1061186X.2010.551402.
84. Hunter AC, Elsom J, Wibroe PP, Moghimi SM. Polymeric particulate technologies for oral drug delivery and targeting: a pathophysiological perspective. *Nanomedicine*. 2012;8 Suppl 1:S5-20. doi:10.1016/j.nano.2012.07.005.
85. Hussain N, Florence AT. Utilizing bacterial mechanisms of epithelial cell entry: invasin-induced oral uptake of latex nanoparticles. *Pharm. Res.* 1998;15(1):153–6.
86. Hussain M, Haggar A, Heilmann C, Peters G, Flock J-I, Herrmann M. Insertional inactivation of Eap in *Staphylococcus aureus* strain Newman confers reduced staphylococcal binding to fibroblasts. *Infect. Immun.* 2002;70(6):2933–40. doi:10.1128/iai.70.6.2933-2940.2002.

87. Hussain M, Hagggar A, Peters G, Chhatwal GS, Herrmann M, Flock J-I, Sinha B. More than One Tandem Repeat Domain of the Extracellular Adherence Protein of *Staphylococcus aureus* Is Required for Aggregation, Adherence, and Host Cell Invasion but Not for Leukocyte Activation ∇ . *Infect. Immun.* 2008;76(12):5615–23. doi:10.1128/IAI.00480-08.
88. Hussain A, Haque MW, Singh SK, Ahmed FJ. Optimized permeation enhancer for topical delivery of 5-fluorouracil-loaded elastic liposome using Design Expert: part II. *Drug Deliv.* 2016;23(4):1242–53. doi:10.3109/10717544.2015.1124473.
89. Infectious Diseases Society of America. The 10 x '20 Initiative: pursuing a global commitment to develop 10 new antibacterial drugs by 2020. *Clin Infect Dis.* 2010;50(8):1081–3. doi:10.1086/652237.
90. Ivanov AI. Pharmacological inhibition of endocytic pathways: is it specific enough to be useful? *Methods Mol Biol.* 2008;440:15–33. doi:10.1007/978-1-59745-178-9_2.
91. Jacobs M, Grégoire N, Mégarbane B, Gobin P, Balayn D, Marchand S, et al. Population Pharmacokinetics of Colistin Methanesulfonate and Colistin in Critically Ill Patients with Acute Renal Failure Requiring Intermittent Hemodialysis. *Antimicrob. Agents Chemother.* 2016;60(3):1788–93. doi:10.1128/AAC.01868-15.
92. Jacobson K, d. Papahadjopoulos. Phase transitions and phase separations in phospholipid membranes induced by changes in temperature, pH, and concentration of bivalent cations. *Biochemistry.* 1975;14(1):152–61. doi:10.1021/bi00672a026.
93. Jain S, Patil SR, Swarnakar NK, Agrawal AK. Oral delivery of doxorubicin using novel polyelectrolyte-stabilized liposomes (layersomes). *Mol Pharm.* 2012;9(9):2626–35. doi:10.1021/mp300202c.
94. Jain S, Kumar D, Swarnakar NK, Thanki K. Polyelectrolyte stabilized multilayered liposomes for oral delivery of paclitaxel. *Biomaterials.* 2012;33(28):6758–68. doi:10.1016/j.biomaterials.2012.05.026.

95. Jantratid E, Janssen N, Reppas C, Dressman JB. Dissolution media simulating conditions in the proximal human gastrointestinal tract: an update. *Pharm. Res.* 2008;25(7):1663–76. doi:10.1007/s11095-008-9569-4.
96. Jesorka A, Orwar O. Liposomes: technologies and analytical applications. *Annu Rev Anal Chem (Palo Alto Calif).* 2008;1:801–32. doi:10.1146/annurev.anchem.1.031207.112747.
97. Jones AT. Macropinocytosis: Searching for an endocytic identity and role in the uptake of cell penetrating peptides. *J Cell Mol Med.* 2007;11(4):670–84. doi:10.1111/j.1582-4934.2007.00062.x.
98. Joost I, Jacob S, Utermöhlen O, Schubert U, Patti JM, Ong M-F, et al. Antibody response to the extracellular adherence protein (Eap) of *Staphylococcus aureus* in healthy and infected individuals. *FEMS Immunol Med Microbiol.* 2011;62(1):23–31. doi:10.1111/j.1574-695X.2011.00783.x.
99. Josse J, Laurent F, Diot A. Staphylococcal Adhesion and Host Cell Invasion: Fibronectin-Binding and Other Mechanisms. *Front Microbiol.* 2017;8:2433. doi:10.3389/fmicb.2017.02433.
100. Kamei N, Morishita M, Eda Y, Ida N, Nishio R, Takayama K. Usefulness of cell-penetrating peptides to improve intestinal insulin absorption. *J Control Release.* 2008;132(1):21–5. doi:10.1016/j.jconrel.2008.08.001.
101. Kamiński ZJ, Kolesińska B, Kolesińska J, Sabatino G, Chelli M, Rovero P, et al. N-triazinylammonium tetrafluoroborates. A new generation of efficient coupling reagents useful for peptide synthesis. *J Am Chem Soc.* 2005;127(48):16912–20. doi:10.1021/ja054260y.
102. Kanlaya R, Sintiprungrat K, Chaiyarit S, Thongboonkerd V. Macropinocytosis is the major mechanism for endocytosis of calcium oxalate crystals into renal tubular cells. *Cell Biochem Biophys.* 2013;67(3):1171–9. doi:10.1007/s12013-013-9630-8.

103. Karaiskos I, Friberg L, Pontikis K, Loannidis K, Tsagkari V, Galani L, et al. Colistin Population Pharmacokinetics after Application of a Loading Dose of 9 MU Colistin Methanesulfonate in Critically Ill Patients. *Antimicrob. Agents Chemother.* 2015;59(12):7240–8. doi:10.1128/AAC.00554-15.
104. Karande P, Mitragotri S. Enhancement of transdermal drug delivery via synergistic action of chemicals. *Biochim Biophys Acta.* 2009;1788(11):2362–73. doi:10.1016/j.bbame.2009.08.015.
105. Karmali PP, Chaudhuri A. Cationic liposomes as non-viral carriers of gene medicines: resolved issues, open questions, and future promises. *Med Res Rev.* 2007;27(5):696–722. doi:10.1002/med.20090.
106. Katayama K, Kato Y, Onishi H, Nagai T, Machida Y. Double liposomes: hypoglycemic effects of liposomal insulin on normal rats. *Drug Dev Ind Pharm.* 2003;29(7):725–31. doi:10.1081/ddc-120021771.
107. Kazakov S. Liposome-Nanogel Structures for Future Pharmaceutical Applications: An Updated Review. *Curr Pharm Des.* 2016;22(10):1391–413. doi:10.2174/1381612822666160125114733.
108. Kesarwani K, Gupta R. Bioavailability enhancers of herbal origin: An overview. *Asian Pacific Journal of Tropical Biomedicine.* 2013;3(4):253–66. doi:10.1016/S2221-1691(13)60060-X.
109. Khafagy E-S, Morishita M. Oral biodrug delivery using cell-penetrating peptide. *Adv. Drug Deliv. Rev.* 2012;64(6):531–9. doi:10.1016/j.addr.2011.12.014.
110. Kheirrolomoom A, Ferrara KW. Cholesterol transport from liposomal delivery vehicles. *Biomaterials.* 2007;28(29):4311–20. doi:10.1016/j.biomaterials.2007.06.008.
111. Koch-Weser JAN. Adverse Effects of Sodium Colistimethate. *Ann Intern Med.* 1970;72(6):857. doi:10.7326/0003-4819-72-6-857.
112. Kokkona M, Kallinteri P, Fatouros D, Antimisiaris SG. Stability of SUV liposomes in the presence of cholate salts and pancreatic lipases: effect

- of lipid composition. *European Journal of Pharmaceutical Sciences*. 2000a;9(3):245–52.
113. Kokkona M, Kallinteri P, Fatouros D, Antimisiaris SG. Stability of SUV liposomes in the presence of cholate salts and pancreatin lipases: effect of lipid composition. *Eur J Pharm Sci*. 2000b;9:245–52.
114. Kowapradit J, Apirakaramwong A, Ngawhirunpat T, Rojanarata T, Sajomsang W, Opanasopit P. Methylated N-(4-N,N-dimethylaminobenzyl) chitosan coated liposomes for oral protein drug delivery. *Eur J Pharm Sci*. 2012;47(2):359–66. doi:10.1016/j.ejps.2012.06.020.
115. Kraker MEA, Stewardson AJ, Harbarth S. Will 10 Million People Die a Year due to Antimicrobial Resistance by 2050? *PLoS Med* 2016. doi:10.1371/journal.pmed.1002184.
116. Kristensen M, Groot AM de, Berthelsen J, Franzyk H, Sijts A, Nielsen HM. Conjugation of cell-penetrating peptides to parathyroid hormone affects its structure, potency, and transepithelial permeation. *Bioconjug. Chem*. 2015;26(3):477–88. doi:10.1021/bc5005763.
117. Kuhn DA, Vanhecke D, Michen B, Blank F, Gehr P, Petri-Fink A, Rothen-Rutishauser B. Different endocytotic uptake mechanisms for nanoparticles in epithelial cells and macrophages. *Beilstein J Nanotechnol*. 2014;5:1625–36. doi:10.3762/bjnano.5.174.
118. Labouta HI, Menina S, Kochut A, Gordon S, Geyer R, Dersch P, Lehr CM. Bacteriomimetic invasin-functionalized nanocarriers for intracellular delivery. *Journal of Controlled Release*. 2015;220:414–24. doi:10.1016/j.jconrel.2015.10.052.
119. Landersdorfer CB, Nguyen T-H, Lieu LT, Nguyen G, Bischof RJ, Meeusen EN, et al. Substantial Targeting Advantage Achieved by Pulmonary Administration of Colistin Methanesulfonate in a Large-Animal Model. *Antimicrob. Agents Chemother*. 2017. doi:10.1128/AAC.01934-16.
120. Laxminarayan R, Matsoso P, Pant S, Brower C, Røttingen J-A, Klugman K, Davies S. Access to effective antimicrobials: a worldwide challenge.

- The Lancet. 2016;387(10014):168–75. doi:10.1016/S0140-6736(15)00474-2.
121. Lee C-M, Lee H-C, Lee K-Y. O-palmitoylcurdlan sulfate (OPCurS)-coated liposomes for oral drug delivery. *J Biosci Bioeng.* 2005;100(3):255–9. doi:10.1263/jbb.100.255.
122. Lehr CM, Bouwstra JA, Kok W, Noach AB, Boer AG de, Junginger HE. Bioadhesion by means of specific binding of tomato lectin. *Pharm. Res.* 1992;9(4):547–53. doi:10.1023/a:1015804816582.
123. Lehr CM, Labouta HI, Gordon S, Castoldi A, Menina S, Geyer R, Kochut A. and Dersch P. *Methods and compositions of carrier systems for the purpose of intracellular drug targeting*; 2016.
124. Lemièrè J, Carvalho K, Sykes C. Cell-sized liposomes that mimic cell motility and the cell cortex. *Methods Cell Biol.* 2015;128:271–85. doi:10.1016/bs.mcb.2015.01.013.
125. Leo L de, Di Toro N, Decorti G, Malusà N, Ventura A, Not T. Fasting increases tobramycin oral absorption in mice. *Antimicrob. Agents Chemother.* 2010;54(4):1644–6. doi:10.1128/AAC.01172-09.
126. Levitte S, Adams KN, Berg RD, Cosma CL, Urdahl KB, Ramakrishnan L. Mycobacterial Acid Tolerance Enables Phagolysosomal Survival and Establishment of Tuberculous Infection In Vivo. *Cell Host Microbe.* 2016;20(2):250–8. doi:10.1016/j.chom.2016.07.007.
127. Li J, Nation RL, Milne RW, Turnidge JD, Coulthard K. Evaluation of colistin as an agent against multi-resistant Gram-negative bacteria. *International Journal of Antimicrobial Agents.* 2005;25(1):11–25. doi:10.1016/j.ijantimicag.2004.10.001.
128. Li J, Nation RJ, Turnidge JD, Milne RW, Coulthard K, Rayner CR, Paterson DL. Colistin: the re-emerging antibiotic for multidrug-resistant Gram-negative bacterial infections. *The Lancet Infectious Diseases.* 2006;6(9):589–601. doi:10.1016/S1473-3099(06)70580-1.

129. Li X, Chen D, Le C, Zhu C, Gan Y, Hovgaard L, Yang M. Novel mucus-penetrating liposomes as a potential oral drug delivery system: preparation, in vitro characterization, and enhanced cellular uptake. *Int J Nanomedicine*. 2011;6:3151–62. doi:10.2147/IJN.S25741.
130. Li K, Chen D, Zhao X, Hu H, Yang C, Pang D. Preparation and investigation of *Ulex europaeus* agglutinin I-conjugated liposomes as potential oral vaccine carriers. *Arch Pharm Res*. 2011;34(11):1899–907. doi:10.1007/s12272-011-1110-3.
131. Li C, Zhang Y, Su T, Feng L, Long Y, Chen Z. Silica-coated flexible liposomes as a nanohybrid delivery system for enhanced oral bioavailability of curcumin. *Int J Nanomedicine*. 2012;7:5995–6002. doi:10.2147/IJN.S38043.
132. Liang JF, Yang VC. Insulin-cell penetrating peptide hybrids with improved intestinal absorption efficiency. *Biochem Biophys Res Commun*. 2005;335(3):734–8. doi:10.1016/j.bbrc.2005.07.142.
133. Lipp R. Major Advances in Oral Drug Delivery over the Past 15 Years. 2013.
134. Liu W, Ye A, Liu W, Liu C, Han J, Singh H. Behaviour of liposomes loaded with bovine serum albumin during in vitro digestion. *Food Chem*. 2015;175:16–24. doi:10.1016/j.foodchem.2014.11.108.
135. Liu C, Kou Y, Zhang X, Cheng H, Chen X, Mao S. Strategies and industrial perspectives to improve oral absorption of biological macromolecules. *Expert Opin Drug Deliv*. 2018;15(3):223–33. doi:10.1080/17425247.2017.1395853.
136. Lowy F d. Is *Staphylococcus aureus* an intracellular pathogen? *Trends in Microbiology*. 2000;8(8):341–3. doi:10.1016/S0966-842X(00)01803-5.
137. Maher S, Mrsny RJ, Brayden DJ. Intestinal permeation enhancers for oral peptide delivery. *Adv. Drug Deliv. Rev.* 2016;106(Pt B):277–319. doi:10.1016/j.addr.2016.06.005.

138. Manconi M, Mura S, Manca ML, Fadda AM, Dolz M, Hernandez MJ, et al. Chitosomes as drug delivery systems for C-phycoerythrin: preparation and characterization. *Int J Pharm.* 2010;392(1-2):92–100. doi:10.1016/j.ijpharm.2010.03.038.
139. Mannock DA, Lewis, R. N. A. H., McElhane RN. Comparative calorimetric and spectroscopic studies of the effects of lanosterol and cholesterol on the thermotropic phase behavior and organization of dipalmitoylphosphatidylcholine bilayer membranes. *Biophys J.* 2006;91(9):3327–40. doi:10.1529/biophysj.106.084368.
140. Martens E, Demain AL. The antibiotic resistance crisis, with a focus on the United States. *J Antibiot.* 2017;70(5):520–6. doi:10.1038/ja.2017.30.
141. Mayor S, Pagano RE. Pathways of clathrin-independent endocytosis. *Nat Rev Mol Cell Biol.* 2007;8(8):603–12. doi:10.1038/nrm2216.
142. McClure EE, Chávez ASO, Shaw DK, Carlyon JA, Ganta RR, Noh SM, et al. Engineering of obligate intracellular bacteria: Progress, challenges and paradigms. *Nat Rev Microbiol.* 2017;15(9):544–58. doi:10.1038/nrmicro.2017.59.
143. McGavin MH, Krajewska-Pietrasik D, Rydén C, Höök M. Identification of a *Staphylococcus aureus* extracellular matrix-binding protein with broad specificity. *Infect. Immun.* 1993;61(6):2479–85.
144. Menina S, Labouta, H. I.:Geyer, R., Krause T, Gordon, S., Dersch, P, Lehr C-M. Invasin-functionalized liposome nanocarriers improve the intracellular delivery of anti-infective drugs. *RSC Adv.* 2016;6(47):41622–9. doi:10.1039/C6RA02988D.
145. Miguel I de, Ioualalena K, Bonnefous M, Peyrot M, Nguyen F, Cervilla M, et al. Synthesis and characterization of supramolecular biovector (SMBV) specifically designed for the entrapment of ionic molecules. *Biochimica et Biophysica Acta (BBA) - Biomembranes.* 1995;1237(1):49–58. doi:10.1016/0005-2736(95)00079-I.

146. Minato S, Iwanaga K, Kakemi M, Yamashita S, Oku N. Application of polyethyleneglycol (PEG)-modified liposomes for oral vaccine: effect of lipid dose on systemic and mucosal immunity. *Journal of Controlled Release*. 2003;89(2):189–97. doi:10.1016/S0168-3659(03)00093-2.
147. Mohammed NN, Pandey P, Khan NS, Elokely KM, Liu H, Doerksen RJ, Repka MA. Clotrimazole-cyclodextrin based approach for the management and treatment of Candidiasis - A formulation and chemistry-based evaluation. *Pharm Dev Technol*. 2016;21(5):619–29. doi:10.3109/10837450.2015.1041041.
148. Mohanraj VJ, Barnes TJ, Prestidge CA. Silica nanoparticle coated liposomes: a new type of hybrid nanocapsule for proteins. *Int J Pharm*. 2010;392(1-2):285–93. doi:10.1016/j.ijpharm.2010.03.061.
149. Morishita M, Kamei N, Ehara J, Isowa K, Takayama K. A novel approach using functional peptides for efficient intestinal absorption of insulin. *J Control Release*. 2007;118(2):177–84. doi:10.1016/j.jconrel.2006.12.022.
150. Mouritsen OG. Lipids, curvature, and nano-medicine. *Eur J Lipid Sci Technol*. 2011;113(10):1174–87. doi:10.1002/ejlt.201100050.
151. Müllertz A, Reppas C, Psachoulias D, Vertzoni M, Fatouros DG. Structural features of colloidal species in the human fasted upper small intestine. *J Pharm Pharmacol*. 2015;67(4):486–92. doi:10.1111/jphp.12336.
152. Muppidi K, Pumerantz AS, Wang J, Betageri G. Development and stability studies of novel liposomal vancomycin formulations. *ISRN Pharm*. 2012;2012:636743. doi:10.5402/2012/636743.
153. Muramatsu K, Maitani Y, Nagai T. Dipalmitoylphosphatidylcholine liposomes with soybean-derived sterols and cholesterol as a carrier for the oral administration of insulin in rats. *Biol Pharm Bull*. 1996;19(8):1055–8. doi:10.1248/bpb.19.1055.
154. Nabi IR, Le PU. Caveolae/raft-dependent endocytosis. *J Cell Biol*. 2003;161(4):673–7. doi:10.1083/jcb.200302028.

155. Nag OK, Awasthi V. Surface engineering of liposomes for stealth behavior. *Pharmaceutics*. 2013;5(4):542–69. doi:10.3390/pharmaceutics5040542.
156. Naisbett B, Woodley J. The potential use of tomato lectin for oral drug delivery. 1. Lectin binding to rat small intestine in vitro. *Int J Pharm*. 1994;107(3):223–30. doi:10.1016/0378-5173(94)90438-3.
157. Nangia S, Sureshkumar R. Effects of nanoparticle charge and shape anisotropy on translocation through cell membranes. *Langmuir*. 2012;28(51):17666–71. doi:10.1021/la303449d.
158. Nation RL, Garonzik SM, Thamlikitkul, J. Li, V, Giamarellos-Bourboulis EJ, Paterson DL, Turnidge JD, et al. Updated US and European Dose Recommendations for Intravenous Colistin: How Do They Perform? *Clinical Infectious Diseases*. 2016;62(5):552–8. doi:10.1093/cid/civ964.
159. Nawroth T, Buch P, Buch K, Langguth P, Schweins R. Liposome formation from bile salt-lipid micelles in the digestion and drug delivery model FaSSIF(mod) estimated by combined time-resolved neutron and dynamic light scattering. *Mol Pharm*. 2011;8(6):2162–72. doi:10.1021/mp100296w.
160. Nguyen TX, Huang L, Liu L, Elamin Abdalla AM, Gauthier M, Yang G. Chitosan-coated nano-liposomes for the oral delivery of berberine hydrochloride. *J. Mater. Chem. B*. 2014;2(41):7149–59. doi:10.1039/C4TB00876F.
161. Nguyen TX, Huang L, Gauthier M, Yang G, Wang Q. Recent advances in liposome surface modification for oral drug delivery. *Nanomedicine (Lond)*. 2016;11(9):1169–85. doi:10.2217/nnm.16.9.
162. Nicolas P, Mor A. Peptides as weapons against microorganisms in the chemical defense system of vertebrates. *Annu Rev Microbiol*. 1995;49:277–304. doi:10.1146/annurev.mi.49.100195.001425.
163. Nielsen LH, Gordon S, Holm R, Selen A, Rades T, Müllertz A. Preparation of an amorphous sodium furosemide salt improves solubility and dissolution rate and leads to a faster T_{max} after oral dosing to

- rats. *European Journal of Pharmaceutics and Biopharmaceutics*. 2013;85(3 PART B):942–51. doi:10.1016/j.ejpb.2013.09.002.
164. Niu M, Lu Y, Hovgaard L, Wu W. Liposomes containing glycocholate as potential oral insulin delivery systems: preparation, in vitro characterization, and improved protection against enzymatic degradation. *Int J Nanomedicine*. 2011;6:1155–66. doi:10.2147/IJN.S19917.
165. Niu M, Lu Y, Hovgaard L, Guan P, Tan Y, Lian R, et al. Hypoglycemic activity and oral bioavailability of insulin-loaded liposomes containing bile salts in rats: the effect of cholate type, particle size and administered dose. *Eur J Pharm Biopharm*. 2012;81(2):265–72. doi:10.1016/j.ejpb.2012.02.009.
166. Okoro CK, Kingsley RA, Connor TR, Harris SR, Parry CM, Al-Mashhadani MN, et al. Intracontinental spread of human invasive *Salmonella* Typhimurium pathovariants in sub-Saharan Africa. *Nat Genet*. 2012;44(11):1215–21. doi:10.1038/ng.2423.
167. Palma M, Haggar A, Flock J-I. Adherence of *Staphylococcus aureus* Is Enhanced by an Endogenous Secreted Protein with Broad Binding Activity. *J Bacteriol*. 1999;181(9):2840–5.
168. Pandey R, Khuller GK. Nanoparticle-based oral drug delivery system for an injectable antibiotic - streptomycin. Evaluation in a murine tuberculosis model. *Chemotherapy*. 2007;53(6):437–41. doi:10.1159/000110009.
169. Pantze SF, Parmentier J, Hofhaus G, Fricker G. Matrix liposomes: A solid liposomal formulation for oral administration. *Eur. J. Lipid Sci. Technol*. 2014;116(9):1145–54. doi:10.1002/ejlt.201300409.
170. Papadimitriou S, Bikiaris D. Novel self-assembled core-shell nanoparticles based on crystalline amorphous moieties of aliphatic copolyesters for efficient controlled drug release. *Journal of Controlled Release*. 2009;138(2):177–84. doi:10.1016/j.jconrel.2009.05.013.
171. d. Papahadjopoulos, Poste G, Schaeffer BE. Fusion of mammalian cells by unilamellar lipid vesicles: Influence of lipid surface charge, fluidity and

- cholesterol. *Biochimica et Biophysica Acta (BBA) - Biomembranes*. 1973;323(1):23–42. doi:10.1016/0005-2736(73)90429-X.
172. Parmentier J, Hartmann FJ, Fricker G. In vitro evaluation of liposomes containing bio-enhancers for the oral delivery of macromolecules. *Eur J Pharm Biopharm*. 2010;76(3):394–403. doi:10.1016/j.ejpb.2010.09.002.
173. Parmentier J, Thewes B, Gropp F, Fricker G. Oral peptide delivery by tetraether lipid liposomes. *Int J Pharm*. 2011;415(1-2):150–7. doi:10.1016/j.ijpharm.2011.05.066.
174. Parmentier J, Thomas N, Müllertz A, Fricker G, Rades T. Exploring the fate of liposomes in the intestine by dynamic in vitro lipolysis. *Int J Pharm*. 2012;437(1-2):253–63. doi:10.1016/j.ijpharm.2012.08.018.
175. Pasut G, Paolino D, Celia C, Mero A, Joseph AS, Wolfram J, et al. Polyethylene glycol (PEG)-dendron phospholipids as innovative constructs for the preparation of super stealth liposomes for anticancer therapy. *J Control Release*. 2015;199:106–13. doi:10.1016/j.jconrel.2014.12.008.
176. Pawar VK, Meher JG, Singh Y, Chaurasia M, Surendar Reddy B, Chourasia MK. Targeting of gastrointestinal tract for amended delivery of protein/peptide therapeutics: strategies and industrial perspectives. *J Control Release*. 2014;196:168–83. doi:10.1016/j.jconrel.2014.09.031.
177. Paz I, Sachse M, Dupont N, Mounier J, Cederfur C, Enninga J, et al. Galectin-3, a marker for vacuole lysis by invasive pathogens. *Cell Microbiol*. 2010;12(4):530–44. doi:10.1111/j.1462-5822.2009.01415.x.
178. Peterson E, Kaur P. Antibiotic Resistance Mechanisms in Bacteria: Relationships Between Resistance Determinants of Antibiotic Producers, Environmental Bacteria, and Clinical Pathogens. *Front Microbiol*. 2018;9:2928. doi:10.3389/fmicb.2018.02928.
179. Petralito S, Spera R, Pacelli S, Relucenti M, Familiari G, Vitalone A, et al. Design and development of PEG-DMA gel-in-liposomes as a new tool for

- drug delivery. *Reactive and Functional Polymers*. 2014;77:30–8. doi:10.1016/j.reactfunctpolym.2014.02.002.
180. Pieters J. Mycobacterium tuberculosis and the macrophage: Maintaining a balance. *Cell Host Microbe*. 2008;3(6):399–407. doi:10.1016/j.chom.2008.05.006.
181. Pizarro-Cerdá J, Moreno E, Desjardins M, Gorvel JP. When intracellular pathogens invade the frontiers of cell biology and immunology. *Histol Histopathol*. 1997;12(4):1027–38.
182. Pizarro-Cerdá J, Cossart P. Bacterial adhesion and entry into host cells. *Cell*. 2006;124(4):715–27. doi:10.1016/j.cell.2006.02.012.
183. Pizarro-Cerdá J, Charbit A, Enninga J, Lafont F, Cossart P. Manipulation of host membranes by the bacterial pathogens *Listeria*, *Francisella*, *Shigella* and *Yersinia*. *Semin Cell Dev Biol*. 2016;60:155–67. doi:10.1016/j.semcdb.2016.07.019.
184. PLOS Medicine Editors. Antimicrobial Resistance: Is the World UNprepared? *PLoS Med*. 2016;13(9):e1002130. doi:10.1371/journal.pmed.1002130.
185. Powers JH. Antimicrobial drug development--the past, the present, and the future. *Clin Microbiol Infect*. 2004;10 Suppl 4:23–31. doi:10.1111/j.1465-0691.2004.1007.x.
186. Pridgen EM, Alexis F, Farokhzad OC. Polymeric nanoparticle drug delivery technologies for oral delivery applications. *Expert Opin Drug Deliv*. 2015;12(9):1459–73. doi:10.1517/17425247.2015.1018175.
187. Qin S-Y, Zhang A-Q, Cheng X, Rong L, Zhang X-Z. Drug self-delivery systems for cancer therapy. *Biomaterials*. 2017;112:234–47. doi:10.1016/j.biomaterials.2016.10.016.
188. Rao GG, Ly NS, Haas CE, Garonzik S, Forrest A, Bulitta JB, et al. New dosing strategies for an old antibiotic: Pharmacodynamics of front-loaded regimens of colistin at simulated pharmacokinetics in patients with kidney

- or liver disease. *Antimicrob. Agents Chemother.* 2014;58(3):1381–8. doi:10.1128/AAC.00327-13.
189. Raza A, Sime FB, Cabot PJ, Maqbool F, Roberts JA, Falconer JR. Solid nanoparticles for oral antimicrobial drug delivery: a review. *Drug Discov. Today.* 2019;24(3):858–66. doi:10.1016/j.drudis.2019.01.004.
190. Rejman J, Oberle V, Zuhorn IS, Hoekstra D. Size-dependent internalization of particles via the pathways of clathrin- and caveolae-mediated endocytosis. *Biochem J.* 2004;377(Pt 1):159–69. doi:10.1042/BJ20031253.
191. Rejman J, Bragonzi A, Conese M. Role of clathrin- and caveolae-mediated endocytosis in gene transfer mediated by lipo- and polyplexes. *Molecular Therapy.* 2005;12(3):468–74. doi:10.1016/j.ymthe.2005.03.038.
192. Ren B, Huang P, Zhang J, He W, Han J, Liu X, Zhang L, editors. *Main Applications of Antibiotics*; 2015.
193. Ribet D, Cossart P. How bacterial pathogens colonize their hosts and invade deeper tissues. *Microbes Infect.* 2015;17(3):173–83. doi:10.1016/j.micinf.2015.01.004.
194. Riethorst D, Baatsen P, Remijn C, Mitra A, Tack J, Brouwers J, Augustijns P. An In-Depth View into Human Intestinal Fluid Colloids: Intersubject Variability in Relation to Composition. *Mol Pharm.* 2016;13(10):3484–93. doi:10.1021/acs.molpharmaceut.6b00496.
195. Riss TL, Moravec RA, Niles AL, Duellman S, Benink HA, Worzella TJ, Minor L. *Assay Guidance Manual: Cell Viability Assays*. Bethesda (MD); 2004.
196. Róg T, Pasenkiewicz-Gierula M. Cholesterol effects on the phospholipid condensation and packing in the bilayer: a molecular simulation study. *FEBS Letters.* 2001;502(1-2):68–71. doi:10.1016/S0014-5793(01)02668-0.
197. Ross BP, DeCruz SE, Lynch TB, Davis-Goff K, Toth I. Design, synthesis, and evaluation of a liposaccharide drug delivery agent: application to the

- gastrointestinal absorption of gentamicin. *J Med Chem.* 2004;47(5):1251–8. doi:10.1021/jm030474j.
198. Rowland RN, Woodley JF. The stability of liposomes in vitro to pH, bile salts and pancreatic lipase. *Biochimica et Biophysica Acta (BBA)/Lipids and Lipid Metabolism.* 1980a;620(3):400–9.
199. Rowland RN, Woodley JF. The stability of liposomes in vitro to pH, bile salts and pancreatic lipase. *Biochimica Biophysica Acta.* 1980b;620(3):400–9. doi:10.1016/0005-2760(80)90131-9.
200. Ryan KJ, Ray CG, Sherris JCM. *Sherris medical microbiology: An introduction to infectious diseases / Kenneth J. Ryan, C. George Ray, editors.* 4th ed. New York, London: McGraw-Hill; 2004.
201. S. E. Autenrieth and I. B. Autenrieth. *Yersinia enterocolitica: Subversion of adaptive immunity and implications for vaccine development.* *International Journal of Medical Microbiology.* 2008;298(1-2):69–77. doi:10.1016/j.ijmm.2007.07.010.
202. Salama AH, Aburahma MH. Ufasomes nano-vesicles-based lyophilized platforms for intranasal delivery of cinnarizine: preparation, optimization, ex-vivo histopathological safety assessment and mucosal confocal imaging. *Pharm Dev Technol.* 2016;21(6):706–15. doi:10.3109/10837450.2015.1048553.
203. Salouti M, Ahangari A. Nanoparticle based Drug Delivery Systems for Treatment of Infectious Diseases. In: Sezer AD, ed. *Application of Nanotechnology in Drug Delivery.* InTech; 2014. doi:10.5772/58423.
204. Samad A, Sultana Y, Aqil M. Liposomal drug delivery systems: an update review. *Curr Drug Deliv.* 2007;4(4):297–305. doi:10.2174/156720107782151269.
205. Sassene P, Kleberg K, Williams HD, Bakala-N'Goma J-C, Carrière F, Calderone M, et al. Toward the establishment of standardized in vitro tests for lipid-based formulations, part 6: effects of varying pancreatin and

- calcium levels. *AAPS J.* 2014;16(6):1344–57. doi:10.1208/s12248-014-9672-x.
206. Schnitzer JE, Oh P, Pinney E, Allard J. Filipin-sensitive caveolae-mediated transport in endothelium: reduced transcytosis, scavenger endocytosis, and capillary permeability of select macromolecules. *J Cell Biol.* 1994;127(5):1217–32.
207. Sercombe L, Veerati T, Moheimani F, Wu SY, Sood AK, Hua S. Advances and Challenges of Liposome Assisted Drug Delivery. *Front Pharmacol.* 2015;6:286. doi:10.3389/fphar.2015.00286.
208. Sharma A, Sharma S, Khuller GK. Lectin-functionalized poly (lactide-co-glycolide) nanoparticles as oral/aerosolized antitubercular drug carriers for treatment of tuberculosis. *J. Antimicrob. Chemother.* 2004;54(4):761–6. doi:10.1093/jac/dkh411.
209. Sheehan J, Hlavka J. The Use of Water-Soluble and Basic Carbodiimides in Peptide Synthesis. *J. Org. Chem.* 1956;21(4):439–41. doi:10.1021/jo01110a017.
210. Shukla A, Khatri K, Gupta PN, Goyal AK, Mehta A, Vyas SP. Oral immunization against hepatitis B using bile salt stabilized vesicles (bilosomes). *J Pharm Pharm Sci.* 2008;11(1):59–66. doi:10.18433/j3k01m.
211. Shukla A, Mishra V, Kesharwani P. Bilosomes in the context of oral immunization: development, challenges and opportunities. *Drug Discov. Today.* 2016;21(6):888–99. doi:10.1016/j.drudis.2016.03.013.
212. Simonzadeh N. An isocratic HPLC method for the simultaneous determination of cholesterol, cardiolipin, and DOPC in lyophilized lipids and liposomal formulations. *J Chromatogr Sci.* 2009;47(4):304–8.
213. Smart AL, Gaisford S, Basit AW. Oral peptide and protein delivery: intestinal obstacles and commercial prospects. *Expert Opin Drug Deliv.* 2014;11(8):1323–35. doi:10.1517/17425247.2014.917077.

214. Smistad G, Bøyum S, Alund SJ, Samuelsen ABC, Hiorth M. The potential of pectin as a stabilizer for liposomal drug delivery systems. *Carbohydr Polym.* 2012;90(3):1337–44. doi:10.1016/j.carbpol.2012.07.002.
215. Song K-H, Chung S-J, Shim C-K. Enhanced intestinal absorption of salmon calcitonin (sCT) from proliposomes containing bile salts. *J Control Release.* 2005;106(3):298–308. doi:10.1016/j.jconrel.2005.05.016.
216. Stetefeld J, McKenna SA, Patel TR. Dynamic light scattering: a practical guide and applications in biomedical sciences. *Biophys Rev.* 2016;8(4):409–27. doi:10.1007/s12551-016-0218-6.
217. Stewart JC. Colorimetric determination of phospholipids with ammonium ferrothiocyanate. *Analytical Biochemistry.* 1980;104(1):10–4.
218. Su L-H, Chiu C-H. Salmonella: Clinical importance and evolution of nomenclature. *Chang Gung Med J.* 2007;30(3):210–9.
219. Sugihara H, Yamamoto H, Kawashima Y, Takeuchi H. Effectiveness of submicronized chitosan-coated liposomes in oral absorption of indomethacin. *Journal of Liposome Research.* 2012;22(1):72–9. doi:10.3109/08982104.2011.621128.
220. Talegaonkar S, Mishra PR, Khar RK, Biju SS. Vesicular systems: An overview. *Indian J Pharm Sci.* 2006;68(2):141. doi:10.4103/0250-474X.25707.
221. Thanou M, Verhoef JC, Junginger HE. Chitosan and its derivatives as intestinal absorption enhancers. *Adv. Drug Deliv. Rev.* 2001;50:S91-S101. doi:10.1016/S0169-409X(01)00180-6.
222. Thompson KM, Abraham N, Jefferson KK. Staphylococcus aureus extracellular adherence protein contributes to biofilm formation in the presence of serum. *FEMS Microbiology Letters.* 2010;305(2):143–7. doi:10.1111/j.1574-6968.2010.01918.x.
223. Thongborisute J, Tsuruta A, Kawabata Y, Takeuchi H. The effect of particle structure of chitosan-coated liposomes and type of chitosan on

- oral delivery of calcitonin. *J Drug Target.* 2006;14(3):147–54. doi:10.1080/10611860600648346.
224. Thornton SJ, Wasan KM. The reformulation of amphotericin B for oral administration to treat systemic fungal infections and visceral leishmaniasis. *Expert Opin Drug Deliv.* 2009;6(3):271–84. doi:10.1517/17425240902802861.
225. Tian J-N, Ge B-Q, Shen Y-F, He Y-X, Chen Z-X. Thermodynamics and Structural Evolution during a Reversible Vesicle-Micelle Transition of a Vitamin-Derived Bolaamphiphile Induced by Sodium Cholate. *J Agric Food Chem.* 2016;64(9):1977–88. doi:10.1021/acs.jafc.5b05547.
226. Torchilin VP, Levchenko TS, Rammohan R., Volodina N, Papahadjopoulos-Sternberg B, D'Souza GG. Cell transfection in vitro and in vivo with nontoxic TAT peptide-liposome-DNA complexes. *Proc. Natl. Acad. Sci. U.S.A.* 2003;100(4):1972–7. doi:10.1073/pnas.0435906100.
227. Truong-Le V, Lovalenti PM, Abdul-Fattah AM. Stabilization challenges and formulation strategies associated with oral biologic drug delivery systems. *Adv. Drug Deliv. Rev.* 2015;93:95–108. doi:10.1016/j.addr.2015.08.001.
228. Uliczka F, Pisan F, Schaake J, Stolz T, Rohde M, Fruth A, et al. Unique Cell Adhesion and Invasion Properties of *Yersinia enterocolitica* O:3, the Most Frequent Cause of Human Yersiniosis. *PLoS Pathog.* 2011;7:e1002117.
229. van Slooten ML, Boerman O, Romøren K, Kedar E, Crommelin DJA, Storm G. Liposomes as sustained release system for human interferon- γ : biopharmaceutical aspects. *Biochimica et Biophysica Acta (BBA) - Molecular and Cell Biology of Lipids.* 2001;1530(2-3):134–45. doi:10.1016/S1388-1981(00)00174-8.
230. Vannuffel P, Cocito C. Mechanism of action of streptogramins and macrolides. *Drugs.* 1996;51 Suppl 1:20–30. doi:10.2165/00003495-199600511-00006.

231. Venkatesan N, Vyas SP. Polysaccharide coated liposomes for oral immunization — development and characterization. *Int J Pharm.* 2000;203(1-2):169–77. doi:10.1016/S0378-5173(00)00442-7.
232. Venter H, Henningsen ML, Begg SL. Antimicrobial resistance in healthcare, agriculture and the environment: the biochemistry behind the headlines. *Essays Biochem.* 2017;61(1):1–10. doi:10.1042/EBC20160053.
233. Vercauteren D, Vandenbroucke RE, Jones AT, Rejman J, Demeester J, Smedt SCD, et al. The use of inhibitors to study endocytic pathways of gene carriers: Optimization and pitfalls. *Mol Ther.* 2010;18(3):561–9. doi:10.1038/mt.2009.281.
234. Vogt A, Batsford S, Rodríguez-Iturbe B, García R. Cationic antigens in poststreptococcal glomerulonephritis. *Clin Nephrol.* 1983;20(6):271–9.
235. Wallace SJ, Li J, Nation RL, Prankerd RJ, Boyd BJ. Interaction of colistin and colistin methanesulfonate with liposomes: Colloidal aspects and implications for formulation. *J Pharm Sci.* 2012;101(9):3347–59. doi:10.1002/jps.23203.
236. Wang N, Wang T, Zhang M, Chen R, Niu R, Deng Y. Mannose derivative and lipid A dually decorated cationic liposomes as an effective cold chain free oral mucosal vaccine adjuvant-delivery system. *Eur J Pharm Biopharm.* 2014;88(1):194–206. doi:10.1016/j.ejpb.2014.04.007.
237. Watson PMD, Paterson JC, Thom G, Ginman U, Lundquist S, Webster CI. Modelling the endothelial blood-CNS barriers: a method for the production of robust in vitro models of the rat blood-brain barrier and blood-spinal cord barrier. *BMC Neurosci.* 2013;14:59. doi:10.1186/1471-2202-14-59.
238. Weissgerber P, Faigle M, Northoff H, Neumeister B. Investigation of mechanisms involved in phagocytosis of *Legionella pneumophila* by human cells. *FEMS Microbiology Letters.* 2003;219(2):173–9. doi:10.1016/S0378-1097(03)00051-X.

239. Weissig V, Pettinger TK, Murdock N. Nanopharmaceuticals (part 1): products on the market. *Int J Nanomedicine*. 2014;9:4357–73. doi:10.2147/IJN.S46900.
240. Werle M, Makhlof A, Takeuchi H. Carbopol-Lectin Conjugate Coated Liposomes for Oral Peptide Delivery. *Chem. Pharm. Bull.* 2010;58(3):432–4. doi:10.1248/cpb.58.432.
241. WHO. WHO Report on Global Surveillance of Epidemic-prone Infectious Diseases - Introduction: Why infectious diseases are still a problem and surveillance is still required. WHO Report; 2018.
242. WHO Report. Global priority list of antibiotic-resistant bacteria to guide research, discovery, and development of new antibiotics. WHO Report; 2017.
243. Wijetunge SS, Wen J, Yeh C-K, Sun Y. Lectin-Conjugated Liposomes as Biocompatible, Bioadhesive Drug Carriers for the Management of Oral Ulcerative Lesions. *ACS Appl. Bio Mater.* 2018;1(5):1487–95. doi:10.1021/acsbm.8b00425.
244. Willats WGT, Knox JP, Mikkelsen JD. Pectin: new insights into an old polymer are starting to gel. *Trends in Food Science & Technology*. 2006;17(3):97–104. doi:10.1016/j.tifs.2005.10.008.
245. Wise R. A review of the mechanisms of action and resistance of antimicrobial agents. *Can Respir J*. 1999;6 Suppl A:20A-2A.
246. Working PK, Newman MS, Huang SK, Mayhew E, Vaage J, Lasic DD. Pharmacokinetics, Biodistribution and Therapeutic Efficacy of Doxorubicin Encapsulated in Stealth® Liposomes (Doxil®). *Journal of Liposome Research*. 2008;4(1):667–87. doi:10.3109/08982109409037065.
247. Wu W, Lu Y, Qi J. Oral delivery of liposomes. *Ther Deliv*. 2015;6(11):1239–41. doi:10.4155/tde.15.69.
248. Yahav D, Farbman L, Leibovici L, Paul M. Colistin: new lessons on an old antibiotic. *Clin Microbiol Infect*. 2012;18(1):18–29. doi:10.1111/j.1469-0691.2011.03734.x.

249. Yan W, Huang L. The effects of salt on the physicochemical properties and immunogenicity of protein based vaccine formulated in cationic liposome. *Int J Pharm.* 2009;368(1-2):56–62. doi:10.1016/j.ijpharm.2008.09.053.
250. Yapa S, Li J, Porter CJH, Nation RL, Patel K, McIntosh MP. Population pharmacokinetics of colistin methanesulfonate in rats: Achieving sustained lung concentrations of colistin for targeting respiratory infections. *Antimicrob. Agents Chemother.* 2013;57(10):5087–95. doi:10.1128/AAC.01127-13.
251. Yoneyama H, Katsumata R. Antibiotic resistance in bacteria and its future for novel antibiotic development. *Biosci Biotechnol Biochem.* 2006;70(5):1060–75. doi:10.1271/bbb.70.1060.
252. Zambito Y, Zaino C, Di Colo G. Effects of N-trimethylchitosan on transcellular and paracellular transcorneal drug transport. *Eur J Pharm Biopharm.* 2006;64(1):16–25. doi:10.1016/j.ejpb.2006.01.004.
253. Zhang X, Qi J, Lu Y, He W, Li X, Wu W. Biotinylated liposomes as potential carriers for the oral delivery of insulin. *Nanomedicine: Nanotechnology, Biology and Medicine.* 2014;10(1):167–76. doi:10.1016/j.nano.2013.07.011.
254. Zhang, Zhu X, Jin Y, Shan W, Huang Y. Mechanism study of cellular uptake and tight junction opening mediated by goblet cell-specific trimethyl chitosan nanoparticles. *Mol Pharm.* 2014;11(5):1520–32. doi:10.1021/mp400685v.
255. Zheng S, Xie Y, Li Y, Li L, Tian N, Zhu W, et al. Development of high drug-loading nanomicelles targeting steroids to the brain. *Int J Nanomedicine.* 2014;9:55–66. doi:10.2147/IJN.S52576.
256. Zhu Q, Guo T, Xia D, Li X, Zhu C, Li H, et al. Pluronic F127-modified liposome-containing tacrolimus-cyclodextrin inclusion complexes: improved solubility, cellular uptake and intestinal penetration. *J Pharm Pharmacol.* 2013;65(8):1107–17. doi:10.1111/jphp.12074.

257. Zhu Z, Zhu W, Yi J, Liu N, Cao Y, Lu J, et al. Effects of sonication on the physicochemical and functional properties of walnut protein isolate. *Food Res Int.* 2018;106:853–61. doi:10.1016/j.foodres.2018.01.060.
258. Ziello JE, Huang Y, Jovin IS. Cellular Endocytosis and Gene Delivery. *Mol Med.* 2010;16(5-6):222–9. doi:10.2119/molmed.2009.00101.

8 Supplementary Figures

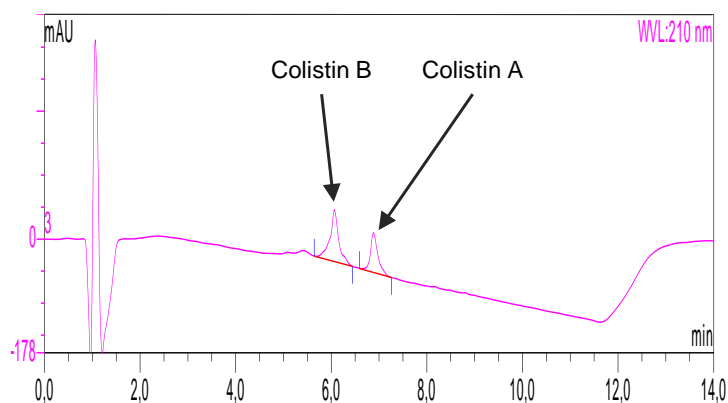


Figure 8.1. Colistin analytic analysis

Chromatograms of colistin A and B obtained by HPLC analysis, using gradient mode composed of 20:80 (v/v) acetonitrile: 0.1% TFA running for 10 min to reach 50:50 (v/v). A flow rate of 1 mL/min was used and peaks were detected using a UV-detector set at 210 nm.

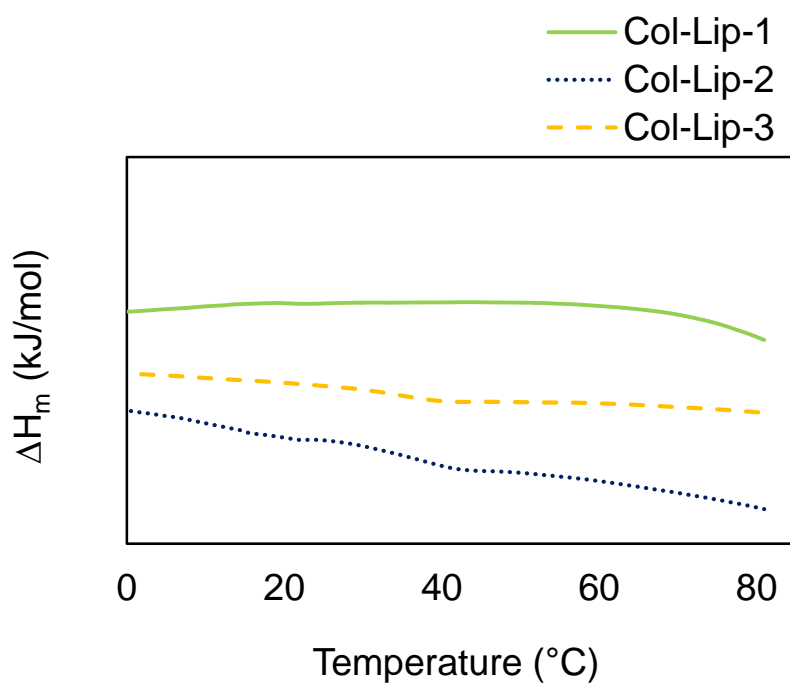


Figure 8.2. Thermal Characterization

Thermal analysis of Col-Lip-1, Col-Lip-2 and Col-Lip-3 using a heating rate from 0 °C to 80 °C with a heating rate of 10 °C/min and the enthalpy changes (ΔH_m) were plotted versus temperature.

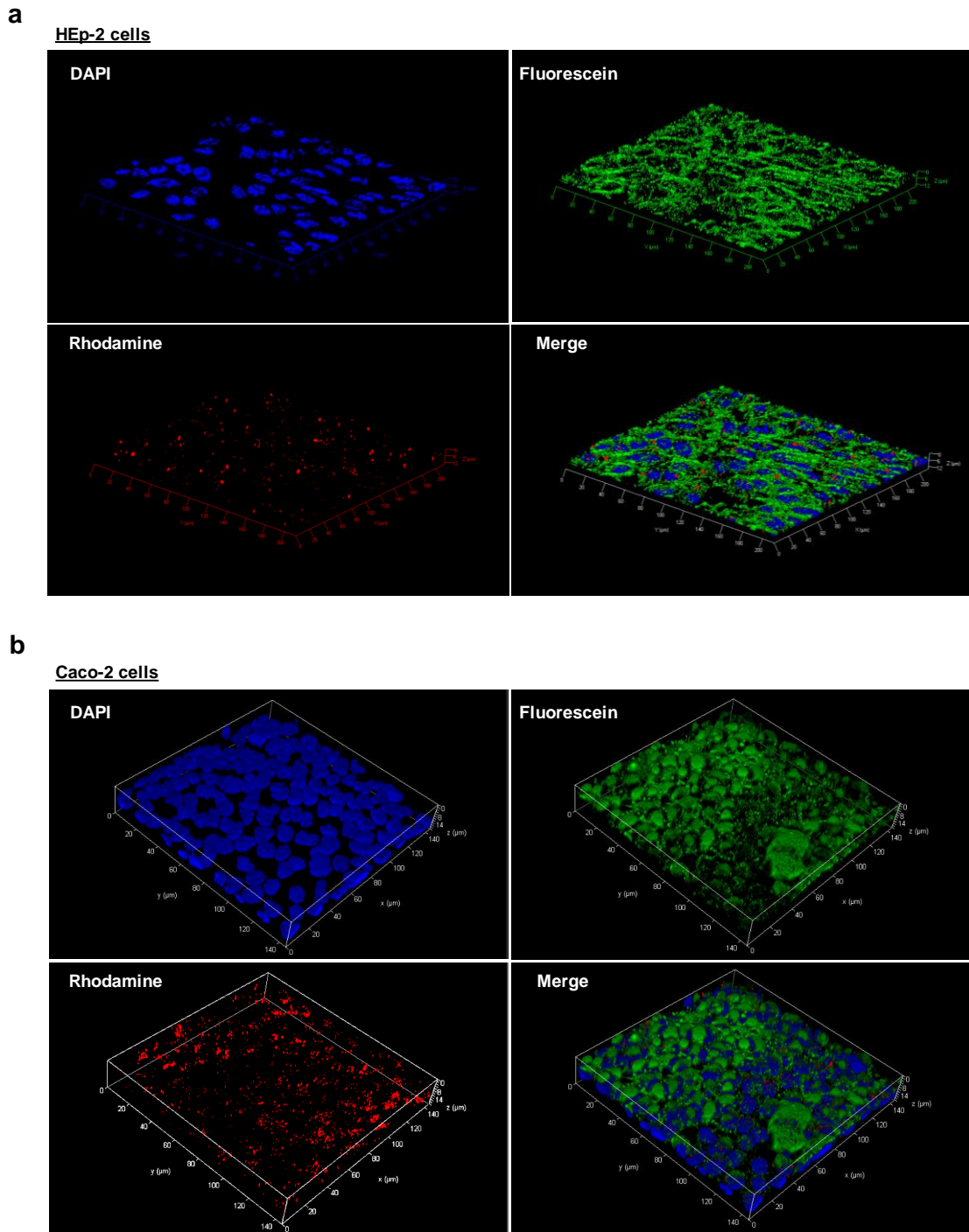
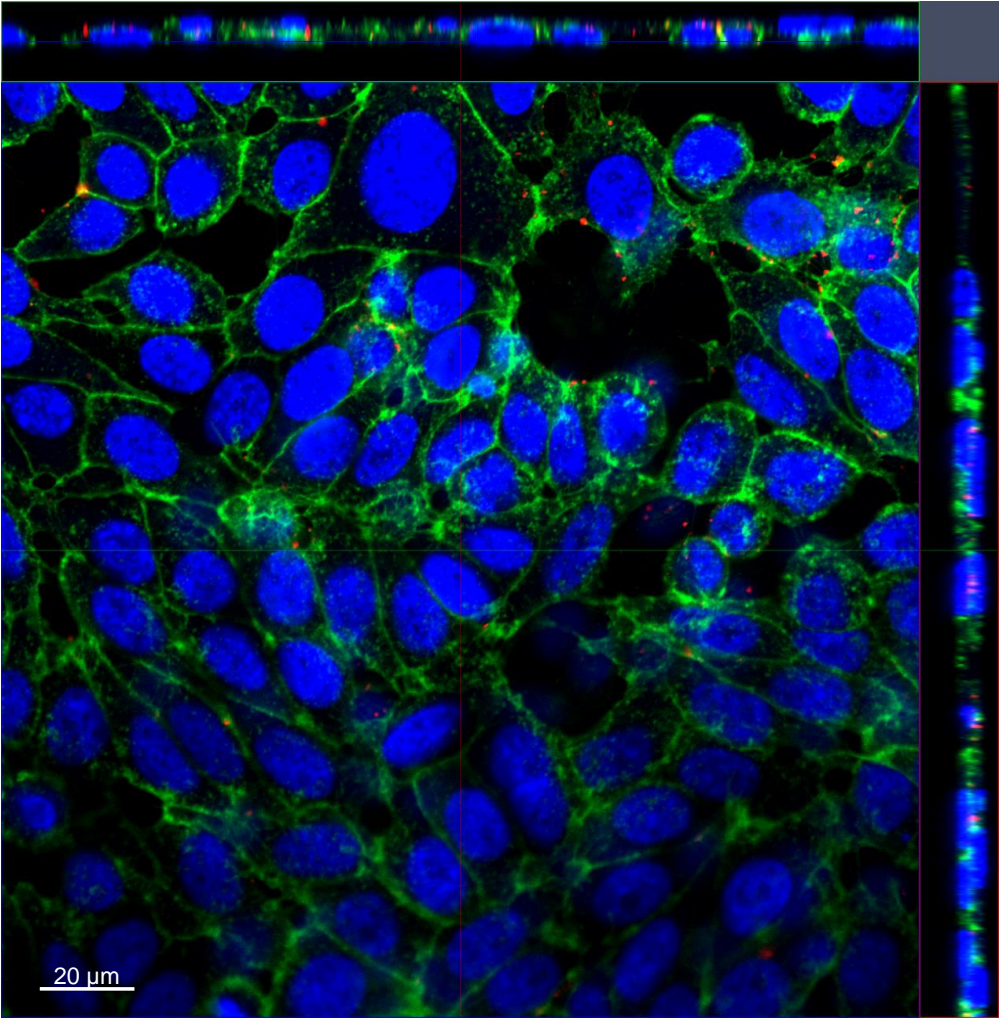


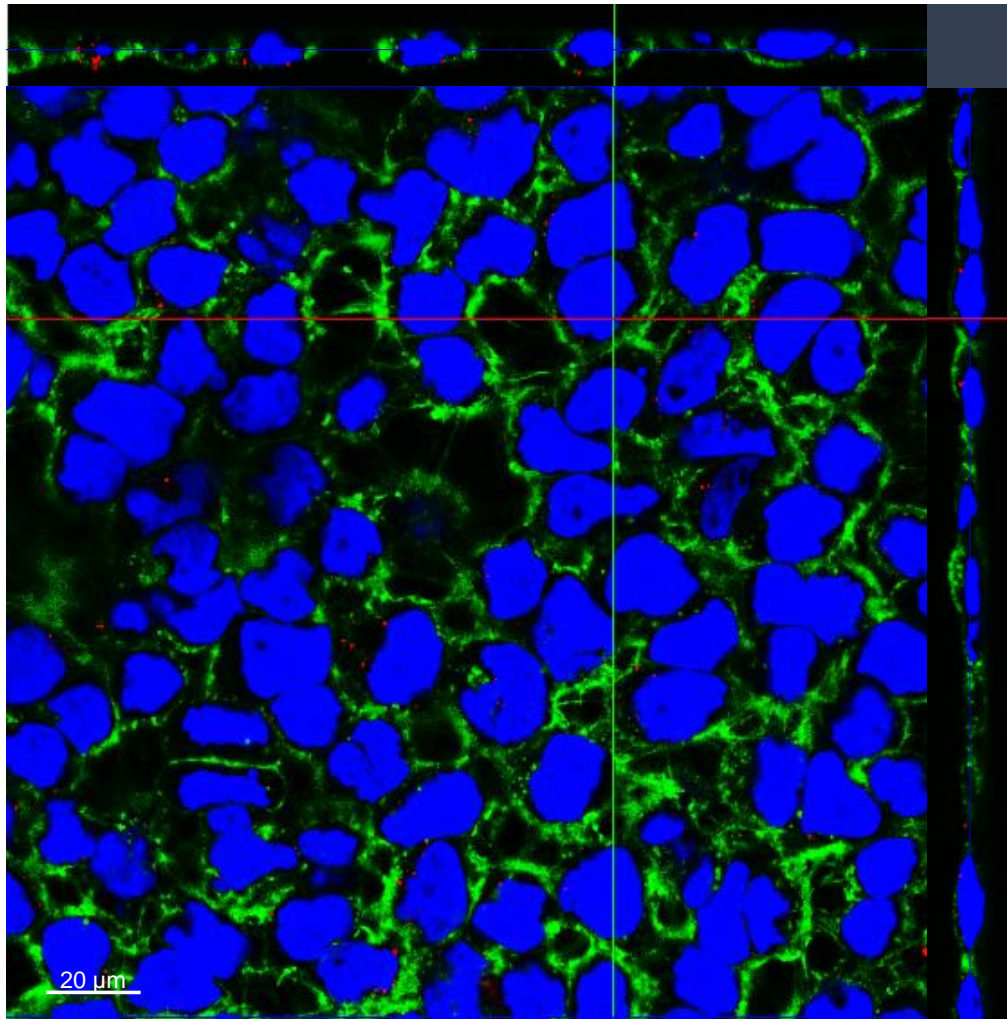
Figure 8.3. 3D fluorescence imaging

Representative confocal 3D uptake images of EapCol-Lip-3 by HEP-2 cells (a) and Caco-2 monolayer (b). Cells were treated with liposomes (labeled with rhodamine, red), stained for cell membrane (green), nucleus (blue), and fixed. Z-Stack sections (20 sections) were taken for an area of $200\ \mu\text{m} \times 200\ \mu\text{m} \times 12\ \mu\text{m}$ (HEP-2 cells), $140\ \mu\text{m} \times 140\ \mu\text{m} \times 14\ \mu\text{m}$ (Caco-2 cells) (x, y, z axes).

a

Hep-2 cells



b**Caco-2 cells****Figure 8.4. Ortho-CLSM images of Eap-Col-Lip-3 uptake**

Representative Ortho view of Z -stack image of EapCol-Lip-3 uptake in HEP-2 cells (a) and Caco-2 monolayer (b). Images were taken using 40x oil immersion objective and cell membrane was stained in green (Fluorescein), nucleus in blue (DAPI) and liposomes pre-labelled with rhodamine (red).

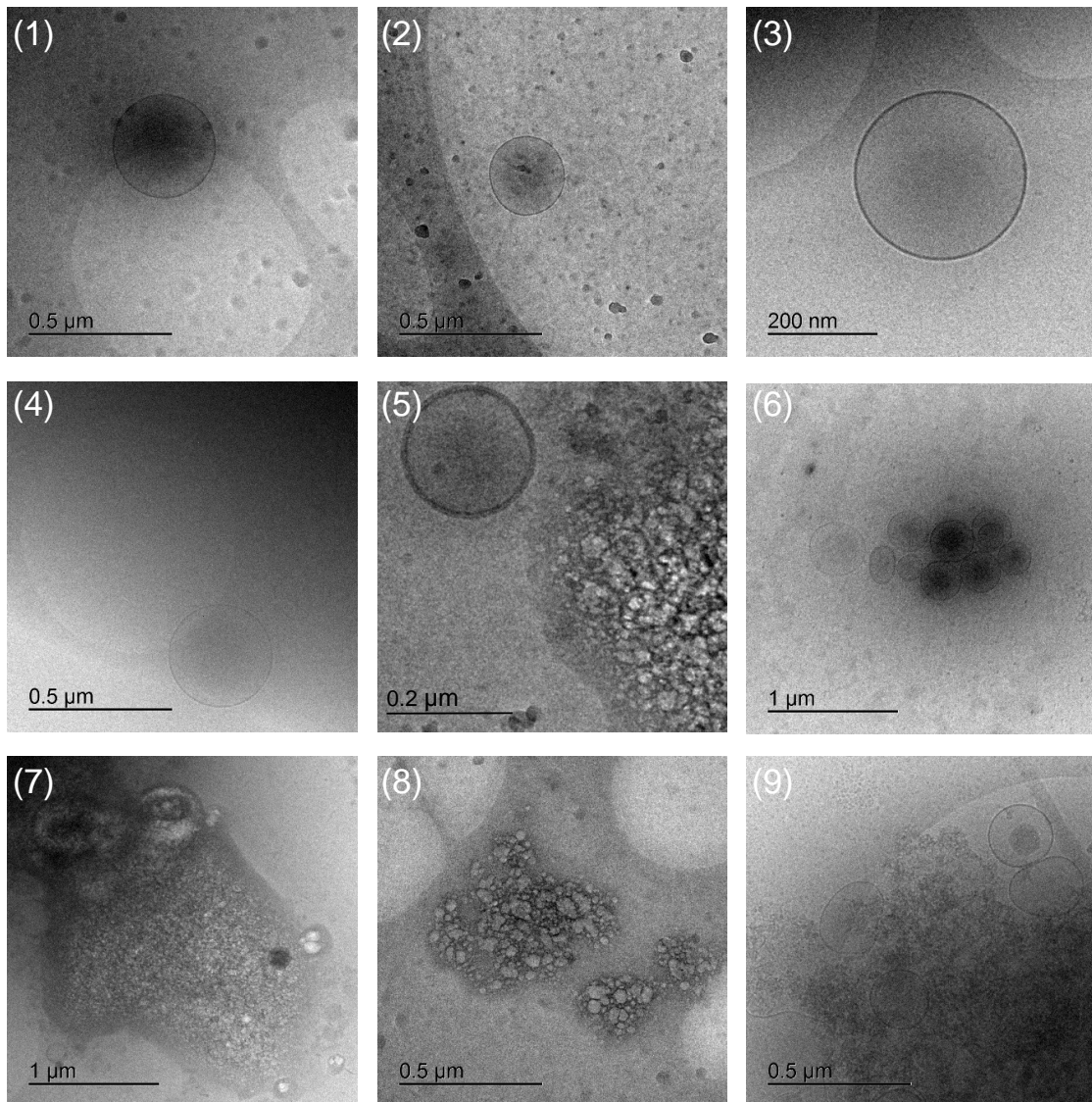


Figure 8.5. Liposomal morphology after stability studies in FaSSIF-Enz

Representative pictures of Cryo-TEM imaging showing simulated medium content and/or liposomes morphology (1, 2 and 3) Col-Lip-1, (4, 5) Col-Lip-2 and (6) Col-Lip-3. Images were taken directly after 5 h incubation in fasted state simulated intestinal fluid containing enzymes (FaSSIF-Enz) at 37° C. (7, 8 and 9) images of FaSSIF-Enz alone without liposomal formulation, indicating the presence of several colloidal structures in the medium.

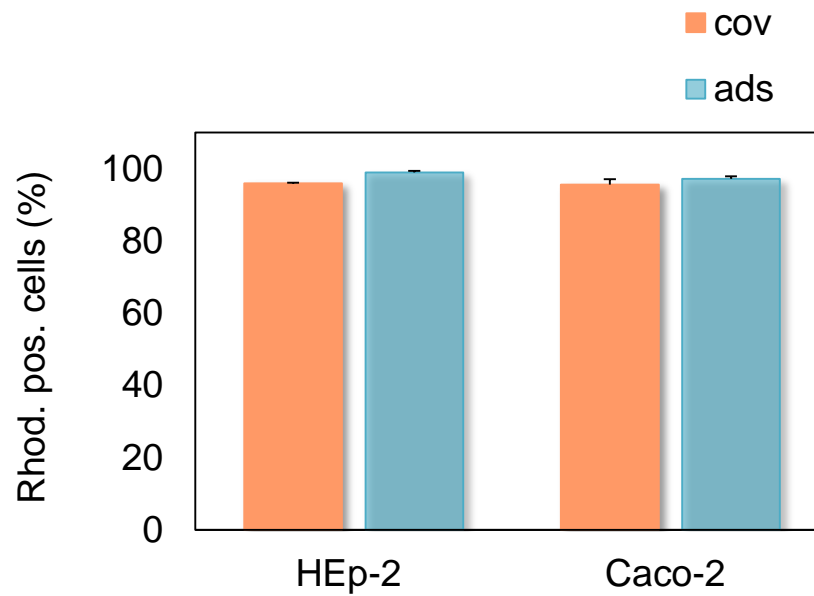


Figure 8.6. EapCol-Lip-3 uptake comparison

EapCol-Lip-3 functionalized with Eap either covalently using DMTMM (Cov) or adsorbed on liposomal surface via direct incubation with Eap (Ads). HEp-2 cells and Caco-2 monolayer were incubated with the samples for 2 h and 4 h respectively at 37° C. Results showed no significant difference between the two methods in achieving high rhodamine-positive cells signal.

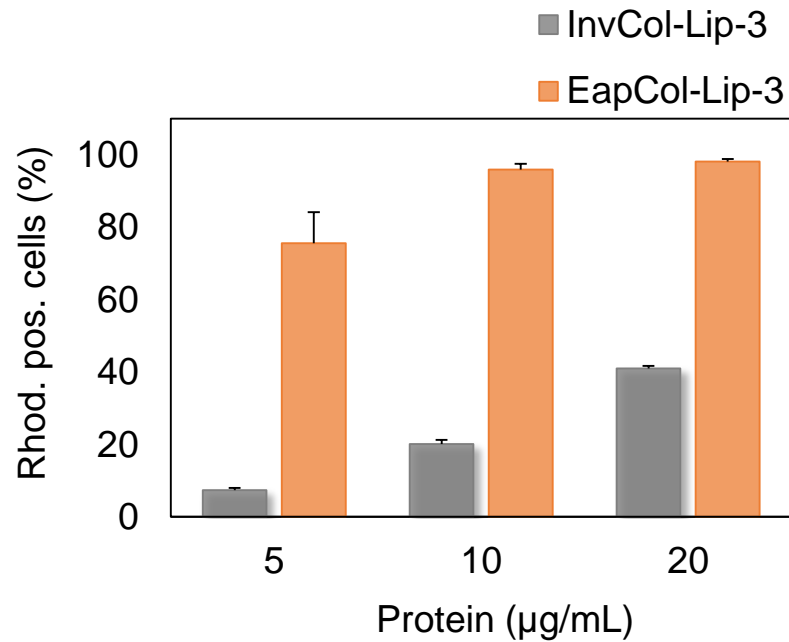


Figure 8.7. Eap- and InvA197-functionalized col-Lip-3 comparison

Col-Lip-3 was functionalized with InvA197 (InvCol-Lip-3) and with Eap (EapCol-Lip-3). Liposomes were applied to HEP-2 cells for 1 h using different concentrations 5, 10 and 20 µg/mL of each protein. Samples were prepared by functionalizing liposomes with each concentration separately and no washing step (to remove non-bounded protein) was performed in order to keep the same liposomal concentration in each applied sample. Results indicates the efficiency of Eap to mediate liposomal binding and/or internalization in comparison to InvA197.

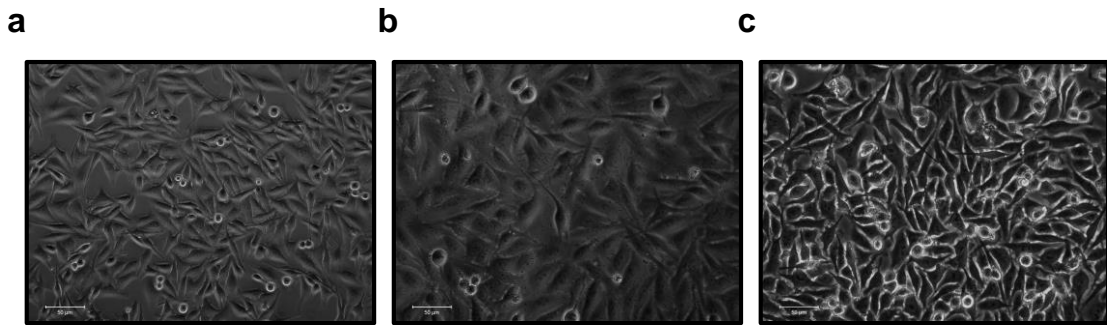


Figure 8.8. Cell imaging during infection

HEp-2 cells images during the infection study showing healthy elongated cells before infection (a), after addition of Salmonella (b) and after gentamicin treatment (c). Cells shared a similar morphology with presence of low number of round-shaped cells at all stages.

Acknowledgements

I am delighted to come to this part in which I will be writing my last words to close this chapter of my life and for that I would like to express my sincere gratitude to everyone who helped in this fascinating research work and in this exciting phase in my life.

First of all, I wish to express my gratitude to my supervisors, Prof. Claus-Michael Lehr for the given opportunity to conduct my PhD work within DDEL group, in which I felt home. Prof. Lehr contributed to a large extent to my professional growth through his exceptional scientific knowledge as well as to my personal development through our compelling social events.

A special thanks and big hugs go to Dr. Sarah Gordon for her great support even before I started my PhD, kind advices throughout my doctoral research work and for the huge impact she had on my English intentionally and unintentionally. It was a privilege and great honor for me to share her scientific knowledge but also her extraordinary human qualities.

I would like to thank Dr. Brigitta Loretz, who welcomed me during my last year in her group and was abundantly helpful and offered invaluable support and guidance.

I also would like to thank Prof. Hartmann for his support and fruitful discussions during thesis committee meetings throughout my dissertation time.

To my collaboration partners Prof. Markus Bischoff and Dr. Janina Eisenbeis, I would like to express my sincere gratitude for providing Eap and for their valuable comments and fruitful discussions. I also would like to thank Prof. Rolf Müller and Karsten Mayr for providing Invasin.

A special thanks to Dr. Chiara De Rossi for her support with analytics, imaging and for being constantly present whenever her help is needed. I further thank Jana Westhues and Petra König for their support with cell culture and Karin Groß and Sarah Müller for their continuous support during my PhD. To Dr. Marcus Koch for his support with Cryo-TEM Imaging. I also would like to acknowledge my student Mohamed Ashraf Kamal, for his valuable help within this work with almost non-ending stability studies and for withstanding my working pressure.

To my all-time besties; starting as office-mates to end up as real-mates; Hanzey Yasar and Jing Wang. I would like to express my gratitude, joy and love for being there for me and more for still being a part of my current life. Thank you for our sad as well as exciting moments, trips, dinners, social-funny events and of course long lasting nights of card games.

To every person I met throughout this path within DDEL group or outside the group and offered me with open arms a great friendship; Herr Richter (Robert), Adriely, Carlos, Sarah N, Khiet, Patrick, Cristina, Jahan, Nashrawan, Rebecca, Junzhe and the Algerian (Samir).

Last and not the least, I must say that I would have not come so far without the continuous and unconditional support and love of my lovely husband Thabet. To him, I wish to express my sincere gratitude and love for being all the way patient, supportive, loving and not just at a personal level but also as a major contributor to my professional development. To my lovely mum, who since day one of my life she believed in me and did everything she could to see me one day achieving high academic degrees, and build a path towards a successful scientific carrier. To my lovely father and lovely little brother for their encouraging, believe and great love. Great thanks to all my family members.

عبارات شكر و تقدير وامتنان لعائلتي الصغيرة، بدءًا من أمي الغالية، التي أقل ما يمكن أن أقدمه لها هو كلمة شكر تحمل خالص المشاعر الطيبة والصادقة تقديرا لها لكل ما قدمته لي ولإيمانها بي وبذل كل ما في وسعها رقيقة لرؤيتي أحقق أعلى الدرجات العلمية، و أبنى مسيرة مهنية ناجحة. إلى والدي الغالي يا نبع العطاء و سند الحياة

وإلى أخي الصغير يا شمعة البيت رسالة شكر و عرفان لكما لوقوفكما بجانبني دوماً و تشجيعكما و حبكما المستمر و اللامتناهي


اختتم كلماتي بشكر خالص لكل فرد من عائلتي الكبيرة صغيرا و كبيرا لتشجيعهم المتواصل ودعواتهم الدائمة

Contributions

I hereby acknowledge the contributions of the following colleagues:

- Prof. Markus Bischoff and Dr. Janina Eisenbeis provided Eap.
- Prof. Rolf Müller and Karsten Mayr provided Invasin.
- Dr. Chiara De Rossi helped with HPLC method development for colistin quantification and performed the TEM imaging.
- Dr. Marcus Koch performed the Cryo-TEM imaging.
- Mohamed Ashraf Kamal helped with stability studies in simulated media.

Award



TOP DOWNLOADED PAPER 2018-2019

CONGRATULATIONS TO

Sara Menina

whose paper has been recognized as
one of the most read in

Advanced Healthcare Materials

WILEY